Isolation of Kaempferol Glycosides from *Ginkgo biloba* Leaves and Synthesis, Identification and Quantification of their major *in vivo* Metabolites

DISSERTATION

ZUR ERLANGUNG DES DOKTORGRADES

DER NATURWISSENSCHAFTEN (DR. RER. NAT.)

DER NATURWISSENSCHAFTLICHEN FAKULTÄT IV

DER UNIVERSITÄT REGENSBURG

vorgelegt von

Daniel Bücherl

aus Dieterskirchen

2013

Die vorliegende Arbeit entstand im Zeitraum vom März 2010 bis Oktober 2013 unter der Leitung von Herrn Prof. Dr. Jörg Heilmann am Lehrstuhl für Pharmazeutische Biologie am Institut für Pharmazie der Naturwissenschaflichen Fakultät IV – Chemie und Pharmazie – der Universität Regensburg.

Das Promotionsgesuch wurde eingereicht im Oktober 2013

Tag der mündlichen Prüfung: 29.11.2013

Prüfungsausschuss:

Prof. Dr. Gerhard Franz	(Vorsitzender)
Prof. Dr. Jörg Heilmann	(Erstgutachter)
Prof. Dr. Joachim Wegener	(Zweitgutachter)
Prof. Dr. Frank-Michael Matysik	(Drittprüfer)

Was du für den Gipfel hältst, ist nur eine Stufe.

Lucius Annaeus Seneca

Danksagung

Ein großes Dankeschön geht an alle die mir während meiner Promotion hilfreich zur Seite gestanden haben. Besonders möchte ich danken:

Prof. Dr. Jörg Heilmann für das Vertrauen und die Möglichkeit mir dieses interessante Projekt zu überlassen, für zahlreiche wertvolle Diskussionen und für die lehrreiche und schöne Zeit in seiner Arbeitsgruppe;

Dr. Egon Koch und Dr. Clemens Erdelmeier der Dr. Willmar Schwabe GmbH und Co. KG, für die Mitbetreuung dieser Arbeit, ihre zahlreichen wertvollen Beiträge, die hilfreichen Diskussionen, die Bereitstellung der Flavonoidfraktionen von EGb 761®, und die Durchführung der Fütterungsexperimente an den Ratten;

Dr. Willmar Schwabe GmbH und Co. KG für die grosszügige finanzielle Unterstützung dieser Arbeit;

meinen Kolleginnen und Kollegen am Lehrstuhl für Pharmazeutische Biologie sowie auch allen Praktikanten, für die freundliche Aufnahme in der Gruppe, das wunderbare Arbeitsklima und ihre Hilfsbereitsschaft. Weiterhin möchte ich mich dafür bedanken, dass die „lebhafte" Gestaltung meines jeweiligen Arbeitsplatzes immer mit einem Lächeln hingenommen wurde. Aus naturwissenschaftlicher Sicht sei angemerkt: „Ordnung ist das Unwahrscheinliche und deswegen eine Erscheinungsweise der Kunst." (Botho Strauß);

besonderer Dank gilt dabei Gabriele Brunner, für die Hilfe bei all den Problemen des Laboralltags und für die stetig freundliche Wegbeschreibung, wenn man mal wieder hektisch und unwissend auf der Suche nach diesem und jenem war;

besonderer Dank gilt auch Anne Grashuber, für die schöne Zusammenarbeit bei der Betreuung der Praktika und ihre freundliche Hilfsbereitschaft;

besonderer Dank gilt auch meinen Laborkolleginnen und Kollegen, Sarah Sutor, Magdalena Motyl, Marcel Flemming, Beata Kling und Michael Saugspier für viele förderliche Diskussionen, das bereitwillige und unkomplizierte Teilen der Arbeitsplätze und Geräte, aber auch für die unterhaltsamen und lustigen Momente im Labor;

besonderer Dank gilt auch Susann Haase, Anne Freischmidt, Susanne Knuth, Rosmarie Scherübl, Monika Untergehrer, Matej Barbič und Sebastian Schmidt für die Geduld beim Erklären der unterschiedlichen Laborgeräte und Methoden;

besonderer Dank gilt auch Markus Löhr und Stefan Wiesneth, für die Hilfe bei Software-Problemen und die damit einhergehende Übernahme der „Computer-Arbeit" innerhalb der Arbeitsgruppe;

der spektroskopischen und spektrometrischen Abteilungen der Fakultät Chemie und Pharmazie der Universiät Regensburg für die nette Zusammenarbeit. Ein besonderer Dank geht hierbei and Herrn Fritz Kastner und Herrn Josef Kiermaier für die hilfreichen Diskussionen und die Ermittlung zahlreicher analytischer Daten;

den Mitarbeitern der Arbeitskreise von Herrn Prof. Dr. Armin Buschauer, Herrn Prof. Dr. Burkhard König und Herrn Prof. Dr. Oliver Reiser für die freundliche Zusammenarbeit;

Paul Baumeister, Petr Jirásek und Andreas Kreuzer für die vielen hilfreichen Diskussionen und die Unterstützung;

meinen Freunden, die immer für Ablenkung gesorgt haben, wenn dies nötig war. Besonders die gemeinsame sportliche Freizeitgestaltung half nach langen Arbeitstagen;

meinen Eltern, Brigitte und Gerhard Bücherl, meinen Geschwistern Tonia und Katrin, und meiner Christina für die jahrelange Unterstützung, das Vertrauen und die Geduld. Ohne sie hätte ich es niemals bis hierhin geschafft. Ihnen ist die vorliegende Arbeit gewidmet.

Abbreviations

2D	two-dimensional
AAPH	2,2'-azobis(2-amidinopropane) dihydrochloride
ABTS	2,2'-azino-bis(3-ethylbenzothiazoline-6-sulphonic acid
ACEI	angiotensin-converting enzyme inhibition
ATP	adenosine-5'-triphosphate
CBG	cytosolic β-glucosidase
CC	column chromatography
CoA	coenzyme A
CVD	cardiovascular disease
DCM	dichloromethane
DMF	*N,N*-dimethylformamide
DMSO	dimethyl sulfoxide
EtOAc	ethyl acetate
EtOH	ethanol
FCS/FKS	fetal calf serum
Glc	β-D-glucose
HCl	hydrochloric acid
HMBC	heteronuclear multiple-bond correlation
HMEC	human microvascular endothelial cells
HPLC	high-performance liquid chromatography
HSQC	heteronuclear single-quantum correlation
IC_{50}	half maximal inhibitory concentration
LOQ	limit of quantification
LPH	lactase phlorozin hydrolase
MeOH	methanol
MMP	matrix metalloproteinase

NADH	nicotinamide adenine dinucleotide
NADPH	nicotinamide adenine dinucleotide phosphate
NMR	nuclear magnetic resonance
NOESY	nuclear Overhauser effect spectroscopy
NOS	nitric oxide synthase
NP	normal phase
ppm	parts per million
R^2	coefficient of determination
ROS	reactive oxygen species
RP	reversed phase
RT	room temperature
S_N2	bi-molecular substitution
SULT	sulfotransferase
TCA	tricarboxylic acid
t_R	retention time
UGT	uridine 5'-diphospho-glucuronosyltransferase
UV	ultraviolet

Table of Contents

1 General Introduction

1.1 Flavonoids and their Role in Plants

Flavonoids are a group of plant secondary metabolites with more than 4000 described members (1999).[1] They occur for instance in the epidermis of leaves and skin of fruits.[2] The basic structure is a flavan skeleton, which consists of two six-membered aromatic rings, connected by a three carbon chain.[2] Further oxidation and hydroxylation can form derivatives and thus the flavonoid family is divided into several subclasses (**Figure 1**).

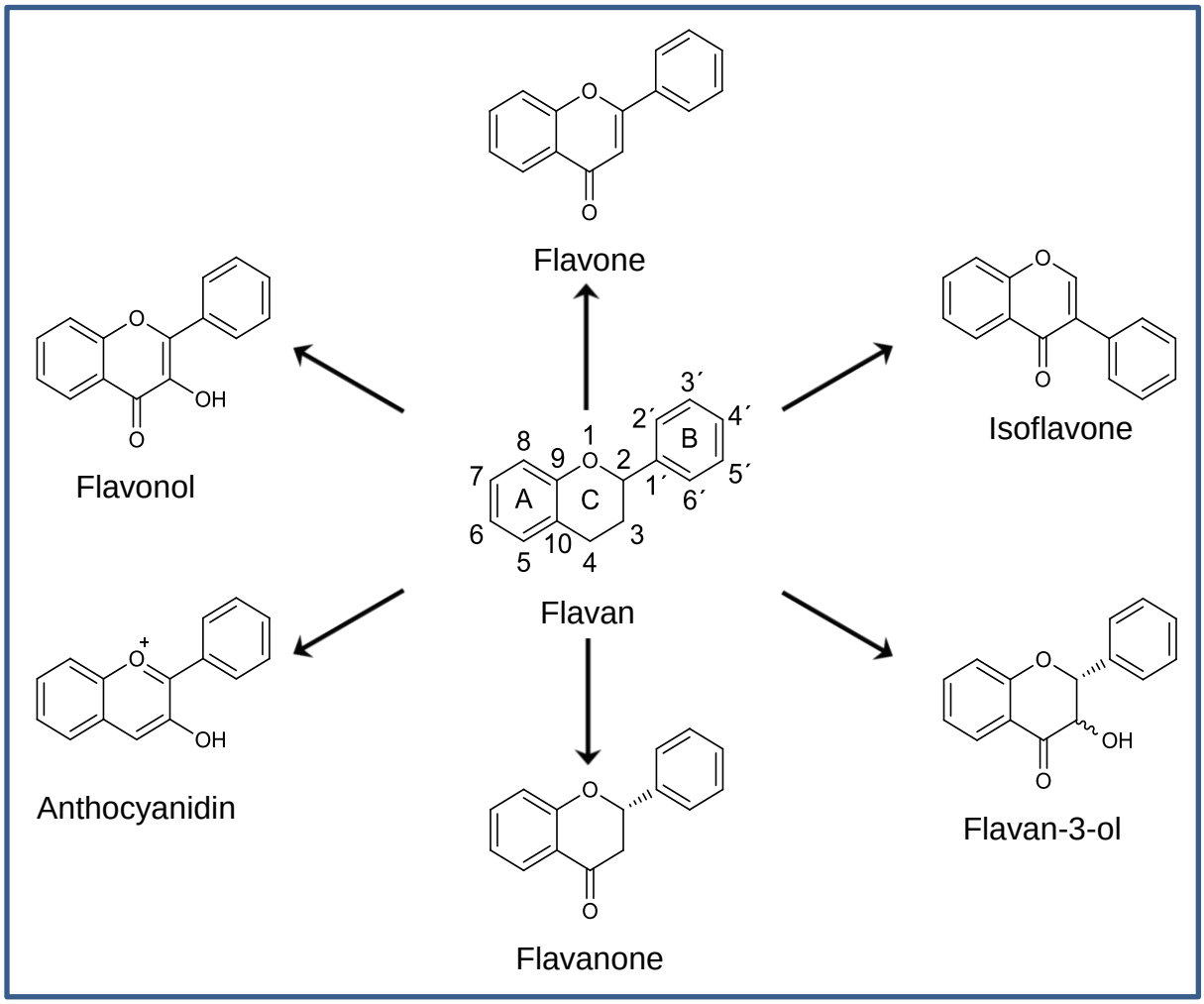

Figure 1: Generic structures of the major flavonoids[2]

Most of these flavonoids are glycosidated, which is, beside the substitution with hydroxyl groups, the reason for their hydrophilic properties.[3] Nevertheless, also several more lipophilic conjugates with O-methyl or isopentyl groups are known.[2]

The substitution with a sugar moiety is favoured at positions 3 or 7. Commonly found sugars are β-D-glucose (Glc), α-L-rhamnose and β-D-galactose. Further on, the glucose can be covalently bonded to a cinnamic acid moiety. In plants, flavonoids play an important role as pigments, to protect the plant from UV damage, in disease resistance and even for pollen development.[4,2] The sub-group of H_2O-soluble anthocyanins forms some pigments with pink, red, violet, blue and purple colors (**Figure 2**). These pigments and their variations are, among others, generated by the pH-depended interactions of anthocyanins with so-called copigments. Copigments like flavonol glycosides are often part of inter- or intra-molecular complexes. But also self-association mechanisms, metal complexation and even covalently linked conjugates *via* malonic acid (in *Allium schoenoprasum*) have been reported.[5,6] The consequence is an enhancement and higher stability of the color.[6] Anthocyanins and their copigments are generally located in the vacuoles of the petal epidermal cells,[5] but also cell wall bounded flavonol glycosides like the yellow kaempferol-3-rhamnosylgalactoside can be found in *Eustoma grandiflorum*, which cannot be regarded as copigment, due to the spatial separation.[5]

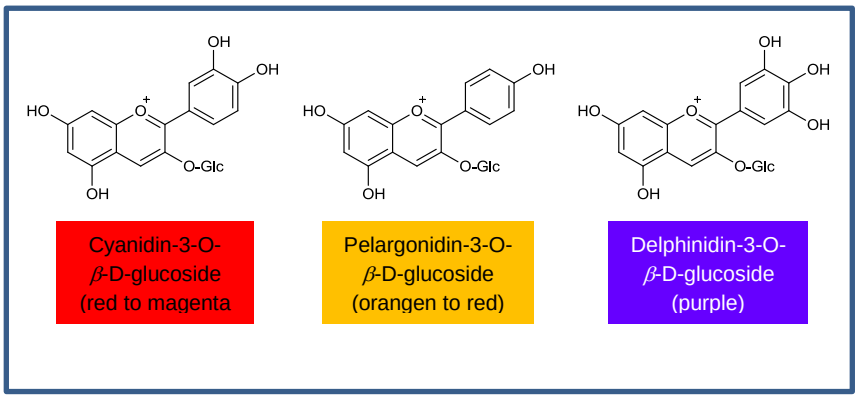

Figure 2: Anthyocyanins and their color

1.2 Biosynthesis

The biosynthesis of the flavonoids is described briefly starting from the photosynthesis, also regarding the ongoing discussions in literature concering the compartimentation of the different steps.

Photosynthesis

Located in the chloroplasts, the photosynthesis uses the energy of the light for an electron transport chain to generate reduction potentials and in particular NADPH and the energy store molecule ATP. These reduction equivalents and "energy carriers" are further used in the Calvin cycle to generate carbohydrates. During the Calvin cycle, a triose phosphate is formed (glyceraldehyde 3-phosphate ↔ dihydroxyacetone-phosphate) which can either be

transferred to the cytosol to support the synthesis of sucrose, or stay in the chloroplast to form starch.[7] The final carbohydrate is not necessarily free glucose, but rather the disaccharide sucrose or the polysaccharide starch.[7,8,9]

Glycolysis

Glycolysis, which is localised in the cytosol and as well in plastids,[7] produces energy in the form of ATP and the reduction equivalents $NADH/H^+$. Starch, sucrose or dihydroxyacetone-phosphate are all able to enter the glycolysis. The first two have to be hydrolyzed to its monomers, phosphorylated and in the case of glucose 6-phosphate, converted to fructose 6-phosphate by hexose phosphate isomerase. Dihydroxyacetone-phosphate can enter the glycolysis directly after conversion to glyceraldehyde 3-phosphate (triose phosphate isomerase). One of the final products of glycolysis is pyruvate.[7,8,9]

Synthesis of Malonyl-CoA

In the next step, pyruvate from plastid located glycolysis undergoes decarboxylation to form acetyl-CoA. The latter is converted by acetyl-CoA carboxylase which involves the conjugation with hydrogen carbonate to form malonyl-CoA and is described as the first step in fatty acid biosynthesis.[7,8,9]

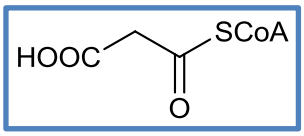

Figure 3: Structure of malonyl-CoA

The pyruvate from cytosol located glycolysis instead can pass the outer membrane of the mitochondria by free diffusion and the inner membrane by a specific carrier protein. In the mitochondria, pyruvate is also converted by the pyruvate dehydrogenase complex to form acetyl-CoA. In the next step, acetyl-CoA undergoes tricarboxyl acid (TCA) cycle which results in the formation of citrate. Citrate is transported to the cytosol *via* an antiporter (oxaloacetate). In the cytoplasm, citrate is converted to acetyl-CoA by ATP citrate lyase. Further on, acetyl-CoA is also transfered by acetyl-CoA carboxylase to form malonyl-CoA.[7, 10,11,12]

In general, acetyl-CoA can be found in at least four compartments namely in mitochondria (for the TCA cycle), in plastids (for *de novo* fatty acid biosynthesis), in peroxisomes (the product of β-oxidation of fatty acids) and in the cytosol.[10,13]

Malonyl-CoA is one of the essential elements for the final flavonoid biosynthesis.

The Prechorismate Pathway or Shikimate Pathway

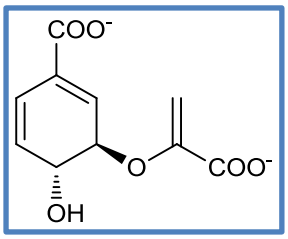

Figure 4: Structure of chorismate

The prechorismate pathway seems to be located exclusively in plastids[14] but also isoenzymes can be found in cytoplasma. The starting materials for this sequence are phosphoenolpyruvate and D-erythrose-4-phosphate. During glycolysis in the plastids, phosphoenolpyruvate is generated. Erythrose-4-phosphate is an intermediate in the regeneration of ribulose-1,5-bisphosphate (Calvin cycle) and in the pentose phosphate pathway. The reaction sequence is catalyzed by six enzymes and yields in chorismate.[7,8,9]

The Postchorismate Pathway

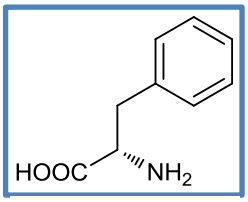

Figure 5: Structure of phenylalanine

It is still not clear whether just plastids or even the cytosol has the ability of further conversion of chorismate to aromatic amino acids and thus, among others, phenylalanine.[15] But most of the enzymes, which are necessary for this step (with the exception of cytosolic phenylpyruvate/4-hydroxyphenylpyruvate aminotransferase) were found in plastids.[16]

The Phenylpropanoid Pathway

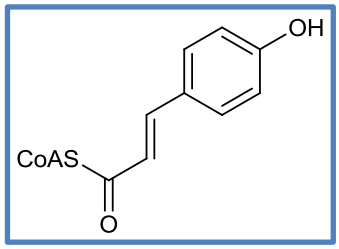

Figure 6: Structure of 4-coumaroyl-CoA

Further enzymatic conversion of phenylalanine to cinnamic acid is catalyzed by phenylalanine ammonia-lyase (PAL), which can be found in the cytosol and is associated to the endoplasmic reticulum.[17] Another enzymatic hydroxylation and conjugation with CoA leads to the formation of 4-coumaroyl-CoA.[7]

Synthesis of Flavonoids

The association of 4-coumaroyl-CoA with three molecules of malonyl-CoA by the cytosol-located chalcone synthase results in the formation of tetrahydroxychalcone, a compound which can already be described as submember of the flavonoid family.[17] Following isomerisation to the flavanone naringenin, hydroxylation at position 3 and finally the generation of a C2-C3 double bond by the oxidoreductase flavonol synthase is one possible way for the synthesis of the flavonol kaempferol.[7]

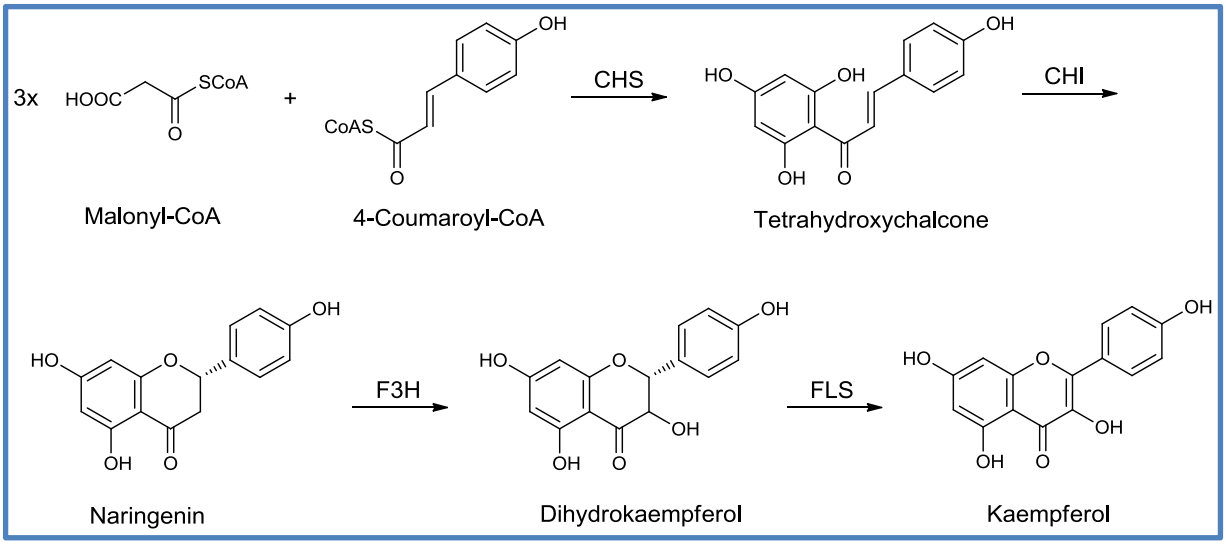

Figure 7: Final biosynthethic pathway to the flavonol kaempferol. Enzyme abbreviations: CHS, chalcone synthase; CHI, chalcone isomerase; F3H, flavanone 3-hydroxylase; FLS, flavonol synthase

An additional glycosylation may also take place in the cytosol. The necessary enzyme, UDPG-flavonoid glucosyl transferase was also detected at the cytoplasmic side of the endoplasmic reticulum.[17] Overall it seems to be most likely and beneficial, that the final steps in flavonoid biosynthesis might be managed by an enzyme complex.[17]

1.3 Flavonoids as Food Ingredients

Flavonoid glycosides are present in several consumed food products and beverages like herbs, vegetables, fruits, tea and wine. The estimated daily flavonoid intake in humans is subject of some studies. But most of the investigations just regard about 2-5 flavonoids. For instance Hertog *et al.* (1993) report a daily intake of the potentially anti-carcinogenic flavonols quercetin, kaempferol, myricetin, together with the flavones apigenin and luteolin of 23 mg/day in the Netherlands.[1] Considering, that Arts *et al.* (2001) have measured an average catechin intake of 50 mg/day in the Netherlands as well, makes the problem for the

investigation of total flavonoid intake obvious.[18] The published averages differ between 0.154 mg/day (4 isoflavones, USA) and 63.9 mg/day (4 flavonols, 1 flavone, 2 isoflavones, Japan) and therefore in a wide range, depending on several variables like analyte, geography, investigated food and possibly even age and gender of the participants.[19,20] A value for an estimated total flavonoid intake for USA adults is 189.7 mg/day based on a database which contains the flavonoid content in foods.[21]

1.4 Flavonoid Activities and their Structural Essentials

In mammals, flavonoids are known to have, among others, anti-inflammatory, anti-oxidative, anti-viral, anti-thrombotic and spasmolytic activities.[22] The knowledge on molecular mechanisms which are responsible for these activities is limited. Nevertheless, flavonoids have, depending on their hydroxyl pattern and presence of a carbonyl group, the ability of free radical scavenging (**Figure 8**, **Figure 9**), metal ion chelating and enzyme inhibition.

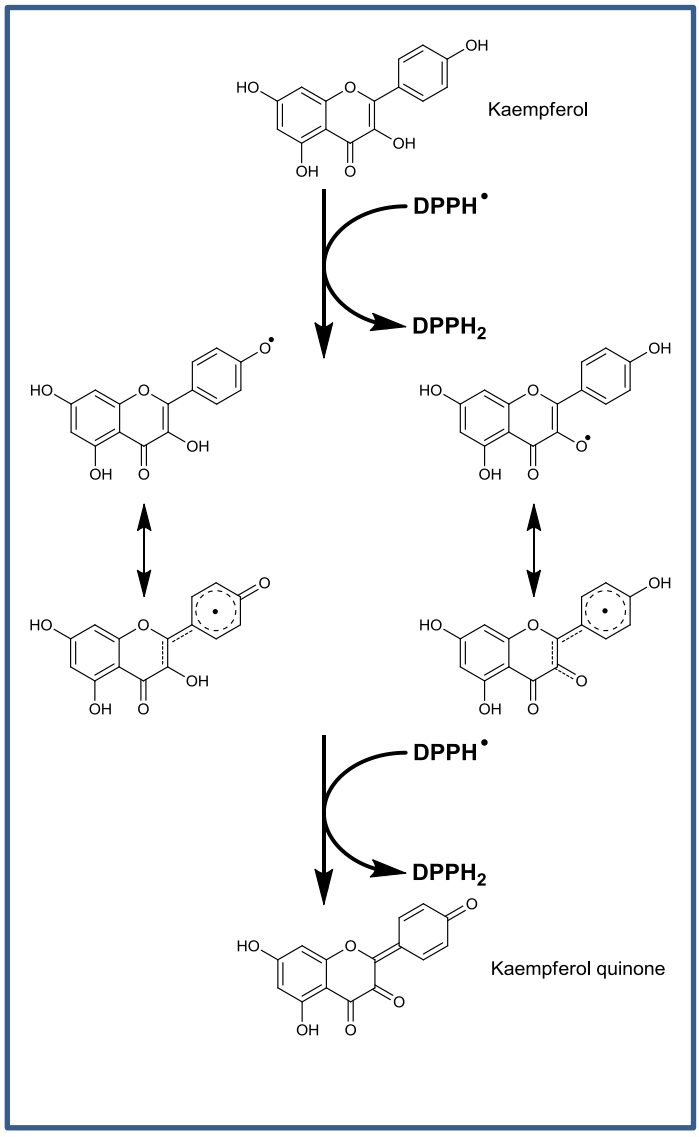

Figure 8: Radical scavenging mechanism of kaempferol.[27] DPPH: 2,2-diphenyl-1-picrylhydrazyl

Some free radicals like the nitric oxide radical NO• or the superoxide radical $O_2^{\bullet -}$, are generated deliberately *in vivo* by phagocytes.[23] The generation of nitric oxide also takes place in neurones and endothelial cells starting from L-arginine by the enzym nitric oxide synthase (NOS).[24,25] This compound plays an important role as intracellular signal, transcellular messenger and cytotoxic species

in the unspecific immune defence.[26] But, as usual, the effect depends on concentration and environment and thus can also be destructive for DNA or important proteins. An excess of NO• can consequently cause cytotoxic and cytostatic effects.[25] A further reaction of nitric oxide with the superoxide radical $O_2^{\bullet -}$ yields in the formation of peroxynitrite, which is directly cytotoxic.[25] The free radical scavenging activity of flavonoids is based on the oxidizability of the B- and C-ring. The oxidation of the compound and thus the reduction and deactivation of the nitric oxide- and other radicals proceeds in two steps.[27]

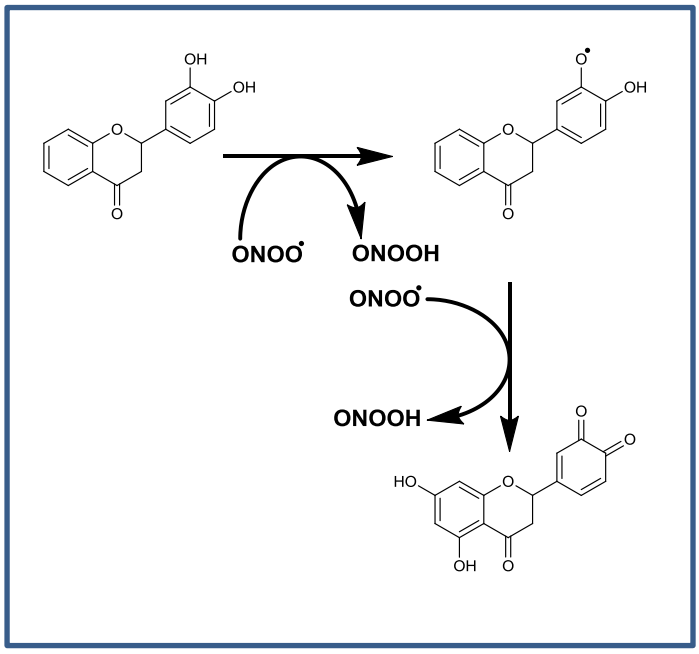

Figure 9: Catechol radical scavening activity[101]

Another part of the anti-oxidative effect of some flavonoids is the interaction with metal ions. The reason for this effect might be on one hand the chelating of the metal and a higher anti-oxidative potential of the resulting complex (e.g. quercetin/2Co^{2+}, **Figure 10**).[28] On the other hand flavonoids can protect for instance low-density lipoprotein from directly Cu^{2+}-induced oxidation by chelating this ion.[29] But in this context it has to be mentioned that these interactions depend strongly on the structure of the flavonoid and metal ion concentration. So even pro-oxidative effects of flavonoids are reported.[30]

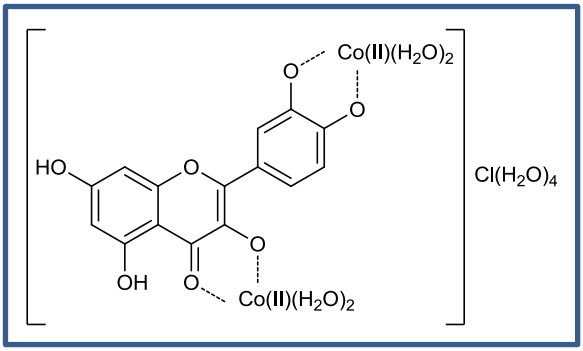

Figure 10: Quercetin-cobalt-complex[28]

Flavonoids are also known to have enzyme inhibiting activity. At first, it can be assumed that either a complexation of the metal ion in the enzyme (if present) or an interaction with amino acids from the active side are responsible for this activity. Concerning the enzyme group of matrix metalloproteinases (MMPs) for instance, the inhibition is based on a

hydrogenbridge bond and hydrophobic interactions in the zinc binding catalytic domain.[31] The chelation of the zinc ion can be discarded in this case, due to the distance from the ion to the flavonoid of more than 5 Å.[31] Hydrogen bonds can also occur between the amino acids and the hydroxyl groups, preferentially at a catechol moiety of the flavonoid.[31] Hydrophobic interactions can be formed, among others, between the amino acid leucin and the chromon scaffold.[31] These non-competitive inhibition of MMPs contributes to anti-metastatic and anti-arteriosclerotic effects, which are reported for some flavonoids.[32] Similar results have been published for the inhibition of the angiotensin-converting enzyme, which is one of the top-selling branches in the pharmaceutical industry. This enzyme is responsible for the maintenance of normal blood pressure *via* the conversion of Angiotensin I into Angiotensin II.[33] Angiotensin II acts vaso-contrictive and can thus cause hypertension and cardiovascular disease (CVD).[34] Concering the flavonoids, the presence or absence of some structural elements changes the ACE-inhibitory (ACEI) activity (**Figure 11**).[34] In a study from Guerrero *et al.* (2012), Luteolin (17 flavonoids were tested) showed the highest effect with an IC_{50} value of 23 µM. The essential structure elements are a double bond between C2 and C3, a carbonyl group in the C-ring, a free hydroxyl function at C3 and a catechol moiety at the B-ring. The latter is with distances of 2.1 Å (oxygen at C3') and 4.3 Å (oxygen at C4') to the zinc ion of the enzym within the range for chelation, but again, hydrophobic interactions and hydrogen bonds play a crucial role.[34] Consequently, even if the ACEI activity of the flavonoids cannot measure up with those of the commercially available drugs, the common, regular dietary intake of flavonoids in a higher dose could prevent or reduce hypertension.[34]

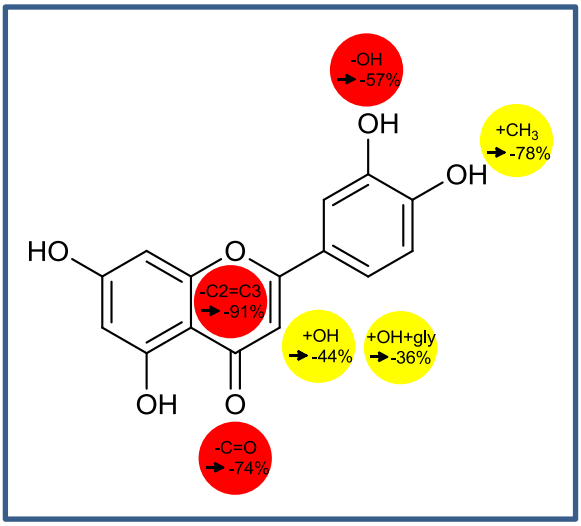

Figure 11: Influence of substitution pattern[37]

1.5 Flavonoids containing Plants in Traditional Medicine

Among the flavonoid subclasses, the flavonols are the most widespread.[2] Kaempferol is beside quercetin the most important member of this group and can be found in some foods like i.e. endive, leek, broccoli, radish, grapefruit and black tea in higher concentrations.[35,36] Further on, significant yields of kaempferol and its conjugates can be found in several traditionally used medicinal plants:

- *Camptosorus sibiricus* (Aspleniaceae), North China, treatment of vascular inflammation, diabetic complication and traumatism[37]
- *Stenochlaena palustris* (Blechnaceae), Papua New Guinea, used as a contraceptive[38]
- *Cinnamomum osmophloeum* (Lauraceae), Taiwan, treatment of inflammation, intestinal infections, astringent, diuretic and diabetic complications[39]
- *Epimedium sagittatum* (Berberidaceae), People's Republic of China, coronary heart disease, chronic bronchitis, frequency/urgency of urination, aphrodisiac[40]
- *Ilex paraguariensis,* mate tea (Aquifoliaceae), South America, choleretic, hypocholesteremic, anti-oxidant, hepatoprotective effects[41]
- *Momordica foetida*, (Cucurbitaceae), East Africa, antimalarial activity[42]
- *Ginkgo biloba,* (Ginkgoaceae), People's Republic of China, treatment of heart and lung dysfunctions, skin infections[43]

Of course it has to be remarked, that this is only a short list of examples among several other plants and furthermore the healing properties may not be only the result of the kaempferol content. In general, it is improbable that the use in traditional medicine is attributed to one compound. But some studies have shown, that kaempferol has various pharmacological activities: anti-oxidant, anti-inflammatory, anti-microbial, anti-cancer, cardioprotective, neuroprotective, anti-diabetic, anti-osteoporotic, estrogenic/anti-estrogenic, anxiolytic, analgesic and anti-allergic.[44]

Some more detailed information on kaempferol glycosides in *Ginkgo* folium, synthetic strategies, *in vivo* metabolism and pharmacology can be found at the beginning of each specific topic.

1.6 Objectives

Kaempferol is beside quercetin one of the most common flavonols in vegetables and herbal medicines. Wherein the *in vivo* metabolism of quercetin is widely understood, the exact structures of *in vivo* kaempferol conjugates and their plasma concentration are unknown or not absolutely evidenced.

The first aim of this thesis was to isolate kaempferol glycosides from two fractions of a *Ginkgo* folium extract, provided from Dr. Willmar Schwabe GmbH und Co. KG. A standard chromatographic scheme should be developed, which allows the facile isolation of compounds in sufficient amounts for *in vivo* pharmacokinetic investigations in rats with a certain dosage.

Five expected metabolites of kaempferol should be chemically synthesized, in order to have reference substances for the analysis of the plasma samples. Therefore, synthetic pathways starting from the aglycone should be developed to yield in the formation of four kaempferol glucuronides and one kaempferol sulfate, wherein the latter is already described in literature.

In the next step, the metabolites of kaempferol in rat plasma should be identified and quantified by HPLC-UV. Therefore some preparatory work has to be accomplished, which includes the development of a combined workup method for the plasma samples and a suitable chromatographic separation with regard to the recovery and the limit of quantification.

Finally, some pharmacological data of kaempferol and its conjugates should be examined, with the focus on potential anti-oxidative, anti-proliferative and anti-inflammatory effects.

2 Isolation and Quantification of Kaempferol Glycosides

2.1 Introduction

Ginkgo biloba LINNÉ (Ginkgoaceae) is described by Charles Darwin as ´living fossil´ due to little or no morphological changes in the past 100 million years.[45] It belongs to the group of gymnosperms, is a dioecious plant and the only member of the Ginkgoaceae family. The tree has a grey bark, reaches a height of 30-40 m and has a diameter of 3-4 m. The plant is probably native in China and Japan and was cultivated in temples. Since the 18th century it can be found in european parks. *Ginkgo* folium consists of the green to yellowish whole leaves (4-10 cm). The leaf is characteristic and bilobate, fan-like and the venation is dichotomously and almost parallel (**Figure 12**).[46,47,48]

Figure 12: Gingko leaf[102]

At least eight kaempferol glycosides are known from literature to occur in *Gingko* folium. In **Figure 13** the structures are presented. For the preparation of the extract, one can find different monographs, all using the powdered drug, which is processed as described briefly in the following :

- U.S. Pharmacopoeia: methanol, c(suspension) = 0.1 g/mL, reflux, 10 min
- Chinese Pharmacopoeia: for flavonoids: methanol, c(suspension) = 0.1 g/mL, reflux, 10 min
  for terpene lactones: 50% acetone, c(suspension) = 0.025 g/mL, reflux, 3 h
- Hong Kong Chinese Materia Medica Standards: methanol, c(suspension) = 0.1 g/mL, sonification, 30 min
- European Pharmacopoeia: methanol, c(suspension) = 0.2 g/mL, 65 °C, 10 min
- EGb 761® complies the monograph in the European Pharmacopoeia "*Ginkgo* dry extract, refined and quantified": 60% acetone

The indications listet in the chinese pharmacopoeia are: obstruction of collaterals by blood stasis, chest impediment and heart pain, hemiplegia caused by windstroke, cough and panting caused by lung deficiency and hyperlipidemia.

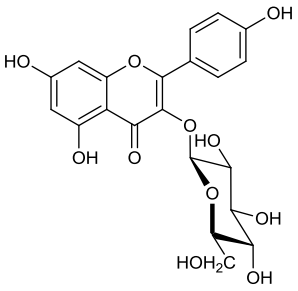

3-O-(β-D-Glucosyl)kaempferol[103,104]

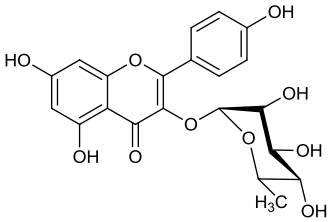

3-O-(α-L-Rhamnosyl)kaempferol[52]

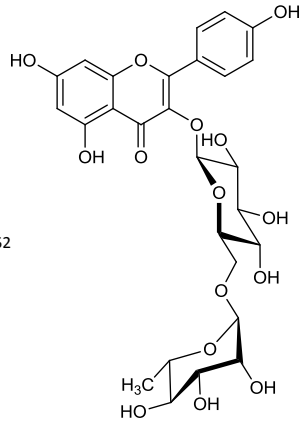

3-O-(6-O-(α-L-Rhamnosyl)-β-D-glucosyl)kaempferol[103,104]

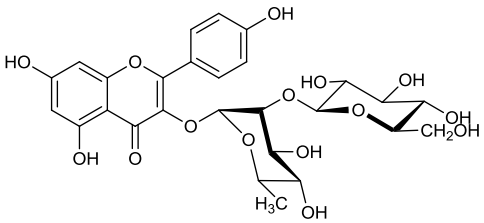

3-O-(2-O-(β-D-Glucosyl)-α-L-hamnosyl)kaempferol[105,103]

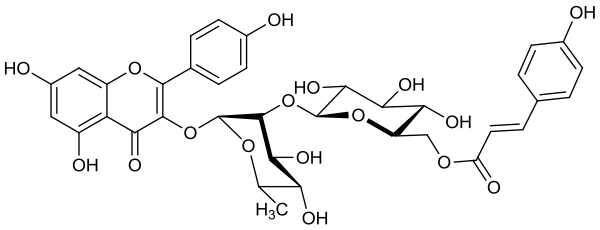

3-O-(2-O-(6-O-(*p*-Hydroxy-trans-cinnamoyl)-β-D-glucosyl)-α-L-rhamnosyl)kaempferol[103,104,108]

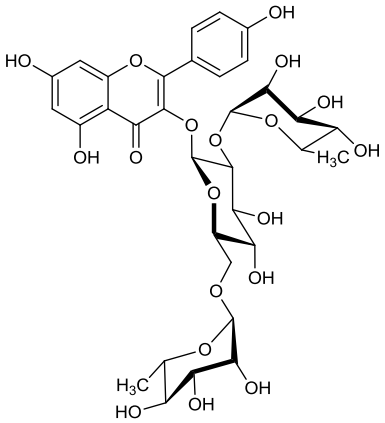

3-O-(2-O, 6-O-Bis(α-L-rhamnosyl)-β-D-glucosyl)kaempferol[106,107]

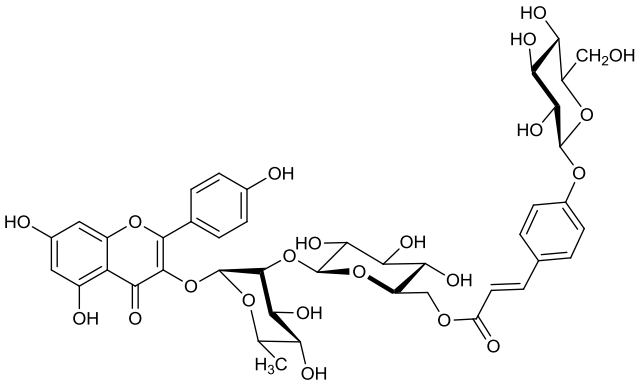

3-O-(2-O, 6-O-(*p*-(β-D-Glucosyl)-oxy-trans-cinnamoyl)-β-D-glucosyl)-α-L-rhamnosyl)kaempferol[105]

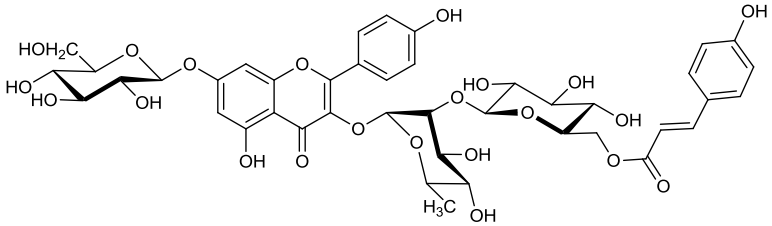

3-O-(2-O, 6-O-(*p*-Hydroxy-trans-cinnamoyl)-β-D-glucosyl)-α-L-rhamnosyl)-7-O-(β-D-glucosyl)kaempferol[104]

Figure 13: Kaempferol glycosides in *Ginkgo* folium

For the isolation of kaempferol glycosides, two flavonol glycosides enriched fractions of EGb 761® were provided from the Dr. Willmar Schwabe GmbH and Co. KG. In the following, a combination of chromatographic methods was developed, which allows the isolation of some kaempferol derivatives for extract quantification and *in vivo* investigation.

The standardized extract EGb 761® consists of about 22-27% flavonoid glycosides and 5-7% terpene lactones.[49] The extract is the active ingredient in Tebonin® caplets and the scope of application covers disturbances of memory, concentration disorders, depressive state, dizziness, tinnitus and headaches.[49] The corresponding aglycones of the flavonoids are mainly quercetin, kaempferol and isorhamnetin. The maximum daily recommended oral dosage for the extract in Tebonin® is 240 mg which is equivalent to about 3.2 mg/kg.

In the present study, it has to be considered, that an administration of 3.2 mg/kg is not sufficient for an *in vivo* investigation in rats due to the different metabolic situation and the expected plasma levels of the metabolites would be with certainity under the limit of quantification (LOQ) using HPLC with UV detection, even if just a pure compound is administered and not the whole extract.

In a comparable study, rats were treated with a dosage of 600 mg/kg of the extract, which yields to a maximum kaempferol concentration (aglycone) of 341 ng/mL after 8 hours.[50] In the present study, not the extract should be used for administration, but different kaempferol glycosides in their pure form and depending on their content in EGb 761®. Consequently, the standardized extract has to be quantified concerning the isolated kaempferol glycosides.

The pure compounds are further on used in the next step as reference substances for the quantification of the standardized extract.

2.2 Material and Methods

2.2.1 Consumable Material

2.2.1.1 Solvents

- Acetone, EMSURE®, for analysis, Merck KGaA, 64271 Darmstadt, Germany
- Ethyl acetate, for analysis, 99.99%, Acros, New Jersey, USA
- H_2O, deionised, further purified by membraPure, Astacus, MembraPure GmbH, Berlin, Germany
- 2-Propanol, EMSURE®, for analysis, 99.8%, Merck KGaA, 64271 Darmstadt, Germany
- 2-Propanol, ROTISOLV® HPLC, ≥ 99.9%, Carl Roth GmbH & Co. KG, 76185 Karlsruhe, Germany
- DMSO, SeccoSolv®, ≥99.9%, Merck KGaA, 64271 Darmstadt, Germany
- Methanol, EMSURE®, for analysis, 99.9%, Merck KGaA, 64271 Darmstadt, Germany

2.2.1.2 Naturstoffreagenz A

- 2-Aminoethyldiphenylborinate, 2 g dissolved in 200 mL MeOH, Fluka®, Sigma-Aldrich Chemie GmbH, 89555 Steinheim, Germany
- Polyethylene glycol 400, 10 g dissolved in 200 mL MeOH, Merck Schuchardt OHG, 85662 Hohenbrunn, Germany

2.2.1.3 TLC

- TLC Silica gel 60 F_{254}, Merck KGaA, 64271 Darmstadt, Germany
- TLC chambers, Camag, Muttenz, Switzerland

2.2.1.4 NMR

- Bruker Avance 300, Bruker Corporation, Billerica, USA
- Methanol-d_4, 99.8%, Deutero GmbH, 56288 Kastellaun, Germany
- NMR tubes, 507-HP, 203 mm, Norell, Landisville, USA

2.2.2 Columns and Stationary Phases for Isolation

- Flash-NP: SuperVarioPrep® D40, 46 x 186 mm, filled with stationary phase Geduran® Si 60 63-200 µm, 90 g, Merck KGaA, 64271 Darmstadt, Germany
- Flash-RP: SuperVarioPrep® D40, 46 x 186 mm, filled with stationary phase RP18 25-40 µm, 90 g, Merck KGaA, 64271 Darmstadt, Germany
- Semipreparative HPLC: Knauer, Vertex, 16 x 250 mm, filled with stationary phase Eurospher-100 C18-7 µm, 14163 Berlin, Germany

2.2.3 Extract and Fractions

The extract of *Ginkgo* folium and flavonoid enriched fractions were obtained from Dr. Willmar Schwabe GmbH & Co. KG.

- Flavonol diglycosides enriched extract: PSC0148/B/Wo06-149-02, 35 g
- Flavonol triglycosides enriched extract: PSC0148/B/Wo06-148-16, 100 g
- Standardised *Ginkgo* folium extract: PSC0148/*Ginkgo*-Extrakt/ Ch.454

2.2.4 Instruments

- Flash: Spot Flash Liquid Chromatography, SPOT-System Ser.-No. 08-01-108, single-beam spectrophotometer, Interchim, 03103 Montlucon, France
- Semipreparative HPLC: Varian ProStar, Model 210, diode array detector, Agilent Technologies Deutschland GmbH, 71034 Böblingen, Germany
- Analytical HPLC:
    - Column: Hibar® 250-4, Purospher® STAR, RP18e (5 µm), Column No.: 027444, Merck KGaA, Darmstadt, Germany
    - Precolumn: LiChroCART® 4-4, Purospher® STAR, RP18e (5 µm), Merck KGaA, Darmstadt, Germany
    - Pump: Hitachi L-2130, VWR, Darmstadt, Germany
    - Autosampler: Hitachi L-2200, VWR, Darmstadt, Germany
    - Column Oven: Hitachi L-2350, VWR, Darmstadt, Germany
    - Diode Array Detector: Hitachi L-2455, VWR, Darmstadt, Germany
    - Software, EZChrom Elite, Version 3.1.7, VWR, Darmstadt, Germany
- Mass spectrometer:
    - TermoQuest Finnigan TSQ 7000, Thermo Fisher Scientific, Waltham, USA
    - Electrospray ionization (ESI)

2.2.5 Isolation of Flavonol Diglycosides

2.2.5.1 First Chromatographic Separation

Instrument:	Flash chromatography
Column:	Merck, SuperVarioPrep® D40, 46 x 186 mm, for 90 g Silica Si 60
Stationary Phase:	Merck, Geduran® Si 60 63-200 µm, 40 x 140 mm
Mobile Phase:	A: EtOAc, B: acetone, C: H_2O
	The solvents where exhaustively mixed in a separatory funnel; after phase separation, the upper phase was used for CC
Application	3.0 g diglycoside extract + 4.5 g silica gel
Fractionation:	52 min
Gradient:	0-25 min: EtOAc: acetone: H_2O ~ 6:2:0,7
	25-40 min: EtOAc: acetone: H_2O ~ 5:3:1
	40-52 min: 100% MeOH
Flow:	50 mL/min

→ 88 fractions each 30 mL

2.2.5.2 Second Chromatographic Separation

Instrument:	Semipreparative HPLC
Column:	Knauer, Vertex, 16 x 250 mm
Stationary Phase:	Eurospher-100 C18-7 µm
Mobile Phase:	A: H_2O, B: 2-propanol
Application:	300 µL (H_2O: 2-propanol 70:30), ~ 33 mg of F3
Fractionation:	31 min
Gradient:	0 min: 15% 2-propanol
	25 min: 30% 2-propanol
	25-27 min: 30% 2-propanol
	29 min: 15% 2-propanol
	29-31: 15% 2-propanol
Flow:	5 mL/min

2.2.6 Isolation of Flavonol Triglycosides

2.2.6.1 First Chromatographic Separation

Instrument:	Flash chromatography
Column:	Merck, SuperVarioPrep® D40, 46 x 186 mm, für 90 g Silica Si 60
Stationary Phase:	Merck, Geduran® Si 60 63-200 µm, 40 x 140 mm
Mobile Phase:	A: EtOAc, B: acetone, C: H_2O
	The listed solvents where exhaustively mixed in a separatory funnel, after phase separation, the upper phase was used for CC
Application:	5.0 g triglycoside extract + 7.5 g silica gel
Fractionation:	55 min
Gradient:	0-10 min: EtOAc: acetone: H_2O ~ 5:3:1
	10-40 min: EtOAc: acetone: H_2O ~ 5:4.5:2
	40-52 min: 100% MeOH
Flow:	30 mL/min

→ 55 fractions each 30 mL

2.2.6.2 Second Chromatographic Separation

Instrument:	Flash chromatography
Column:	Merck, SuperVarioPrep® D40, 46 x 186 mm, 90 g
Stationary Phase:	Merck, RP18 25-40 µm, 90 g, 40 x 115 mm
Mobile Phase:	A: H_2O, B: 2-propanol
Application:	1.7 g F2 + 2.5 g RP18
Fractionation:	33 min
Gradient:	0 min: 15% : 2-propanol
	22 min: 28%: 2-propanol
	22-33 min: 2-propanol
Flow:	30 mL/min

→ 33 fractions each 30 mL

2.2.6.3 Third Chromatographic Separation

Instrument:	Semipreparative HPLC
Column:	Knauer, Vertex, 16 x 250 mm
Stationary Phase:	Eurospher-100 C18-7 µm
Mobile Phase:	A: H_2O, B: 2-propanol
Application:	100 µL (H_2O: 2-propanol 95:5), ~ 36 mg of F2
Fractionation:	33 min
Gradient:	0 min: 10% 2-propanol
	24 min: 20% 2-propanol
	24-27 min: 20% 2-propanol
	30 min: 10% 2-propanol
	30-33: 10% 2-propanol
Flow:	7.5 mL/min

2.2.7 Quantification of four Kaempferol Glycosides in EGb 761®

2.2.7.1 Principles

- Two times, 5.0 mg of each reference substance were dissolved in DMSO ≙ two 1st stock solution for each compound
- 60 µL of the 1st stock solution were diluted with 1940 µL of 7% aqueous 2-propanol ≙ 2nd stock solution
- Depending on the desired concentration, 75-260 µL of the 2nd stock solution were brought to the volume of 1 mL with 7% aqueous 2-propanol
- One calibration curve based on six points
- Only three points of each calibration curve are based on a single 1st stock solution
- Three calibration curves for each reference substance
- These three calibration curves were arithmetically averaged
- The single calibrations curves are interday
- Interday precision und intraday precision based on a single 1st stock solution
- Three times, 5.0 mg of the standardized extract were dissolved in 3320 µL of 7% aqueous 2-propanol and 7.5 µL DMSO

2.2.7.2 Analytical HPLC for Extract Quantification

Instrument:	Analytical HPLC	
Oven:	30 °C	
Thermo Unit:	4 °C	
Column:	Precolumn: LiChroCART® 4-4, Purospher® STAR RP-18e (5 µm)	
	Main column: Hibar® 125-4, Purospher® STAR RP-18e (3 µm)	
Mobile Phase:	A: H_2O + 0.1% TFA, B: 2-propanol	
Injection Volume:	20 µL	
Gradient/Flow:	0 min: 7% 2-propanol	0.7 mL/min
	60 min: 20% 2-propanol	0.7 mL/min
	70 min: 30% 2-propanol	0.6 mL/min
	77 min: 30% 2-propanol	0.6 mL/min
	80: 7% 2-propanol	0.6 mL/min
	90: 7% 2-propanol	0.7 mL/min

2.3 Results and Discussion

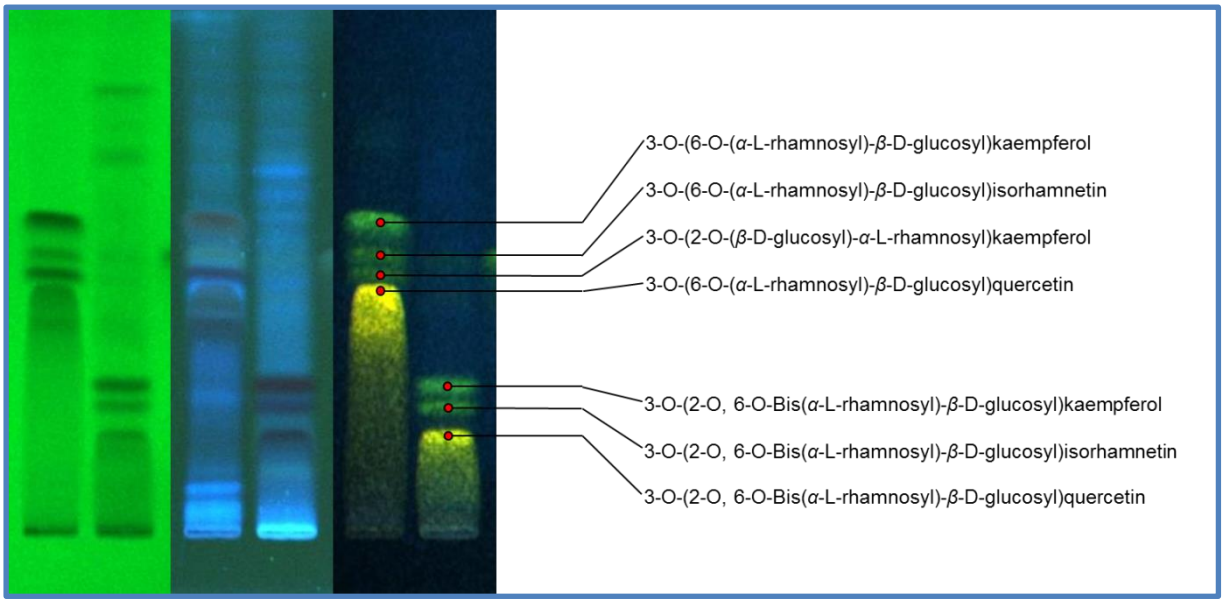

Figure 14: NP-TLC of flavonol glycoside enriched extracts. Application: diglycoside-enriched extract; triglycoside-enriched extract. Mobile phase: EtOAc:acetone:H_2O ~ 5:3:1, 6 runs. Detection at 254 and 366 nm (bands 1-4); 366 nm after derivatisation with Naturstoffreagenz A (band 5 and 6)

The aim of the isolation was to get kaempferol glycosides for the *in vivo* investigations and as references for extract quantification. A combination of chromatographic methods was developed to isolate these compounds from two flavonol-enriched subfractions of the extract EGb 761®. For the isolation of kaempferol diglycosides, two chromatographic steps were needed, whereas 3-O-(2-O, 6-O-bis(α-L-rhamnosyl)-β-D-glucosyl)kaempferol was isolated within three steps. The final purification was successful by use of a H_2O/2-propanol gradient. The crucial separation of the kaempferol- from the isorhamnetin derivatives could not be achieved with H_2O/MeOH or H_2O/acetonitrile mixtures. The final assignment of the flavonol glycosides to the corresponding region on the TLC is depicted in **Figure 14**.

At the beginning, the enriched extract was analyzed by TLC. It could be seen, that the addition of formic or acetic acid leads to a good separation on normal phase. Nevertheless, it was tried to avoid acid in the mobile phase, because hydrolysation can occur during the use of the rotation evaporator.

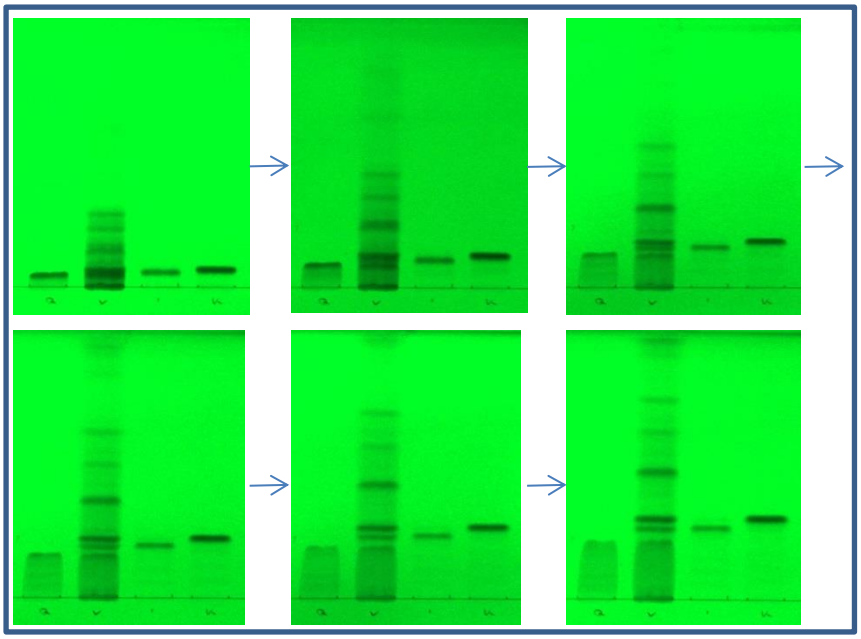

Figure 15: Six times development on NP-TLC of the triglycoside-enriched extract compared to isolated substances. Application (bands 1—4): 3-O-(2-O, 6-O-bis(α-L-rhamnosyl)-β-D-glucosyl)quercetin; triglycoside enriched fraction; 3-O-(2-O, 6-O-bis(α-L-rhamnosyl)-β-D-glucosyl)isorhamnetin; 3-O-(2-O, 6-O-bis(α-L-rhamnosyl)-β-D-glucosyl)kaempferol. Mobile phase: EtOAc:acetone:H_2O ~ 5:3:1

A mixture of EtOAc, acetone and H_2O showed a good separation on TLC. It was necessary to develop the TLC plate about six times, but this procedure results in a good separation of the compounds, which is exemplarily shown for the triglycoside enriched fraction in **Figure 15**. Consequently, different mixtures of these three solvents with varying elution strength were prepared for the first normal phase column chromatography.

Isolation of Kaempferol Diglycosides

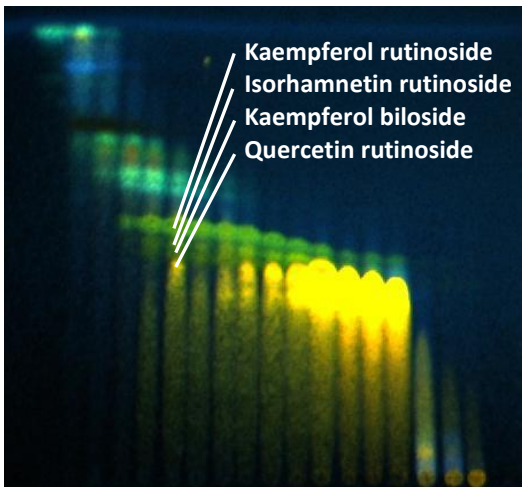

Figure 16: NP-TLC after CC of the diglycoside enriched fraction. Mobile phase: EtOAc:acetone:H_2O ~ 5:3:1; 6 developments; detection at 366 nm after derivatisation with Natursoffreagenz A. CC according to 2.2.5.1

The first separation with flash column chromatography visualized on TLC showed, after derivatisation with Naturstoffreagenz A, four fluorescent areas (366 nm) at an R_f value between 0.34 and 0.56 (**Figure 16**). The upper three have a greenish yellow fluorescens, which indicates one free hydroxyl group at the B-ring of the flavonoid and can thus be assigned, with regard to the metabolite spectrum of *Ginkgo* folium, possibly to kaempferol- and/or isorhamnetin derivatives.[51] The lower, more orange spot can be associated to a flavonoid with two free hydroxyl functions at the B-ring.[51]

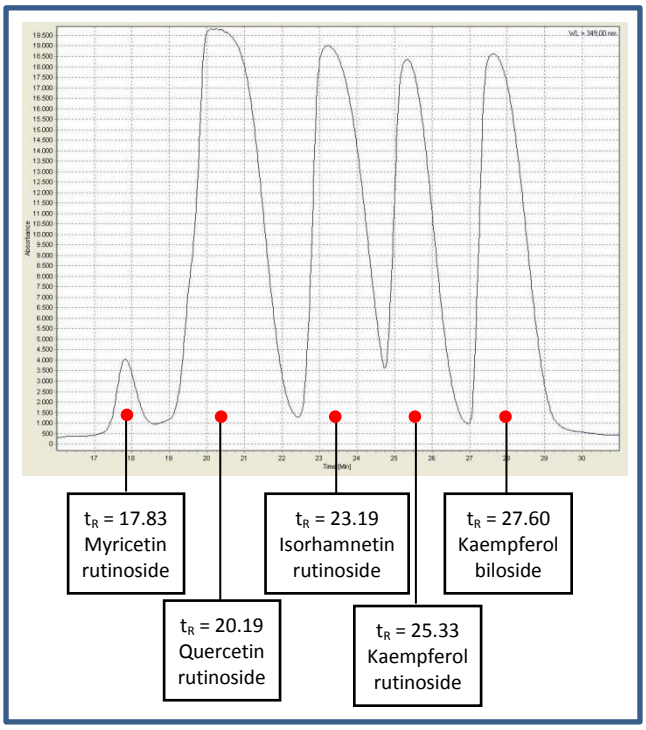

Figure 17: Semipreparative HPLC chromatogram of the diglycosides at 349 nm. CC according to 2.2.5.2

Overall, the separation is not perfect, due to the overlap of the four spots from test tube 28-73. Nevertheless, it can be noted that a combination of the test tubes 18-38 would give a fraction of mainly the desired compounds (greenish yellow fluorescens) and avoids the major part of the quercetin glycoside. Further on, some more lipophilic ingredients could be separated from the kaempferol diglycosides, which allowed the subsequent use of reversed phase HPLC. With the application of a H_2O/2-propanol gradient, a sufficient separation of the remaining flavonoid glycosides could be achieved **(Figure 17**). Beside the already expected flavonols, a myricetin glycoside could be isolated. Overall, five flavonol diglycosides were isolated, wherein two are kaempferol derivatives.

Isolation of Kaempferol Triglycosides

The flavonol triglycoside enriched fraction was first subjected to normal phase flash column chromatography, wherein some traces of remaining diglycosides with a medium R_f-value could be removed. In contrast, the separation form the orange fluorescent quercetin glycoside is unsatisfactory (**Figure 18**).

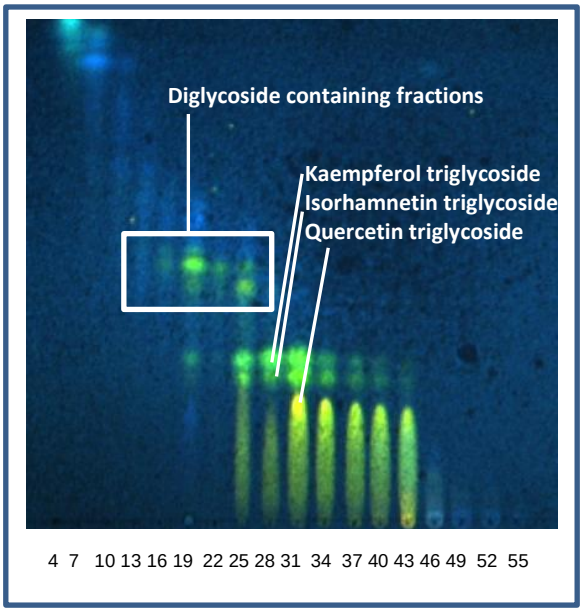

Figure 18: NP-TLC after CC of the triglycoside enriched fraction. Mobile phase: EtOAc:acetone:H_2O ~ 5:3:1; 6 developments; detection at 366 nm after derivatisation with Natursoffreagenz A. CC according to 2.2.6.1

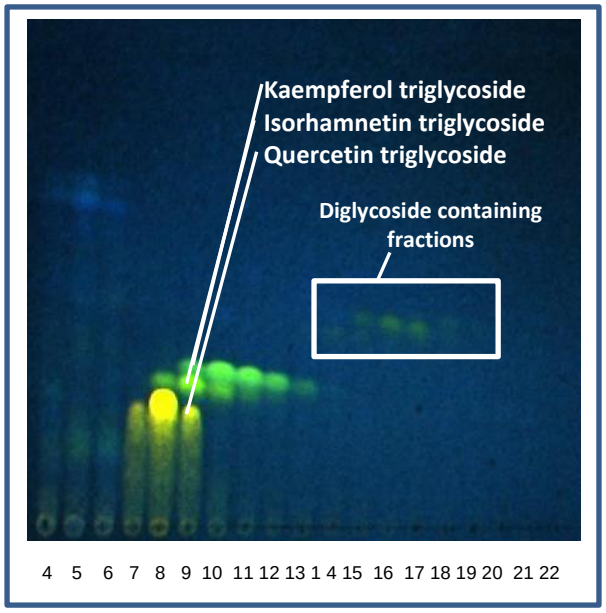

Figure 19: NP-TLC after CC of the triglycoside enriched fraction. Mobile phase: EtOAc:acetone:H_2O ~ 5:3:1; 6 developments; detection at 366 nm after derivatisation with Natursoffreagenz A. CC according to 2.2.6.2

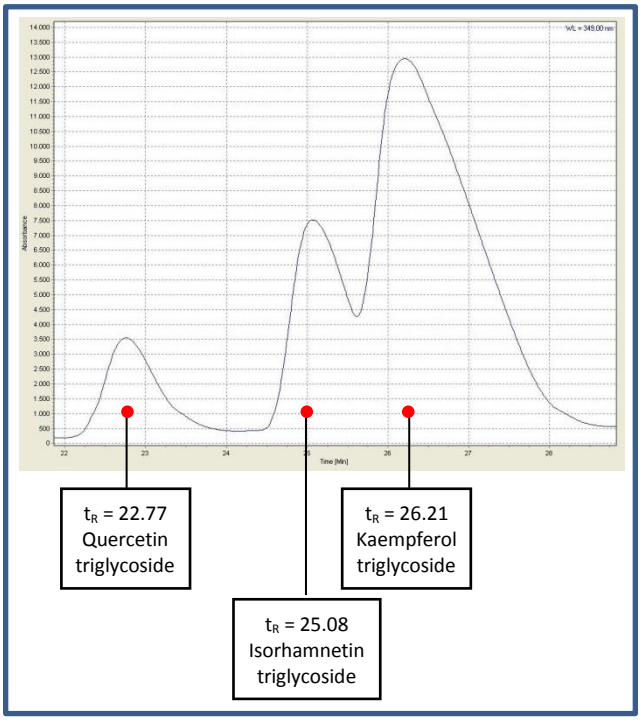

Figure 20: Semipreparative HPLC chromatogram of the triglycosides at 349 nm. CC according to 2.2.6.3

An additional reversed phase flash column chromatography was accomplished with an H_2O/2-propanol gradient. This step could remove the major part of quercetin triglycosides (fraction 8) from kaempferol- and isorhamnetin triglycosides (**Figure 19**).

The final purification step was again achieved by semipreparative HPLC (H_2O/2-propanol gradient), which yielded in the isolation of the three flavonol glycosides (**Figure 20**).

Overall, both isolation sequences results in chromatograms which do not show baseline separation of the compounds. Nevertheless, the methods are a relatively affordable and fast way to get the flavonoids in sufficient amounts for the following projects. In addition, the intermediate fractions which comprises two or more glycosides can be combined and added to the extract. Thereby, unnecessary loss of substance is avoided.

Finally the following eight flavonoid glycosides were isolated.

Isolated diglycosides:

- 3-O-(2-O-(β-D-Glucosyl-α-L-rhamnosyl)kaempferol (calculated yield for 3 g enriched extract: 170 mg, 5.7%)
- 3-O-(6-O-(α-L-Rhamnosyl)-β-D-glucosyl)kaempferol (calculated yield for 3 g enriched extract: 230 mg, 7.7%)
- 3-O-(6-O-(α-L-Rhamnosyl)-β-D-glucosyl)isorhamnetin
- 3-O-(6-O-(α-L-Rhamnosyl)-β-D-glucosyl)quercetin
- 3-O-(6-O-(α-L-rhamnosyl)-β-D-glucosyl)myricetin

Isolated triglycosides:

- 3-O-(2-O, 6-O-Bis(α-L-rhamnosyl)-β-D-glucosyl)kaempferol (calculated yield for 5 g enriched extract: 65 mg, 1.3%)
- 3-O-(2-O, 6-O-Bis(α-L-rhamnosyl)-β-D-glucosyl)isorhamnetin
- 3-O-(2-O, 6-O-Bis(α-L-rhamnosyl)-β-D-glucosyl)quercetin

The yields for the myricetin-, quercetin- and isorhamnetin glycosides are not presented, because the chromatographic separation was not focused on their isolation and thus, the calculated contents would not be informative.

The identification of the kaempferol glycosides was achieved by comparison with ^{1}H NMR literature values[52] (**Table 1-Table 8**) and the further down presented analysis by HPLC-MS (**Figure 21**) .

Table 1: ^{1}H NMR spectral data of 3-O-(6-O-(α-L-rhamnosyl)-β-D-glucosyl)myricetin (300 MHz, 294 K, *J* in Hz, in CD_3OD) compared to literature values[52]

Position	^{1}H	$^1H_{LIT}$
6	6.21 (1H, d, 2.0)	6.20 (1H, d, 2.0)
8	6.39 (1H, d, 2.0)	6.39 (1H, d, 2.0)
2′,6′	7.28 (2H, s)	7.29 (2H, s)
1′′	5.08 (1H, d, 7.7)	5.08 (1H, d, 7.6)
$6''_A$	3.80 (1H, d, 10.5)	3.80 (1H, d, 10.7)
1′′′	4.52 (1H, d, 1.3)	4.52 (1H, d, 1.2)
2′′′	3.62 (1H, dd, 1.5, 3.3)	3.62 (1H, dd, 1.2, 3.5)
3′′′	3.55 (1H, dd, 3.3, 9.3)	3.55 (1H, dd, 3.5, 9.4)
6′′′	1.12 (3H, d, 6.2)	1.12 (3H, d, 6.2)
Remaining sugar protons	3.51-3.23 (7H, m)	3.50-3.25 (7H, m)

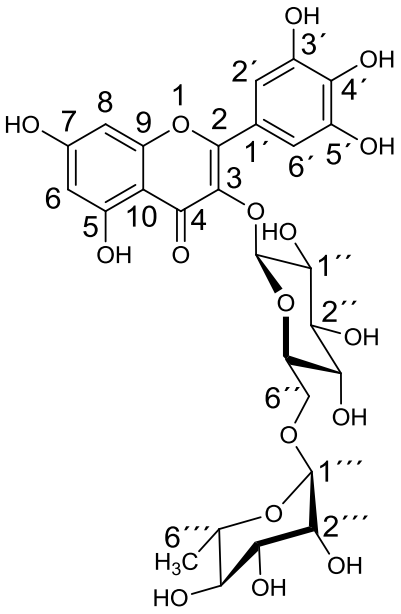

Table 2: ^{1}H NMR spectral data of 3-O-(6-O-(α-L-rhamnosyl)-β-D-glucosyl)quercetin (300 MHz, 295 K, *J* in Hz, in CD_3OD) compared to literature values[52]

Position	^{1}H	$^1H_{LIT}$
6	6.21 (1H, d, 2.1)	6.19 (1H, d, 2.1)
8	6.40 (1H, d, 2.1)	6.37 (1H, d, 2.1)
2′	7.66 (1H, d, 2.1)	7.67 (1H, d, 2.2)
5′	6.87 (1H, d, 8.4)	6.87 (1H, d, 8.4)
6′	7.63 (1H, dd, 2.2, 8.4)	7.63 (1H, dd, 2.2, 8.4)
1′′	5.10 (1H, d, 7.5)	5.09 (1H, d, 7.2)
$6''_A$	3.80 (1H, d, 10.9)	3.81 (1H, d, 10.0)
1′′′	4.51 (1H, s)	4.53 (1H, br s)
2′′′	3.62 (1H, dd, 1.4, 3.4)	3.65 (1H, m)
3′′′	3.53 (1H, dd, 3.6, 9.4)	3.55 (1H, dd, 3.1, 9.4)
6′′′	1.12 (3H, d, 6.2)	1.13 (3H, d, 6.1)
Remaining sugar protons	3.50-3.33 (7H, m)	3.82-3.25 (7H, m)

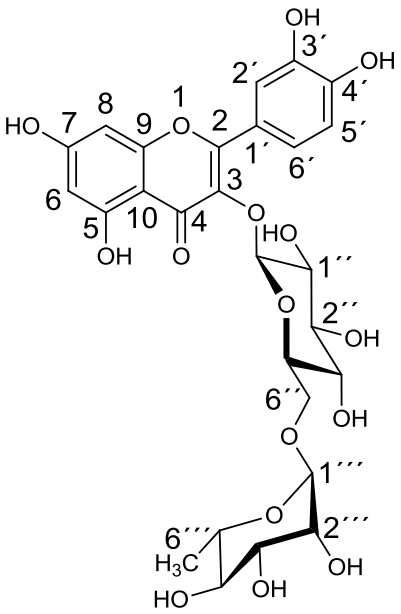

Table 3: ^{1}H NMR spectral data of 3-O-(6-O-(α-L-rhamnosyl)-β-D-glucosyl)isorhamnetin (300 MHz, 297 K, *J* in Hz, in CD_3OD) compared to literature values[52]

Position	^{1}H	$^{1}H_{LIT}$
6	6.20 (1H, d, 2.1)	6.19 (1H, d, 2.1)
8	6.40 (1H, d, 2.1)	6.37 (1H, d, 2.1)
2´	7.94 (1H, d, 2.0)	7.94 (1H, d, 2.1)
3´-O-CH_3	3.94 (3H, s)	3.95 (3H,s)
5´	6.91 (1H, d, 8.5)	6.91 (1H, d, 8.5)
6´	7.62 (1H, dd, 2.1, 8.4)	7.59 (1H, dd, 2.1, 8.5)
1´´	5.23 (1H, d, 7.4)	5.22 (1H, d, 7.6)
6´´$_A$	3.81 (1H, d, 10.2)	3.81 (1H, d, 10.6)
1´´´	4.52 (1H, d, 1.3)	4.54 (1H, d, n.r.)
2´´´	3.61 (1H, dd, 1.6, 3.3)	3.63 (1H, d, 3.4)
6´´´	1.09 (3H, d, 6.2)	1.11 (3H, d, 7.6)
Remaining sugar protons	3.51-3.20 (7H, m)	3.51-3.24 (7H, m)

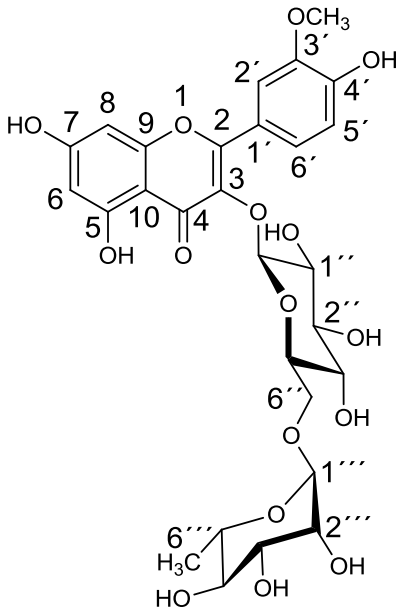

Table 4: ^{1}H NMR spectral data of 3-O-(6-O-(α-L-rhamnosyl)-β-D-glucosyl) kaempferol (300 MHz, 294 K, *J* in Hz, in CD_3OD) compared to literature values;[52] n.r.: not reported

Position	^{1}H	$^{1}H_{LIT}$
6	6.21 (1H, d, 2.1)	6.19 (1H, d, 1.9)
8	6.40 (1H, d, 2.1)	6.38 (1H, d, 1.9)
2´,6´	8.06 (2H, d, 8.9)	8.06 (2H, d, 8.9)
3´,5´	6.89 (2H, d, 8.9)	6.88 (2H, d, 8.9)
1´´	5.13 (1H, d, 7.5)	5.12 (1H, d, 7.6)
6´´$_A$	3.80 (1H, dd, 1.9, 7.6)	3.81 (1H, d, 10.6)
1´´´	4.51 (1H, d, 1.4)	4.52 (1H, d, n.r.)
2´´´	3.63 (1H, dd, 1.6, 3.3)	3.64 (1H, m)
3´´´	3.52 (1H, dd, 3.4, 9.5)	3.53 (1H, dd, 3.3, 9.4)
6´´´	1.12 (3H, d, 6.2)	1.13 (3H, d, 6.2)
Remaining sugar protons	3.48-3.23 (7H, m)	3.48-3.25 (7H, m)

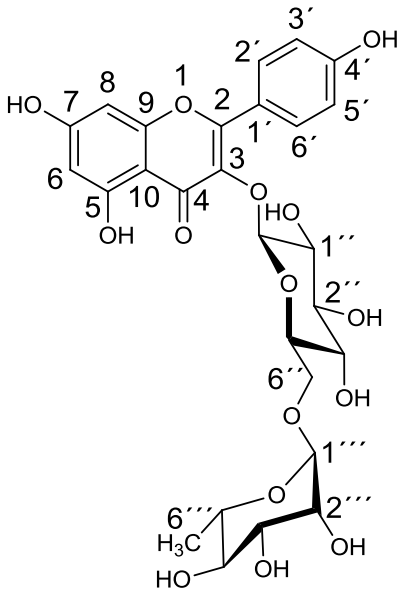

Table 5: ^{1}H NMR spectral data of 3-O-(2-O-(β-D-glucosyl-α-L-rhamnosyl)kaempferol (300 MHz, 297 K, *J* in Hz, in CD_3OD) compared to literature values[52]

Position	^{1}H	$^{1}H_{LIT}$
6	6.20 (1H, d, 1.9)	6.20 (1H, d, 1.9)
8	6.37 (1H, d, 2.1)	6.37 (1H, d, 1.9)
2´,6´	7.77 (2H, d, 8.8)	7.76 (2H, d, 8.9)
3´,5´	6.94 (2H, d, 8.8)	6.94 (2H, d, 8.9)
1´´	5.72 (1H, d, 1.4)	5.73 (1H, d, 1.1)
2´´	4.28 (1H, dd, 1.5, 3.5)	4.29 (1H, dd, 1.3, 3.5)
3´´	3.80 (1H, dd, 3.5, 9.4)	3.81 (1H, dd, 3.5, 9.3)
6´´	0.93 (3H, d, 5.9)	0.94 (3H, d, 5.9)
1´´´	4.41 (1H, d, 7.7)	4.42 (1H, d, 7.7)
6´´´	3.73-3.65 (2H, m)	3.70 (2H,m)
Remaining sugar protons	3.44-3.17 (6H, m)	3.43-3.19 (6H, m)

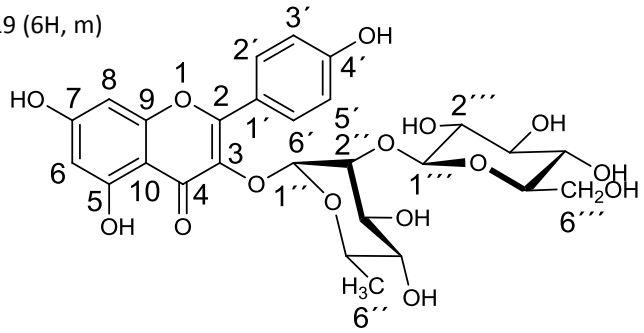

Table 6: ^{1}H NMR spectral data of 3-O-(2-O, 6-O-bis(α-L-rhamnosyl)-β-D-glucosyl)quercetin (300 MHz, 297 K, *J* in Hz, in CD_3OD) compared to literature values;[52] n.r.: not reported

Position	^{1}H	$^{1}H_{LIT}$
6	6.18 (1H, d, br s)	6.18 (1H, d, 2.0)
8	6.36 (1H, br s)	6.37 (1H, d, 2.0)
2´	7.59 (1H, br s)	7.59 (1H, br s)
5´	6.87 (1H, d, 8.4)	6.87 (1H, d, 8.8)
6´	7.62 (1H, d, 1.9)	7.61 (1H, dd, 2.1, n.r)
1´´	5.59 (1H, d, 7.6)	5.59 (1H, d, 7.6)
1´´´	5.22 (1H, br s)	5.22 (1H, d, 1.3)
2´´´	4.00 (1H, dd, 1.7, 2.8)	4.01 (1H, dd, 1.5, 3.3)
5´´´	4.08 (1H, dd, 6.2, 9.6)	4.09 (1H, dd, 6.2, 9.6)
6´´´	1.00 (3H, d, 6.2)	1.00 (3H, d, 6.2)
1´´´´	4.50 (1H, br s)	4.51 (1H, d,1.5)
6´´´´	1.07 (3H, d, 6.2)	1.09 (3H, d, 6.2)
Remaining sugar protons	3.90-3.18 (12H, m)	4.07-3.21 (12H, m)

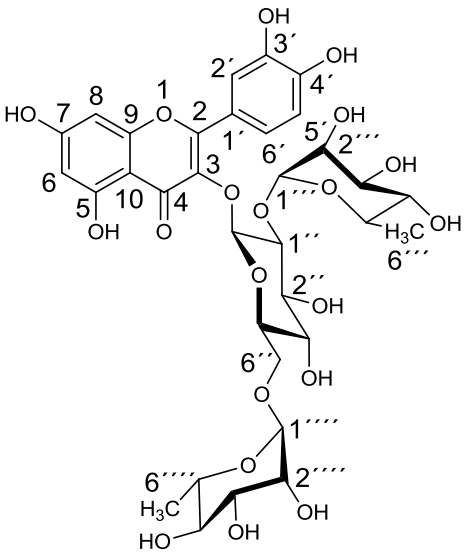

Table 7: ^{1}H NMR spectral data of 3-O-(2-O, 6-O-bis(α-L-rhamnosyl)-β-D-glucosyl)isorhamnetin (300 MHz, 297 K, *J* in Hz, in CD_3OD) compared to literature values;[52] n.r.: not reported

Position	^{1}H	$^{1}H_{LIT}$
6	6.18 (1H, d, 2.1)	6.18 (1H, d, 2.0)
8	6.38 (1H, d, 2.1)	6.39 (1H, d, 2.0)
2´	7.94 (1H, d,2.0)	7.94 (1H, d,1.9)
3´-O-CH_3	3.97 (3H,s)	3.97 (3H,s)
5´	6.91 (1H, d, 8.5)	6.92 (1H, d, 8.5)
6´	7.57 (1H, dd, 2.0, 8.5)	7.57 (1H, dd,1.9, 8.5)
1´´	5.73 (1H, d, 7.4)	5.74 (1H, d, 7.3)
6´´$_A$	3.81 (1H, d, 10.3)	3.81 (1H, d, 10.3)
1´´´	5.19 (1H, d, 1.2)	5.19 (1H, d, n.r.)
2´´´	4.00 (1H, dd, 1.6, 3.4)	4.00 (1H, dd, n.r)
3´´´	3.77 (1H, dd, 3.3, 9.5)	3.73 (1H, dd, 3.4, 9.6)
5´´´	4.06 (1H, dd, 6.3, 9.7)	4.04 (1H, dd, 6.3, 9.7)
6´´´	0.91 (3H, d, 6.2)	0.92 (3H, d, 6.2)
1´´´´	4.53 (1H, d, 1.4)	4.54 (1H, d, n.r.)
6´´´	1.06 (3H, d, 6.2)	1.07 (3H, d, 6.2)
Remaining sugar protons	3.89-3.17 (10H, m)	4.07-3.19 (10H, m)

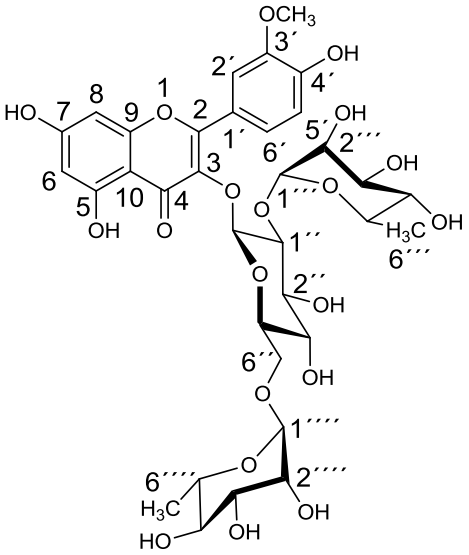

Table 8: ^{1}H NMR spectral data of 3-O-(2-O, 6-O-bis(α-L-rhamnosyl)-β-D-glucosyl)kaempferol (300 MHz, 297 K, *J* in Hz, in CD_3OD) compared to literature values;[52] n.r.: not reported

Position	^{1}H	$^{1}H_{LIT}$
6	6.18 (1H, d, 2.1)	6.20 (1H, d, 2.0)
8	6.38 (1H, d, 2.1)	6.40 (1H, d, 1.9)
2´, 6´	8.01 (2H, d, 8.9)	8.05 (2H, d, 8.9)
3´, 5´	6.89 (2H, d, 8.9)	6.92 (2H, d, 8.9)
1´´	5.60 (1H, d, 7.3)	5.63 (1H, d, 7.2)
1´´´	5.22 (1H, d, 1.2.)	5.25 (1H, d, n.r.)
2´´´	4.00 (1H, dd, 1.6, 3.3j)	4.02 (1H, m)
5´´´	4.06 (1H, dd, 6.2, 9.6)	4.08 (1H, dd, 6.3, 9.6)
6´´´	0.97 (3H, d, 6.2)	0.99 (3H, d, 6.2)
1´´´´	4.49 (1H, d, 1.4)	4.52 (1H, d, n.r.)
6´´´´	1.07 (3H, d, 6.2)	1.08 (3H, d, 6.2)
Remaining sugar protons	3.88-3.19 (12H, m)	3.85-3.22 (12H, m)

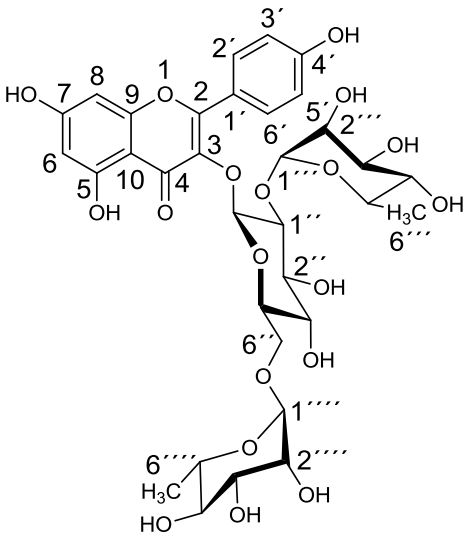

Extract Quantification

The isolated kaempferol glycosides and an additional acylated kaempferol glycoside, which was a kind gift from Dr. Willmar Schwabe GmbH und Co. KG., were used in the next step for their quantification in the standardized extract EGb 761®. The following list contains these four compounds and their used abbreviations:

- 3-O-(2-O, 6-O-Bis(*α*-L-rhamnosyl)-*β*-D-glucosyl)kaempferol **(Triglycoside)**
- 3-O-(6-O-(*α*-L-Rhamnosyl)-*β*-D-glucosyl)kaempferol **(Rutinoside)**
- 3-O-(2-O-(*β*-D-Glucosyl-*α*-L-rhamnosyl)kaempferol **(Biloside)**
- 3-O-(2-O-(6-O-(*p*-Hydroxy-trans-cinnamoyl)-*β*-D-glucosyl)-*α*-L-rhamnosyl)kaempferol **(Acylated Biloside)**

At first, the questions arises whether these four kaempferol glycosides are those with the highest content in EGb 761®. The extract was therefore analyzed by HPLC followed and high resolution mass spectrometry (**Figure 21**). The isolated kaempferol glycosides can clearly be assigned in the chromatogram of EGb 761® by comparison of the retention times and MS data with the pure reference compounds. Further on several other flavonoid glycosides and two ginkgolides can be assigned based on HR *m*/*z* values, which is consequently not an absolute evidence. The retention time of the two kaempferol monoglycosides cannot be associated to a certain peak in the chromatogram, because of similar molecular masses of the following substances:

- Kaempferol-3-O-*β*-D-glucoside (448), luteolin-3´-O-*β*-D-glucoside, quercetin-3-O-*α*-L rhamnoside
- Kaempferol-3-O- *α*-L-rhamnoside (432), apigenin-7-O-*β*-D-glucoside

All conceivable signals for the monoglycosides have multiple smaller integrals compared to the four isolated compounds. Consequently, these substances can be regarded as the predominat kaempferol glycosides in EGb 761®.

The chosen chromatographic method gives a good separation of the ingredients, which is sufficient for the quantification, although for instance the acylated biloside shows a little shoulder in the chromatogram (**Figure 22**)

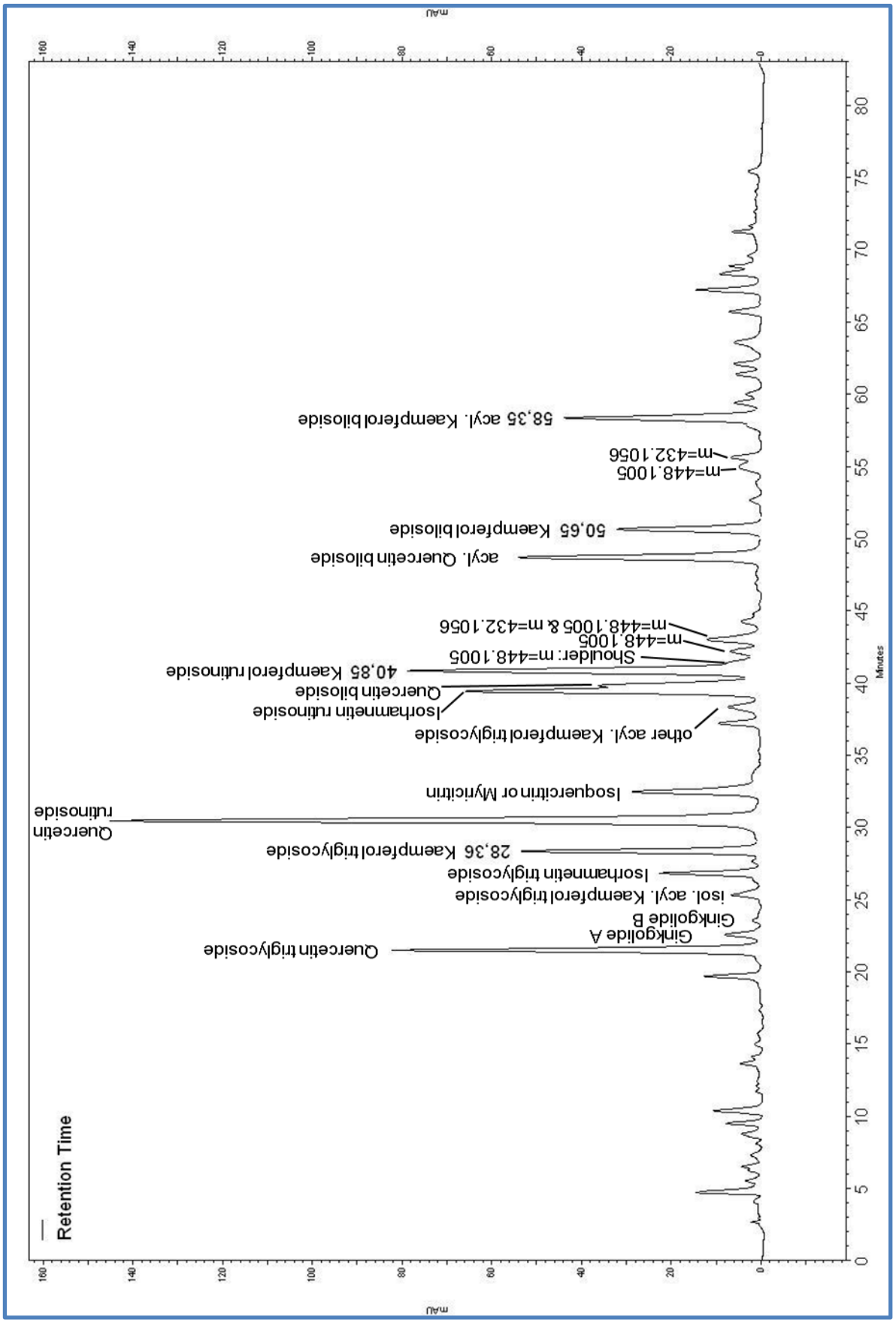

Figure 21: Combination of HPLC (350 nm) and high resolution mass spectrometry (ESI) analysis of EGb 761® and tentative assignment of other compounds based on MS data. CC according to 2.2.7.2, but with formic acid instead of trifluoracetic acid

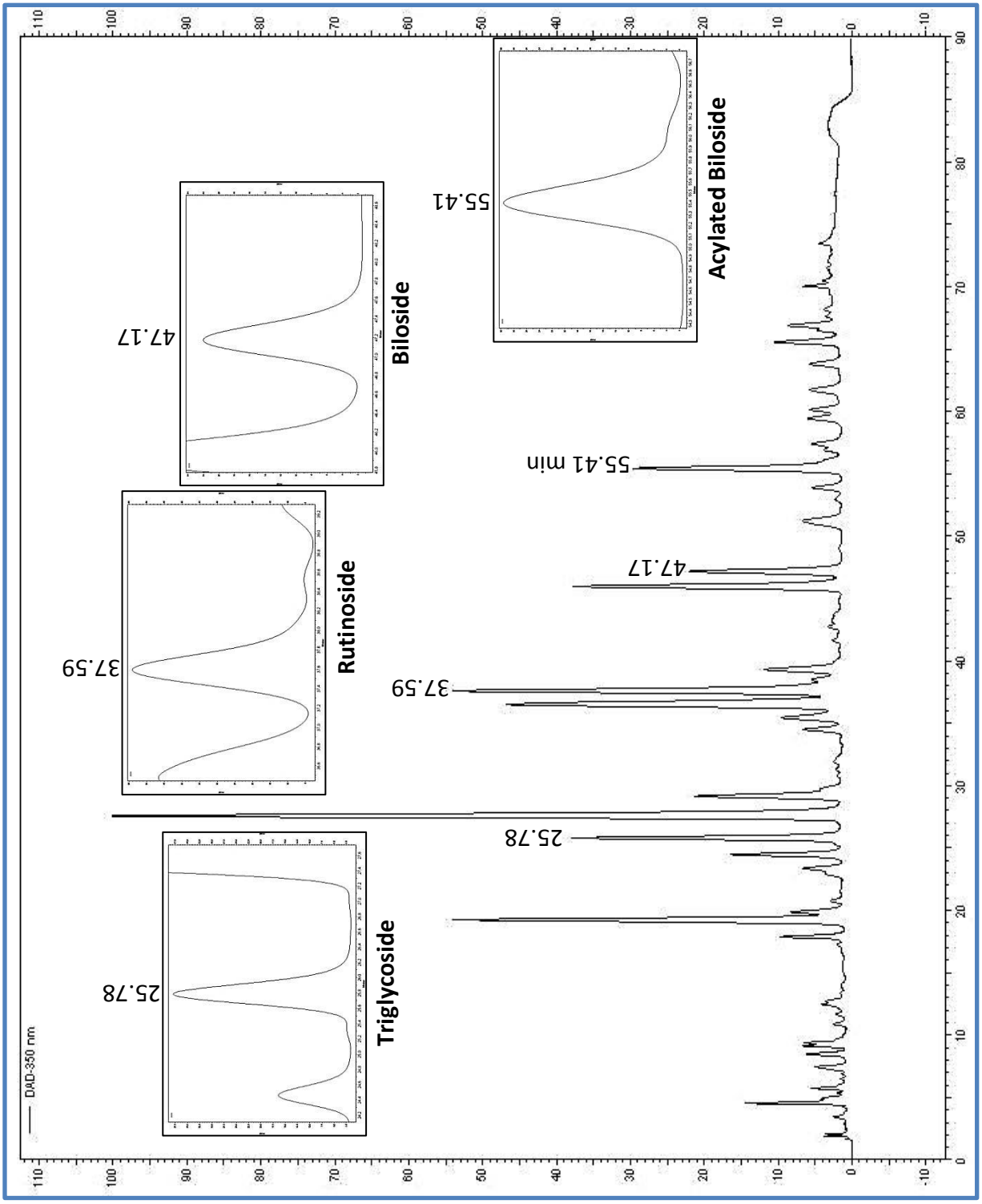

Figure 22: HPLC of EGb 761® at 350 nm. CC according to 2.2.7.2

In the following step the calibration curves for the four kaempferol glycosides were determinated (R^2 = 0.9965-0.9993) and particular contents in EGb 761® were calculated as values between 1.58 and 2.17 % w/w (**Table 9**)

Table 9: Content of four kaempferol glycosides in EGb 761®; the chromatographic purity of the references was considered for the calculation

	Chromatographic purity of reference	Content in EGb 761® [% w/w]	Interday precision (n = 6)	Intraday precision (n = 6)
Triglycoside	98.1%	**1.58 ± 0.02%**	3.24%	1.84%
Rutinoside	98.6%	**2.17 ± 0.01%**	2.09%	1.10%
Biloside	100.0%	**0.89 ± 0.01%**	2.12%	1.84%
Acyl. Biloside	95.4%	**1.59 ± 0.01%**	1.02%	1.26%

Further on, to exclude any loss during the indispensable filtration step before the HPLC analysis, the integrals of the flavonoid signals were calculated for different extract concentrations. It could be shown, that the signal areas are linear to the used extract concentrations (**Figure 23**) which is a proof for the good solubility of the substances in the prepared HPLC samples.

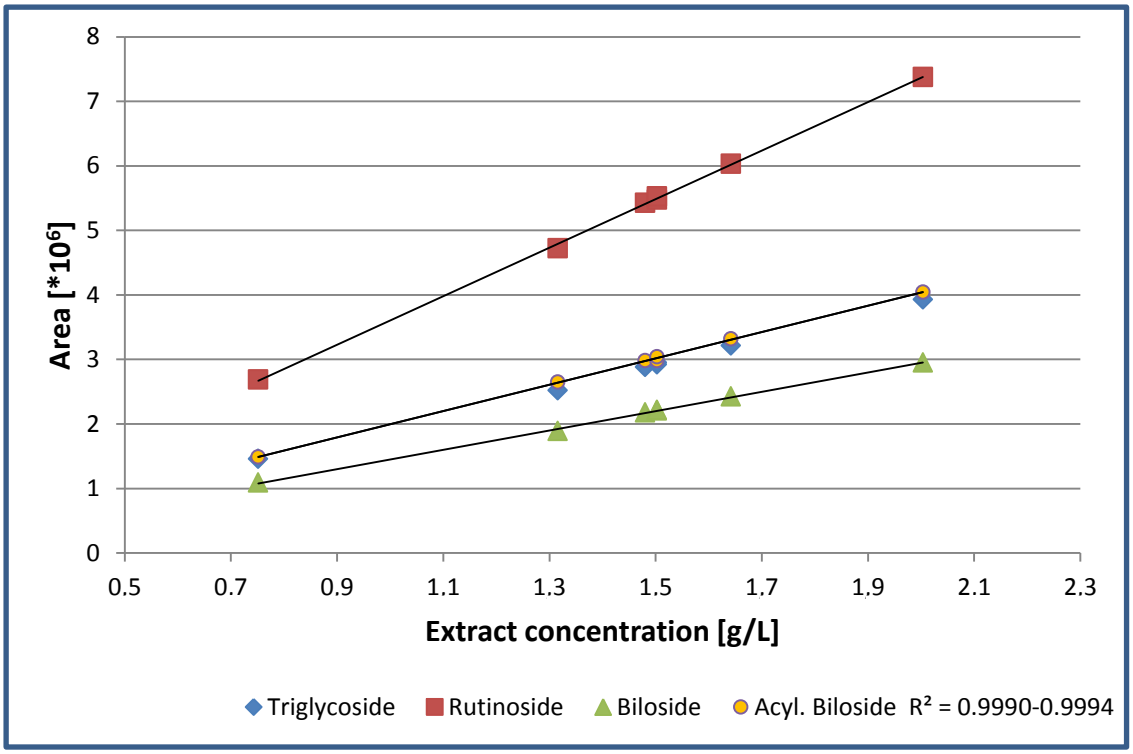

Figure 23: Linearity of the calibration curves of the four kaempferol glycosides using different extract concentrations. CC according to 2.2.7.2

3 Synthesis of five expected Kaempferol Metabolites

3.1 Introduction: Synthetic Approach towards Flavonoid Glucuronides

The flavonol kaempferol can be conjugated *in vivo* within phase-II-metabolism with a sulfate moiety or a glucuronic acid (for more details see page 84). The substitution takes place at the hydroxyl functions of the molecule. Although the reaction is catalyzed *in vivo* by an enzyme, it should be noted that not all four hydroxyl groups have the same reactivity. For instance, regarding published sulfation or methylation reactions, the proton with the highest acidity and consequently the highest reactivity seems to be at 7-OH.[53,54] This could be partly based on the fact that the corresponding alkoxide is resonance stablized by the 4-pyrone carbonyl group. The proton at 5-OH has, as expected, the lowest reactivity, due to the hydrogen bond to the 4-pyrone carbonyl. Based on this information, some possible metabolites of kaempferol should be synthesized in the laboratory to confirm their presence or absence in rat plasma in the following *in vivo* tests.

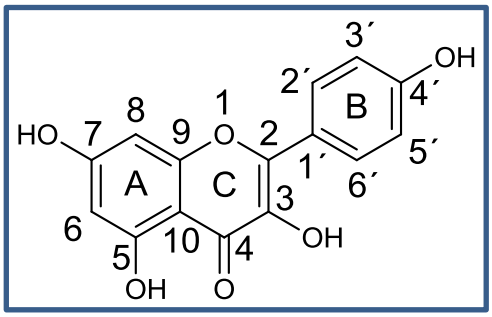

Figure 24: The flavonol kaempferol

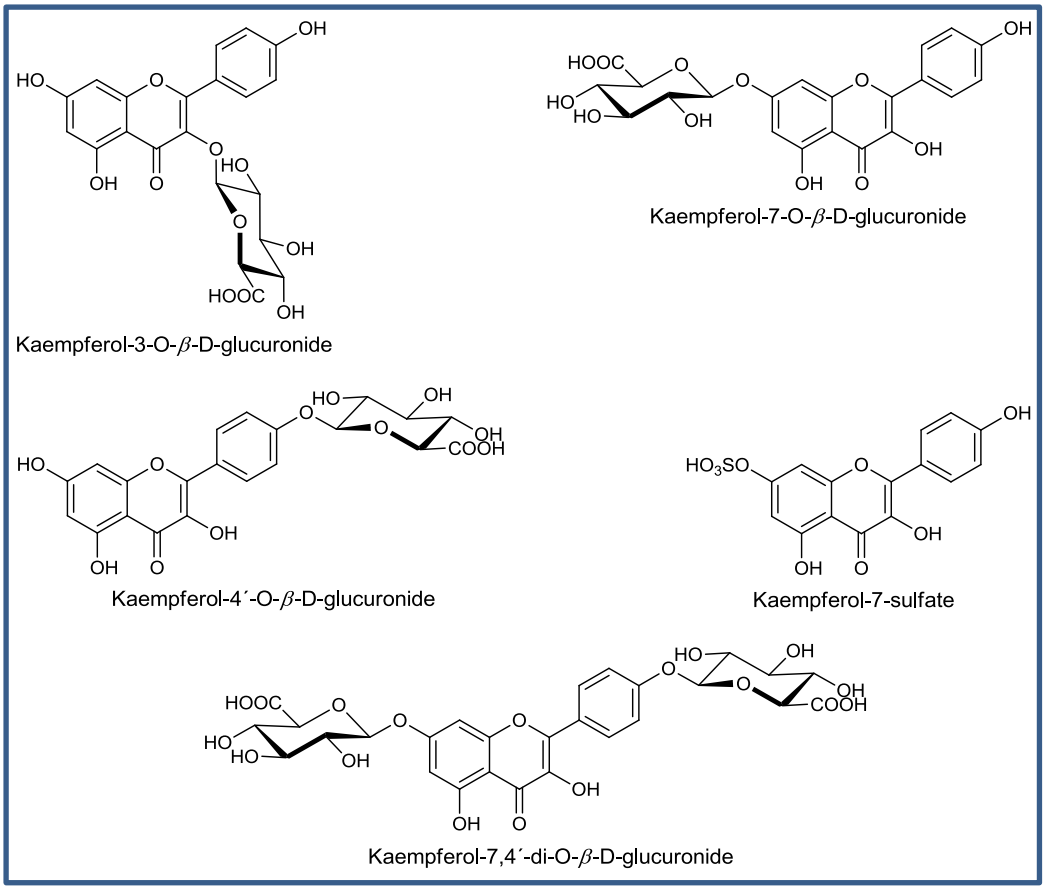

Figure 25: Possible phase-II-metabolites of kaempferol in rat plasma

In general the following reaction conditions, which are briefly summarized here, are conceivable for the formation of the glycosidic bond. The literature suggest different methods for the synthesis of flavonoid glycosides:

For the generation of glucuronides:

- Ag_2O, $CaSO_4$, pyridine (quinoline[55]), 1-bromo-2,3,4-tri-O-acetyl-*α*-D-glucuronic acid methyl ester, RT, 2 h, 45% yield[56]
- BF_3*Et_2O, 3 Å molecular sieve, DCM, 2,3,4-tri-O-acetyl-*α*-D-glucuronic acid methyl ester trichloroacetimidate, -15 °C, over night, 58% yield[57]
- K_2CO_3, DMF, 1-bromo-2,3,4,6-tetra-O-acetyl-*α*-D-glucopyranoside, RT, 12 h, 54% yield[54,58]

For the generation of glucosides:

- Saturated aqueous $KHCO_3$, TDA (tris(3,6-dioxaheptyl)amine, phase transfer catalyst), DCM, 1-bromo-2,3,4,6-tetra-O-acetyl-*α*-D-glucopyranoside, 40 °C, 48 h, 30% yield[59]
- Aqueous K_2CO_3, TBAB (tetra-*n*-butylammonium bromide, phase transfer catalyst), $CHCl_3$, 1-bromo-3,6-Di-O-acetyl-2,4-di-O-benzyl-*α*-D-glucopyranoside, 50 °C, 8 h, 54% yield[60]

Usually, also the synthesis of a kaempferol glucoside followed by a TEMPO (2,2,6,6-tetramethylpiperidinyloxyl) oxidation, which is known to be selective for primary alcohols, would yield in the formation of the desired kaempferol glucuronides. Nevertheless, with regard to the additional synthetic step, direct glucuronidation is favoured. Furthermore, there is no evidence why the shown reaction condition for the generation of glucosides could not be accomplished with the glucuronic acid, instead.

The bromo derivate of the glucuronic acid is about 18 fold cheaper compared to the trichloroacetimidate.[61] Further on, the published yields do not differ in a large scale from each other and consequently a modified Koenigs-Knorr reaction seemed to be the right choice to start with.

3.2 Material and Methods

3.2.1 Consumable Material

3.2.1.1 Solvents

- Acetone, EMSURE®, Merck KGaA, Darmstadt, Germany
- Methanol, ≥ 99% (GC), Merck KGaA, Darmstadt, Germany
- Tetrahydrofuran, dried, Merck KGaA, Darmstadt, Germany
- H_2O, deionised, further purified by membraPure, Astacus, MembraPure GmbH, Berlin, Germany
- Pyridine, ≥ 99.5%, Merck KGaA, Darmstadt, Germany
- *N,N*-Dimethylformamide (H_2O ≤ 0.01%), ≥ 99.8% (GC), Sigma-Aldrich, Steinheim, Germany
- Acetonitrile, LiChrosolv®, ≥ 99.9%, Merck KGaA, Darmstadt, Germany
- Ethanol, ≥ 99.9%, J.T.Baker®, Avantor Performance Materials, Center Valley, PA, USA

3.2.1.2 TLC

- TLC Silica gel 60 RP-18 F_{254S}, Merck KGaA, 64271 Darmstadt, Germany
- TLC chambers, Camag, Muttenz, Switzerland
- UV-viewing cabinet, Camag, Muttenz, Switzerland

3.2.1.3 NMR

- Acetone-d_6, 99.8%, Deutero GmbH, 56288 Kastellaun, Germany
- Bruker Avance 300, Bruker Corporation, Billerica, USA
- Chloroform–d, 99.8%, Sigma-Aldrich, Steinheim, Germany
- Dimethylsulfoxid-d_6, 99.8%, Deutero GmbH, Kastellaun, Germany
- Methanol-d_4, 99.8%, Deutero GmbH, 56288 Kastellaun, Germany
- NMR tubes, 507-HP, 203 mm, Norell, Landisville, USA

3.2.1.4 Chemicals

- Amano Lipase PS, from *Burkholderia cepacia*, ≥ 30000 U/g, Sigma-Aldrich, Steinheim, Germany
- Benzyl bromide, ≥ 98%(GC), Merck Schuchardt OHG, Hohenbrunn, Germany
- Calcium sulfate, -325 mesh, 99%, Sigma-Aldrich, Steinheim, Germany
- Cyclohexene, ≥ 99% (GC), Merck Schuchardt OHG, Hohenbrunn, Germany
- Dowex 50 W X 4, H^+-form, 20-50 mesh, Fluka, Neu-Ulm, Germany
- Kaempferol, ≥ 90**%,** Lyon, France
- *N,N'*-Dicyclohexylcarbodiimide, 99%, Alfa Aesar, Heysham, England
- Palladium hydroxide, 20 wt.% Pd (Dry Basis) on carbon, moist, Sigma-Aldrich, Steinheim, Germany
- Potassium acetate extra pure, Merck KGaA, Darmstadt, Germany

- Potassium carbonate, Honeywell Riedel-de Haën, Seelze, Germany
- Silver(I) oxide, 99+% (metal basis) Powder, Alfa Aesar GmbH & Co KG, Karlsruhe, Germany
- Sodium hydrogen carbonate, Merck KGaA, Darmstadt, Germany
- Tetrabutylammonium hydrogen sulfate, pure, AppliChem, Darmstadt, Germany
- Trifluoroacetic acid, 99%, Sigma-Aldrich, Steinheim, Germany
- Celite® 560, particle size ≤ 148.5 µm, 56%, Sigma-Aldrich, Steinheim, Germany
- Acetic anhydride, ≥ 98.5%, Merck KGaA, Darmstadt, Germany
- Potassium chloride, ≥ 99.5%, Merck KGaA, Darmstadt, Germany
- Sodium carbonate, anhydrous, ≥ 99.5%, Merck KGaA, Darmstadt, Germany
- Acetic acid, ≥ 99.8%, Merck KGaA, Darmstadt, Germany
- 1-Bromo-2,3,4-tri-O-acetyl-α-D-glucuronic acid methyl ester, > 95%, ReseaChem GmbH, Burgdorf, Switzerland

3.2.2 Columns

- Flash-RP: SuperVarioPrep® D40, 46 x 186 mm, filled with stationary phase RP18 25-40 µm, 90 g, Merck KGaA, 64271 Darmstadt, Germany
- Semipreparative HPLC: Knauer, Vertex, 16 x 250 mm, filled with stationary phase Eurospher-100 C18-7 µm, Dr. Ing. Herbert Knauer GmbH, Berlin, Germany

3.2.3 Instruments

- 1D NMR: Avance 300, Bruker, Billerica, USA
- 1D NMR: Avance 400, Bruker, Billerica, USA
- 2D NMR: Avance III 600, Bruker, Billerica, USA
- Flash-RP: SuperVarioPrep® D40, 46 x 186 mm, filled with stationary phase RP18 25-40 µm, 90 g, Merck KGaA, 64271 Darmstadt, Germany
- Mass spectrometer:
    - TOF 6540 UHD, Agilent, Santa Clara, USA
    - Electrospray ionization (ESI)
- Semipreparative HPLC: Knauer, Vertex, 16 x 250 mm, filled with stationary phase Eurospher-100 C18-7 µm, 14163 Berlin, Germany
- UV-Visible Spectrophotometer, 50 Scan, Varian, Agilent, Santa Clara, USA

3.3 Chemistry and Analytical Data

3.3.1 Synthesis of Kaempferol-4´-O-β-D-glucuronide

3.3.1.1 Synthesis of 3,7-Di-O-benzyl-kaempferol

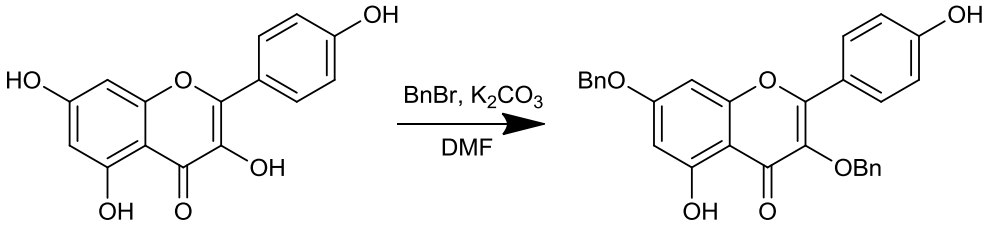

Kaempferol (350.0 mg, 1.22 mmol) and dry potassium carbonate (997.0 mg, 7.21 mmol, 5.9 eq) were suspended in 12.2 mL DMF and 291 µL benzyl bromide (2.45 mmol, 2.0 eq) were added. After stirring in the dark for 2 h and under nitrogen atmosphere the reaction mixture was filtrated and the solvent was removed under nitrogen stream. The crude product was purified by flash column chromatography using a H_2O/acetonitrile gradient.[62,58]

Chromatographic parameter:

Instrument:	Flash chromatography
Column:	Merck, SuperVarioPrep® D40, 46 x 186 mm
Stationary phase:	Merck, RP18 25-40 µm, 90 g, 40 x 115 mm
Mobile phase:	A: H_2O, B: acetonitrile
Application:	Suspension in 80% aqueous acetonitrile
Fractionation:	33 min
Gradient:	0 min: 80% acetonitrile
	15 min: 95% acetonitrile
	25-33 min: 100% MeOH
Flow:	45 mL/min
Region of Retention:	6–15 min, 270–675 mL
File:	120125-1016-1

→ 50 fractions each 30 mL

Table 10: ^{1}H NMR spectral data of 3,7-di-O-benzyl-kaempferol (300 MHz, 295 K, *J* in Hz, in $CDCl_3$)

Position	^{1}H
6	6.45 (1H, d, 2.2)
8	6.51 (1H, d, 2.2)
2´,6´	7.94 (2H, d, 8.8)
3´,5´	6.89 (2H, d, 8.8)
O-CH_2	5.13 (2H, s)
O-CH_2	5.06(2H, s)
Ph-protons	7.44-7.27 (10H, m)
OH	12.71 (1H, s)

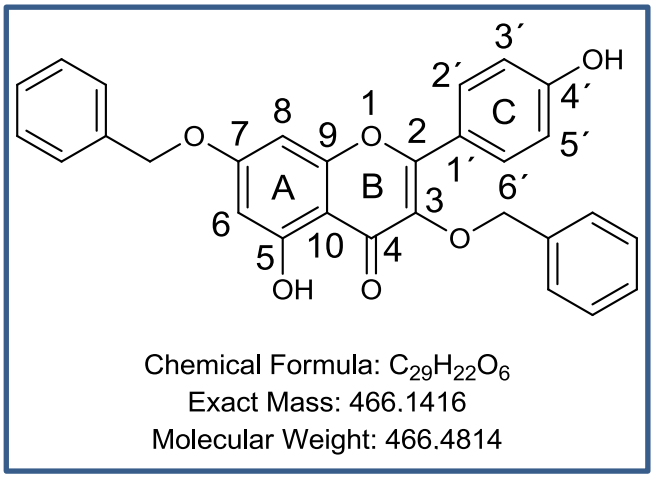

Figure 26: Structure of 3,7-di-O-benzyl-kaempferol

Table 11:Data of 3,7-di-O-benzyl-kaempferol

State of aggregation	Yellow solid
Amount [mg]	200
Yield [%]	35
m/z $[M+H]^+$	467.1492
Calc *m/z* $[M+H]^+$	467.1489

3.3.1.2 Synthesis of 3,7-Di-O-benzyl-kaempferol-4'-O-(2", 3", 4"-tri-O-acetyl)-β-D-glucuronic acid methyl ester

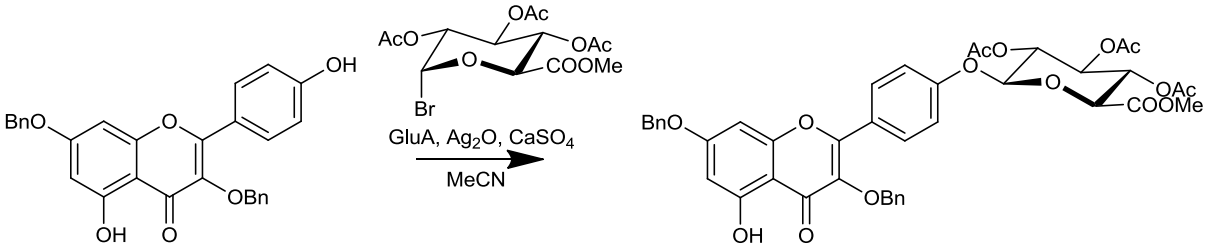

3,7-Di-O-benzyl-kaempferol (200.0 mg, 429.2 µmol), calcium sulfate (470.0 mg) and silver-(I)oxide (248.6 mg, 1.07 mmol, 2.5 eq) were suspended in 5.6 mL acetonitrile at 0 °C. Afterwards, 1-bromo-2,3,4-tri-O-acetyl-α-D-glucuronic acid methyl ester (210.0 mg, 536.5 µmol, 1.25 eq) and 925 µL pyridine were added. After 15 minutes, the ice bath was removed. The reaction mixture was stirred at room temperature for 3.5 h and then filtered. The crude product was purified within two steps by flash column chromatography followed by semipreparative HPLC using a H_2O/acetonitrile-gradient each time.

1. Chromatographic parameter:

Instrument:	Flash chromatography
Column:	Merck, EasyVarioPrep®, 30 x 142 mm, self packed
Stationary phase:	Merck, LiChroprep® RP-18, 25-40 µm, ~35 g, 25 x 110 mm
	+ 5 g precolumn
Mobile phase:	A: H_2O, B: acetonitrile
Application:	527 mg crude product + 700 mg RP18
Fractionation:	25 min
Gradient:	0 min: 85% acetonitrile
	20 min: 95% acetonitrile
	20-25 min: 100% acetonitrile
Flow:	25 mL/min
File:	120306-0924-1
Region of Retention:	4-6.5 min, 100-160 mL

→ 31 fractions each 20 mL

2. Chromatographic parameter:

Instrument:	Semipreparative HPLC
Column:	Knauer, Vertex, 16 x 250 mm
Stationary phase:	Eurospher-100 C18-7 µm
Mobile phase:	A: H_2O, B: acetonitrile
Application:	Liquid injection in 95% aqueous acetonitrile
Fractionation:	12 min
Gradient:	0 min: 85% acetonitrile
	10 min: 95% acetonitrile
	10-11 min: 95% acetonitrile
	12 min: 85% acetonitrile
Flow:	10 mL/min
Retention time (t_R):	7.3 min
λ_{max} [nm] at t_R:	221, 266, 345
File:	2012-03/158-160

Table 12: ^{1}H NMR spectral data of 3,7-di-O-benzyl-kaempferol-4´-O-(2‘‘,3‘‘,4‘‘-tri-O-acetyl)-β-D-glucuronic acid methyl ester (300 MHz, 295 K, *J* in Hz, in DMSO-d_6)

Position	^{1}H
6	6.47 (1H, d, 2.0)
8	6.82 (1H, d, 1.9)
2´,6´	7.97 (2H, d, 9.0)
3´,5´	7.13 (2H, d, 9.0)
1´´	5.79 (1H, d, 7.9)
Sugar proton	5.48 (1H, t, 9.0)
Sugar protons	5.04-5.18 (2H, m)
Sugar proton	4.72 (1H, t, 9.9)
O-CH_3	3.62 (3H, s)
CO-CH_3	2.00 (3H, s)
CO-CH_3	2.01 (3H, s)
CO-CH_3	1.99 (3H, s)
O-CH_2	5.21 (2H, s)
O-CH_2	5.03 (2H, s)
Ph-protons	7.48-7.30 (10H, m)

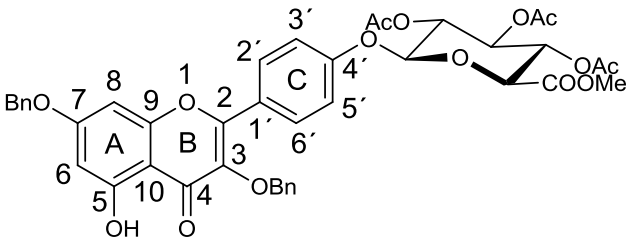

Chemical Formula: $C_{42}H_{38}O_{15}$
Exact Mass: 782.2211
Molecular Weight: 782.7421

Figure 27: Structure of 3,7-di-O-benzyl-kaempferol-4´-O-(2‘‘,3‘‘,4‘‘-tri-O-acetyl)-β-D-glucuronic acid methyl ester

Table 13: Data of 3,7-di-O-benzyl-kaempferol-4´-O-(2‘‘,3‘‘,4‘‘-tri-O-acetyl)-β-D-glucuronic acid methyl ester

State of aggregation	Pale yellow solid
Amount [mg]	77
Yield [%]	18
m/z $[M+H]^+$	783.2287
Calc *m/z* $[M+H]^+$	783.2283

3.3.1.3 Synthesis of Kaempferol-4'-O-(2", 3", 4"-tri-O-acetyl)-β-D-glucuronic acid methyl ester

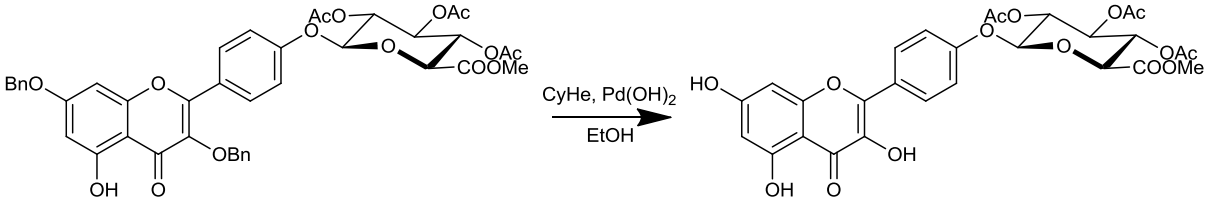

3,7-Di-O-benzyl-kaempferol-4´-O-(2",3",4"-tri-O-acetyl)-β-D-glucuronic acid methyl ester (53.6 mg, 68.5 µmol) was suspended in 8 mL ethanol and 2 mL cyclohexene (CyHe). Afterwards, $Pd(OH)_2$ on charcoal (12.0 mg) was added. The mixture was stirred under nitrogen atmosphere and reflux for 45 min.[57] After cooling the suspension was filtrated and the solvent was evaporated under nitrogen stream. The product was used without any further purification in the next step.

Table 14: ^{1}H NMR spectral data of kaempferol-4´-O-(2",3",4"-tri-O-acetyl)-β-D-glucuronic acid methyl ester, (300 MHz, 295 K, *J* in Hz, in acetone-d_6)

Position	^{1}H
6	6.31 (1H, d, 2.0)
8	6.61 (1H, d, 2.1)
2´,6´	8.28 (2H, d, 9.1)
3´,5´	7.38 (2H, d, 9.0)
1´´	6.06 (1H, d, 3.6)
Sugar proton	5.73 (1H, t, 9.8)
Sugar proton	5.26 (1H, t, 9.7)
Sugar proton	5.18 (1H, dd, 3.6, 10.1)
Sugar proton	4.48 (1H, t, 10.0)
O-CH_3	3.68 (3H, s)
CO-CH_3	2.05 (3H, s)
CO-CH_3	2.04 (3H, s)
CO-CH_3	2.01 (3H, s)

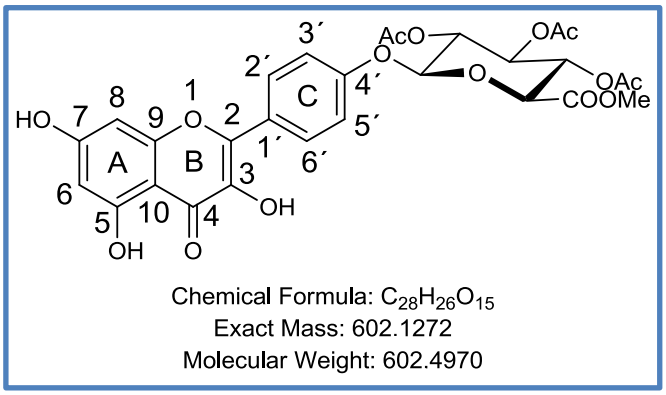

Figure 28: Structure of kaempferol-4'-O-(2",3",4"-tri-O-acetyl)-β-D-glucuronic acid methyl ester

Table 15: Data of kaempferol-4'-O-(2",3",4"-tri-O-acetyl)-β-D-glucuronic acid methyl ester

State of aggregation	Pale yellow solid
Amount [mg]	36.4
Yield [%]	88
m/z $[M-H]^-$	601.1198
Calc *m/z* $[M-H]^-$	601.1199

3.3.1.4 Synthesis of Kaempferol-4'-O-β-D-glucuronide

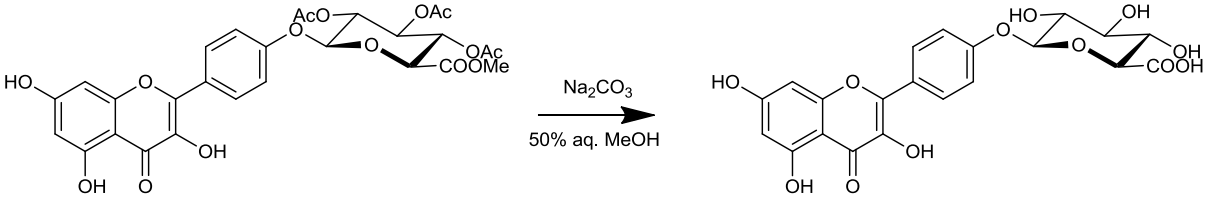

Kaempferol-4'-O-(2'',3'',4''-tri-O-acetyl)-β-D-glucuronic acid methyl ester (36.4 mg, 60.4 µmol) was dissolved in 20 mL 50% aq. MeOH. After addition of 0.6 mL aq. sodium carbonate (0.5 M), the reaction mixture was stirred at room temperature for 90 min. After cooling the pH was ajusted ≤ 3 with Dowex 50 W X 4 resin. The mixture was filtrated and the residue was washed with 20 mL 50% aq. MeOH and 20 mL MeOH. The crude product was purified by semipreparative HPLC.

Chromatographic parameter:

Instrument:	Semipreparative HPLC
Column:	Knauer, Vertex, 16 x 250 mm
Stationary phase:	Eurospher-100 C18-7 µm
Mobile phase:	A: H_2O+0.1% TFA, B: acetonitrile+0.1% TFA
Application:	Liquid injection in 15% aqueous acetonitrile
Fractionation:	19 min
Gradient:	0 min: 10% acetonitrile+0.1% TFA
	35 min: 35% acetonitrile+0.1% TFA
	35-40 min: 35% acetonitrile+0.1% TFA
	45 min: 10% acetonitrile+0.1% TFA
Flow:	10 mL/min
Retention Time (t_R):	30.0 min
λ_{max} [nm] at t_R:	221, 264, 318, 362
File:	2012-03/178-179

Table 16: ^{1}H and ^{13}C NMR spectral data of kaempferol-4´-O-β-D-glucuronide (600/150 MHz, 298 K, *J* in Hz, in DMSO-d_6)

Position	^{1}H	^{13}C
2		146.3
3		136.5
4		176.3
5		160.8
6	6.19 (1H, d, 2.1)	98.5
7		164.1
8	6.46 (1H, d, 2.1)	93.9
9		156.6
10		103.4
2´,6´	8.10 (2H, d, 9.1)	129.6
3´,5´	7.17 (2H, d, 9.1)	116.4
1´´	5.16 (1H, d, 7.5)	99.7
2´´	3.32-3.28 (1H, m)	73.0
3´´	3.36-3.32 (1H, m)	75.8
4´´	3.40 (1H, t, 9.2)	71.5
5´´	3.95 (1H, d, 9.7)	75.6
6´´		170.3

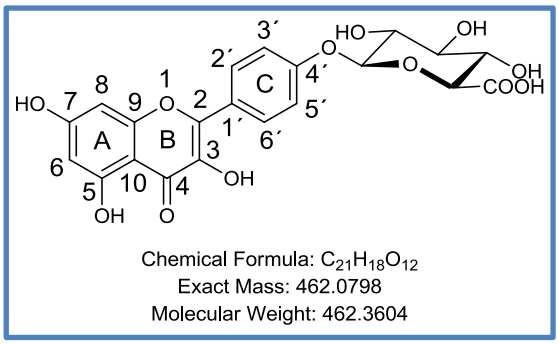

Figure 29: Structure of kaempferol-4´-O-β-D-glucuronide

Table 17: Data of kaempferol-4´-O-β-D-glucuronide

State of aggregation	yellow solid
Amount [mg]	10.5
Yield [%]	38
m/z $[M-H]^-$	461.0725
Calc *m/z* $[M-H]^-$	461.0725
λ_{max} in acetonitrile	249.9, 267.0, 318.0, 363.0
Molar absorptivity (n=3) $[L \cdot mol^{-1} \cdot cm^{-1}]$	10333 (362.7 nm)

3.3.2 Synthesis of Kaempferol-7-O-β-D-glucuronide and Kaempferol-7,4'-di-O-β-D-glucuronide

3.3.2.1 Synthesis of 3,5,7,4'-Tetra-O-acetyl-kaempferol

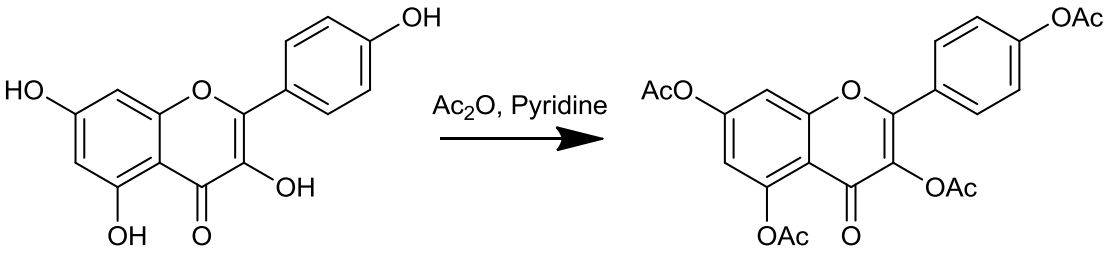

Kaempferol (500 mg, 1.75 mmol) was dissolved in 4.95 mL acetic anhydride. After the addition of 524 µL pyridine, the reaction mixture was heated to reflux (145 °C) for 5 h. 8.7 mL of ice-cold H_2O were added and the precipitate was filtered off and washed with ice-cold H_2O. The crude product was used without further purification in the next step.

Table 18: ^{1}H NMR spectral data of 3,5,7,4'-tetra-O-acetyl-kaempferol (300 MHz, 298 K, *J* in Hz, in acetone-d_6)

Position	^{1}H
6	7.03 (1H, d, 2.2)
8	7.52 (1H, d, 2.2)
2´,6´	8.03 (2H, d, 8.8)
3´,5´	7.38 (2H, d, 8.8)
4x CO-CH_3	2.35 (3H, s)
	2.34 (3H, s)
	2.32 (3H, s)
	2.30 (3H, s)

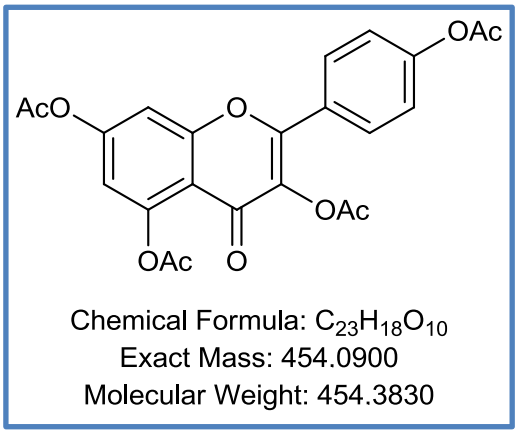

Figure 30: Structure of 3,5,7,4'-tetra-O-acetyl-kaempferol

Table 19: Data of 3,5,7,4'-tetra-O-acetyl-kaempferol

State of aggregation	white solid
Amount [mg]	728
Yield [%]	92%
m/z $[M+H]^+$	455.0973
Calc *m/z* $[M+H]^+$	455.0973

3.3.2.2 Synthesis of 3,5-Di-O-acetyl-kaempferol

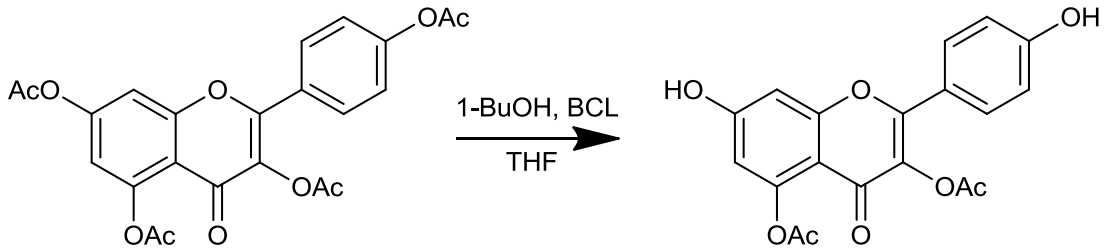

Peracetylated kaempferol (727.0 mg, 1.60 mmol) was dissolved in 87.5 mL dry THF. 1-Butanol (801 µL, 8.75 mmol, ~ 5 eq) and *Burkholderia cepacia* lipase (BCL, 1.75 g, 20 mg/mL) were added. The reaction mixture was stirred for 8 days at 42 °C. The lipase was filtered off and the solvent was evaporated under nitrogen stream. The crude product was purified by flash column chromatography.

Chromatographic parameter:

Instrument:	Flash chromatography
Column:	Merck, SuperVarioPrep® D40, 46 x 186 mm
Stationary Phase:	Merck, RP18 25-40 µm, 90 g, 40 x 115 mm + 5 g precolumn
Mobile Phase:	A: H_2O, B: acetone
Application:	Suspension in 30% aqueous acetone
Fractionation:	35 min
Gradient:	0 min: 20% acetone
	20 min: 75% acetone
	23 min: 100% acetone
	35 min: 100% acetone
Flow:	50 mL/min
Region of Retention:	5.5-8.5 min, 275–425 mL
File:	120307-1254-1

Table 20: ^{1}H NMR spectral data of 3,5-di-O-acetyl-kaempferol (300 MHz, 298 K, *J* in Hz, in acetone-d_6)

Position	^{1}H
6	6.64 (1H, d, 2.3)
8	6.95 (1H, d, 2.3)
2´,6´	7.83 (2H, d, 8.9)
3´,5´	7.03 (2H, d, 8.9)
2x CO-CH_3	2.30 (3H, s)
	2.28 (3H, s)

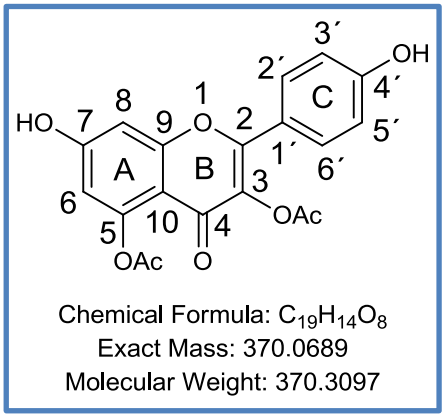

Figure 31: Structure of 3,5-di-O-acetyl-kaempferol

Table 21. Data of 3,5-di-O-acetyl-kaempferol

State of aggregation	white solid
Amount [mg]	94.4
Yield [%]	15
m/z $[M+H]^+$	371.0761
Calc *m/z* $[M+H]^+$	371.0762

3.3.2.3 One-Pot synthesis of 3,5-Di-O-acetyl-kaempferol-7-O-(2“,3“,4“-tri-O-acetyl)-β-D-glucuronic acid methyl ester and 3,5-Di-O-acetyl-kaempferol-7,4’-O-di-(2“, 3“, 4“-tri-O-acetyl)-β-D-glucuronic acid methyl ester

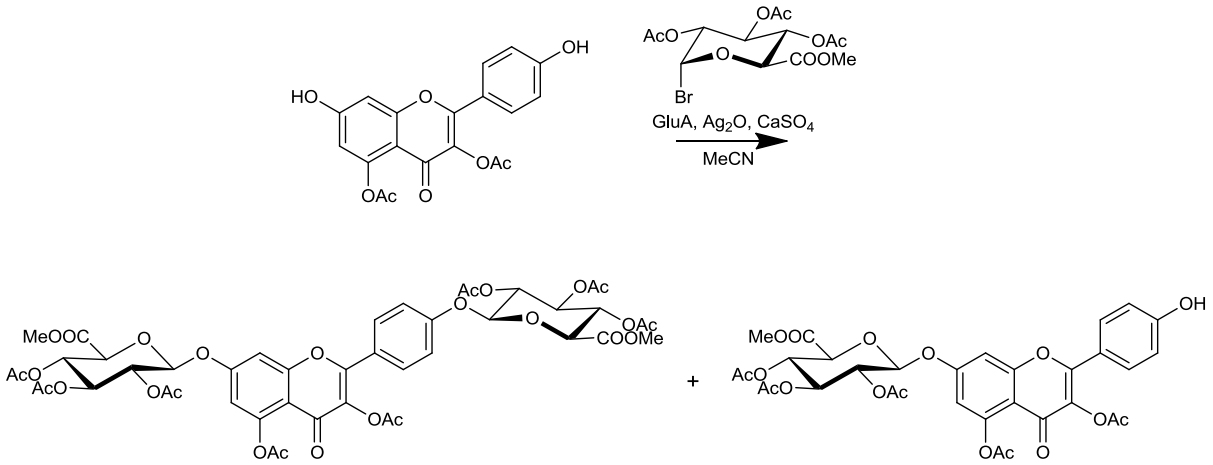

3,5-Di-O-acetyl-kaempferol (106.4 mg, 335.1 µmol), calcium sulfate (558.0 mg) and silver(I)-oxide (163.1 mg, 707.8 µmol, 2.1 eq) were suspended in 4.5 mL acetonitrile. Afterwards 1-bromo-2,3,4-tri-O-acetyl-α-D-glucuronic acid methyl ester (197.2 mg, 502.7 µmol, 1.5 eq) was added. After 2.5 and 3 h another 15 mg of the glucuronic acid were added. The reaction mixture was stirred overall for 4 h at room temperature. Subsequently, 22 mL aq. KCl (10%, w/w) and 112 mL aqueous acetic acid (10%, v/v) were added and the mixture was filtered through celite.[57] The residue was washed with 100 mL H_2O and the crude product was eluted with 100 mL acetone. The solvent was evaporated under nitrogen stream before the crude product was purified by semipreparative HPLC.

Chromatographic parameter:

Instrument:	Semipreparative HPLC
Column:	Knauer, Vertex, 16 x 250 mm
Stationary phase:	Eurospher-100 C18-7 µm
Mobile phase:	A: H_2O, B: acetonitrile
Application:	Liquid injection in 55% aqueous acetonitrile
Fractionation:	17 min
Gradient:	0 min: 45% acetonitrile
	15 min: 70% acetonitrile
	15-17 min: 70% acetonitrile
	18 min: 45% acetonitrile

Flow:	10 mL/min	
Retention time (t_R):	7-Glucuronide	7,4´-Diglucuronide
	11.0 min	15.5 min
λ_{max} [nm] at t_R:	7-Glucuronide	7,4´-Diglucuronide
	209, 248, 324	222, 249, 307
File:	2012-03/166-173	

Table 22: ^{1}H NMR spectral data of 3,5-di-O-acetyl-kaempferol-7-O-(2“,3“,4“-tri-O-acetyl)-β-D-glucuronic acid methyl ester (400 MHz, 298 K, *J* in Hz, in acetone-d_6)

Position	^{1}H
6	6.87 (1H, d, 2.4)
8	7.33 (1H, d, 2.4)
2´,6´	7.84 (2H, d, 8.9)
3´,5´	7.04 (2H, d, 8.9)
1´´	5.87 (1H, d, 7.6)
Sugar proton	5.50 (1H, t, 9.5)
Sugar proton	5.30 (1H, dd, 7.6, 9.5)
Sugar proton	5.26 (1H, t, 9.6)
Sugar proton	4.71 (1H, d, 9.7)
O-CH_3	3.69 (3H, s)
2x CO-CH_3	2.32 (3H, s)
(aglycone)	2.29 (3H, s)
3x CO-CH_3 (sugar)	2.04 (3H, s)
	2.02 (3H, s)
	2.01 (3H, s)

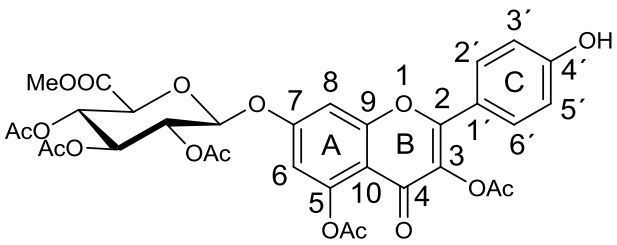

Chemical Formula: $C_{32}H_{30}O_{17}$
Exact Mass: 686.1483
Molecular Weight: 686.5704

Figure 32: Structure of 3,5-di-O-acetyl-kaempferol-7-O-(2“,3“,4“-tri-O-acetyl)-β-D-glucuronic acid methyl ester

Table 23: Data of 3,5-di-O-acetyl-kaempferol-7-O-(2“,3“,4“-tri-O-acetyl)-β-D-glucuronic acid methyl ester

State of aggregation	pale yellow solid
Amount [mg]	11.2
Yield [%]	10
m/z $[M+H]^+$	687.1559
Calc *m/z* $[M+H]^+$	687.1556

Table 24: ^{1}H NMR spectral data of 3,5-di-O-acetyl-kaempferol-7,4´-di-O-(2‘‘, 3‘‘, 4‘‘-tri-O-acetyl)-β-D-glucuronic acid methyl ester (400 MHz, 298 K, *J* in Hz, in acetone-d_6)

Position	^{1}H
6	6.89 (1H, d, 2.4)
8	7.34 (1H, d, 2.4)
2´,6´	7.93 (2H, d, 9.0)
3´,5´	7.28 (2H, d, 9.0)
Anomeric	5.87 (1H, d, 7.6)
protons	5.74 (1H, d, 7.8)
Sugar protons	5.49 (2H, t, 9.5)
Sugar protons	5.33-5.22 (4H, m)
Sugar proton	4.71 (1H, d, 9.8)
Sugar proton	4.67 (1H, d, 9.9)
O-CH_3	3.71 (3H, s)
O-CH_3	3.68 (3H, s)
2x CO-CH_3	2.32 (3H, s)
(aglycone)	2.28 (3H, s)
6x CO-CH_3	2.04 (3H, s)
(sugar)	2.03 (3H, s)
	2.02 (6H, s)
	2.014 (3H,s)
	2.013 (3H,s)

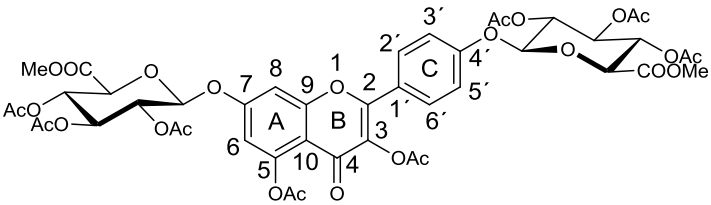

Figure 33: Structure of 3,5-di-O-acetyl-kaempferol-7,4´-di-O-(2‘‘, 3‘‘, 4‘‘-tri-O-acetyl)-β-D-glucuronic acid methyl ester

Table 25: Data of of 3,5-di-O-acetyl-kaempferol-7,4´-di-O-(2‘‘, 3‘‘, 4‘‘-tri-O-acetyl)-β-D-glucuronic acid methyl ester

State of aggregation	white solid
Amount [mg]	28.0
Yield [%]	11
m/z $[M+H]^+$	1003.2359
Calc *m/z* $[M+H]^+$	1003.2350

3.3.2.4 Synthesis of Kaempferol-7-O-β-D-glucuronide

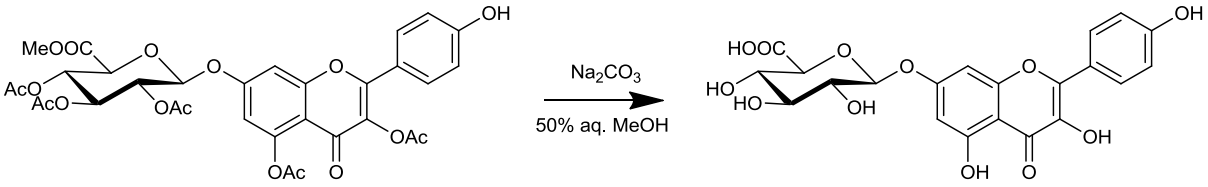

3,5-Di-O-acetyl-kaempferol-7-O-(2‘‘,3‘‘,4‘‘-tri-O-acetyl)-β-D-glucuronic acid methyl ester (11.2 mg, 16.3 µmol) was dissolved in 10 mL 50% aq. MeOH. After the addition of 0.3 mL aq. sodium carbonate (0.5 M), the reaction mixture was stirred at room temperature for 1 h. After cooling the pH was ajusted ≤ 3 with Dowex 50 W X 4 resin. The mixture was filtrated and the residue was washed with 10 mL 50% aq. MeOH and 10 mL MeOH. The crude product was purified by semipreparative HPLC.

Chromatographic parameter:

Instrument:	Semipreparative HPLC
Column:	Knauer, Vertex, 16 x 250 mm
Stationary phase:	Eurospher-100 C18-7 µm
Mobile phase:	A: H_2O+0.1% TFA, B: Acetonitrile+0.1% TFA
Application:	Liquid injection in 15% aqueous acetonitrile
Fractionation:	19 min
Gradient:	0 min: 10% acetonitrile+0.1% TFA
	15 min: 45% acetonitrile+0.1% TFA
	16 min: 90% acetonitrile+0.1% TFA
	16-18 min: 90% acetonitrile+0.1% TFA
	19 min: 10% acetonitrile+0.1% TFA
Flow:	10 mL/min
Retention Time (t_R):	14.0 min
λ_{max} [nm] at t_R:	225, 251, 262, 364
File:	2012-03/174-175

Table 26: ^{1}H and ^{13}C NMR spectral data of kaempferol-7-O-β-D-glucuronide (600/150 MHz, 298 K, *J* in Hz, in DMSO-d_6)

Position	^{1}H	^{13}C
2		147.9
3		136.2
4		176.2
5		160.5
6	6.43 (1H, d, 2.2)	98.9
7		162.5
8	6.80 (1H, d, 2.1)	94.6
9		156.1
10		105.1
1´		121.8
2´,6´	8.04 (2H, d, 9.0)	130.0
3´,5´	6.93 (2H, d, 9.0)	115.8
4´		159.5
1´´	5.22 (1H, d, 7.6)	99.4
2´´	3.30-3.26(1H, m)	72.9
3´´	3.33 (1H, t, 8.9)	75.6
4´´	3.39 (1H, t, 9.3)	71.4
5´´	4.03 (1H, d, 9.6)	75.5
6´´		170.3

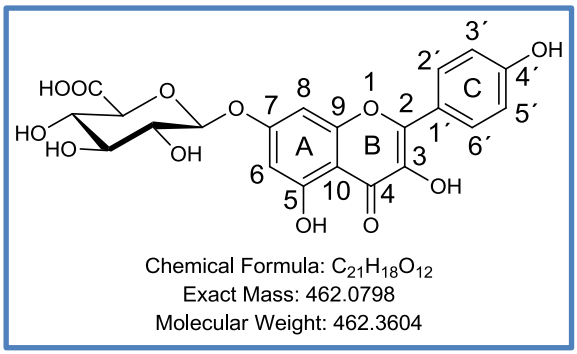

Chemical Formula: $C_{21}H_{18}O_{12}$
Exact Mass: 462.0798
Molecular Weight: 462.3604

Figure 34: Structure of kaempferol-7-O-β-D-glucuronide

Table 27: Data of kaempferol-7-O-β-D-glucuronide

State of aggregation	yellow solid
Amount [mg]	5.0
Yield [%]	66
m/z $[M-H]^-$	461.0726
Calc *m/z* $[M-H]^-$	461.0725
λ_{max} in acetonitrile	252.0, 267.0, 323.0 365.0
Molar absorptivity (n=3) $[L \cdot mol^{-1} \cdot cm^{-1}]$	14140 (364.7 nm)

3.3.2.5 Synthesis of Kaempferol-7,4'-di-O-β-D-glucuronide

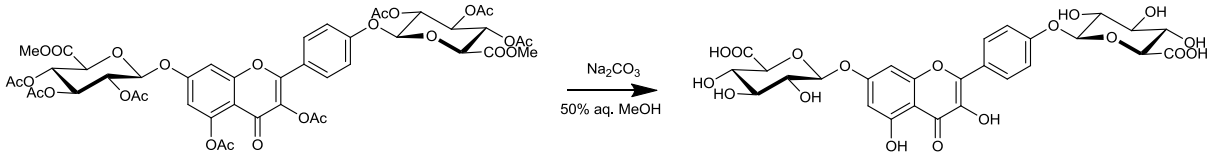

3,5-Di-O-acetyl-kaempferol-7,4'-di-O-(2'', 3'', 4''-tri-O-acetyl)-β-D-glucuronic acid methyl ester (28.0 mg, 32.9 µmol) was dissolved in 20 mL 50% aq. MeOH. After the addition of 0.6 mL aq. sodium carbonate (0.5 M), the reaction mixture was stirred at room temperature for 180 min. After cooling the pH was ajusted ≤ 3 with Dowex 50 W X 4 resin. The mixture was filtrated and the residue was washed with 20 mL 50 % aq. MeOH and 20 mL MeOH. The crude product was purified by semipreparative HPLC.

Chromatographic parameter:

Instrument:	Semipreparative HPLC
Column:	Knauer, Vertex, 16 x 250 mm
Stationary phase:	Eurospher-100 C18-7 µm
Mobile phase:	A: H_2O+0.1% TFA, B: acetonitrile+0.1% TFA
Application:	Liquid injection in 15% aqueous acetonitrile
Fractionation:	19 min
Gradient:	0 min: 10% acetonitrile+0.1% TFA
	15 min: 45% acetonitrile+0.1% TFA
	16 min: 90% acetonitrile+0.1% TFA
	16-18 min: 90% acetonitrile+0.1% TFA
	19 min: 10% acetonitrile+0.1% TFA
Flow:	10 mL/min
Retention Time (t_R):	10.0 min
λ_{max} [nm] at t_R:	245, 265, 319, 357
File:	2012-03/176-177

Table 28: ^{1}H and ^{13}C NMR spectral data of kaempferol-7,4´-di-O-β-D-glucuronide (600/150 MHz, 298 K, *J* in Hz, in DMSO-d_6)

Position	^{1}H	^{13}C
2		147.0
3		136.9
4		176.5
5		160.5
6	6.44 (1H, d, 2.1)	99.0
7		162.6
8	6.83 (1H, d, 2.1)	94.7
9		156.2
10		105.2
1´		124.8
2´,6´	8.14 (2H, d, 9.0)	129.7
3´,5´	7.18 (2H, d, 9.1)	116.4
4´		158.4
1´´	5.17 (1H, d, 7.5)	99.6
2´´	3.31-3.27 (1H, m)*	73.0*
3´´	3.36-3.31 (1H, m)*	75.8*
4´´	3.42-3.37 (1H, m)*	71.5*
5´´	3.96 (1H, d, 9.6)	75.5*
6´´		170.3
1´´´	5.22 (1H, d, 7.5)	99.4
2´´´	3.31-3.27 (1H, m)*	72.9*
3´´´	3.36-3.31 (1H, m)*	75.7*
4´´´	3.42-3.37 (1H, m)*	71.4*
5´´´	4.03 (1H, d, 9.6)	75.5*
6´´´		170.3

* signals are exchangeable, COSY suggests: δ(H4´´) > δ(H4´´´), δ(H2´´) > δ(H2´´´)

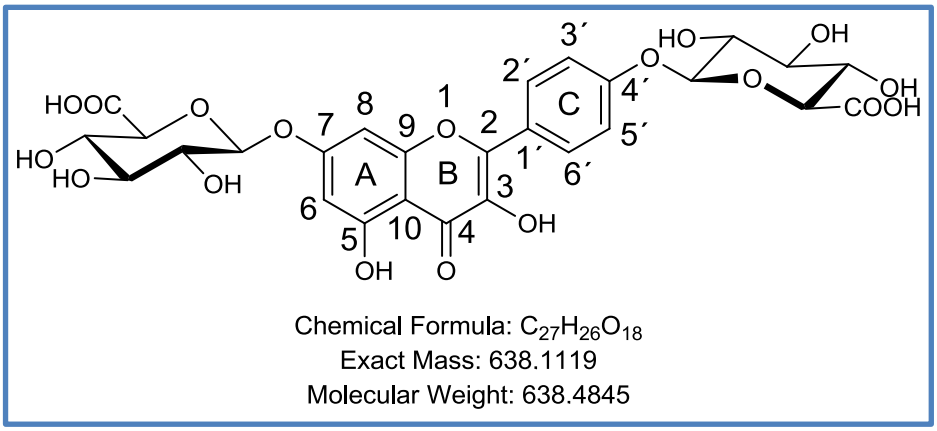

Figure 35: Structure of kaempferol-7,4´-di-O-β-D-glucuronide

Table 29: Data of kaempferol-7,4´-di-O-β-D-glucuronide

State of aggregation	yellow solid
Amount [mg]	11.3
Yield [%]	54
m/z $[M-H]^-$	637.1046
Calc *m/z* $[M-H]^-$	637.1043
λ_{max} in acetonitrile	251.0, 267.0, 318.9, 363.0
Molar absorptivity (n=3) $[L \cdot mol^{-1} \cdot cm^{-1}]$	10540 (363.0 nm)

3.3.3 Synthesis of Kaempferol-3-O-β-D-glucuronide

3.3.3.1 Synthesis of Kaempferol-3-O-(2“, 3“, 4“-tri-O-acetyl)-β-D-glucuronic acid methyl ester

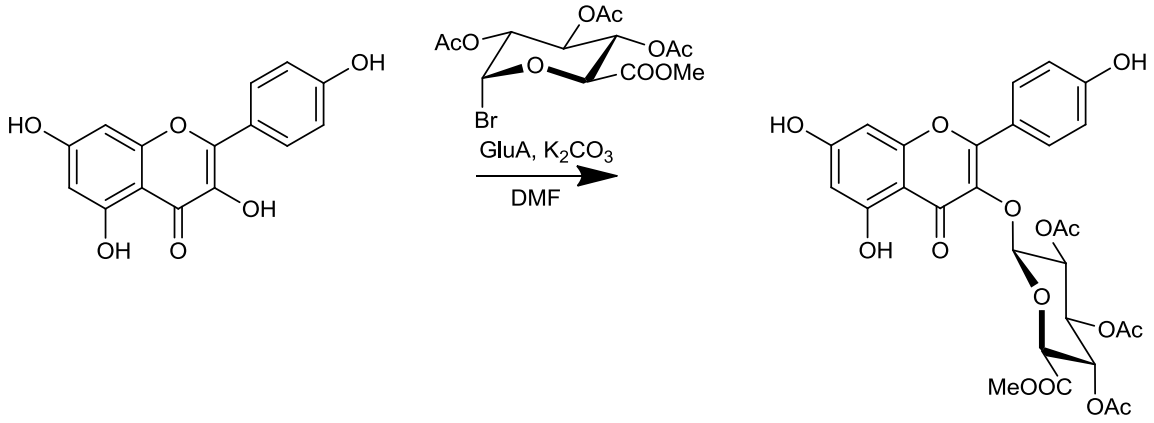

Kaempferol (75.0 mg, 262 µmol), potassium carbonate (36.0 mg, 262 µmol, 1 eq) and 1-bromo-2,3,4-tri-O-acetyl-α-D-glucuronic acid methyl ester (728.0 mg, 1833 µmol, 7 eq) were suspended under nitrogen atmosphere and 0 °C in 2.6 mL DMF. The ice bath was removed and after 72 h another 36.0 mg of potassium carbonate were added. The reaction mixture was stirred overall for 96 h at room temperature. Subsequently, 50 mL of EtOAc were added to the reaction mixture, which was extracted two times with 50 mL H_2O, each. The organic phase was dried under nitrogen stream before the crude product was purified by semipreparative HPLC.

Chromatographic parameter:

Instrument:	Semipreparative HPLC
Column:	Knauer, Vertex, 16 x 250 mm
Stationary phase:	Eurospher-100 C18-7 µm
Mobile phase:	A: H_2O, B: acetonitrile
Application:	Liquid injection in 80% aqueous acetonitrile
Fractionation:	22 min
Gradient:	0 min: 25% acetonitrile
	15 min: 65% acetonitrile
	18 min: 90% acetonitrile
	18-20 min: 90% acetonitrile
	22 min: 25% acetonitrile

Flow: 10 mL/min

Retention Time (t_R): 15.8 min

λ_{max} [nm] at t_R: 224, 239, 264, 346

File: 2013-08/207-209

Table 30: ^{1}H NMR spectral data of kaempferol-3-O-(2'', 3'', 4''-tri-O-acetyl)-β-D-glucuronic acid methyl ester (300 MHz, 298 K, *J* in Hz, in DMSO-d_6)

Position	^{1}H
6	6.21 (1H, d, 2.0)
8	6.43 (1H, d, 2.0)
2´,6´	7.98 (2H, d, 8.9)
3´,5´	6.90 (2H, d, 8.9)
1´´	5.76 (1H, d, 7.9)
Sugar proton	5.45 (1H, t, 9.7)
Sugar proton	5.02 (1H, dd, 8.3, 10.5)
Sugar proton	4.96 (1H, t, 9.9)
Sugar proton	4.46 (1H, d, 9.9)
O-CH_3	3.51 (3H, s)
3x CO-CH_3	2.02 (3H, s)
(sugar)	1.99 (3H, s)
	1.97 (3H, s)

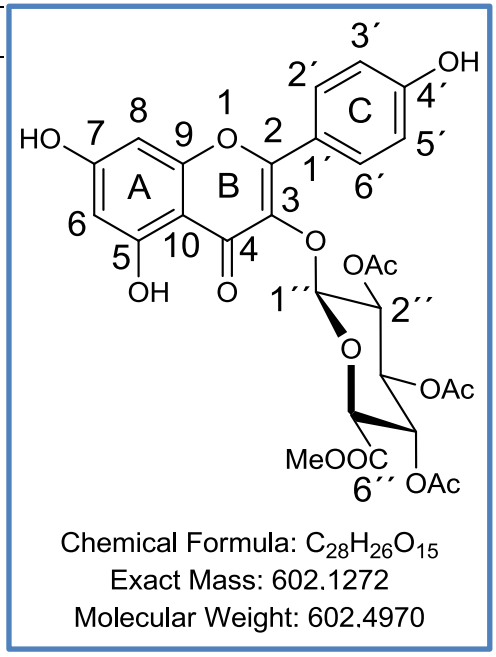

Figure 36: Structure of kaempferol-3-O-(2'', 3'', 4''-tri-O-acetyl)-β-D-glucuronic acid methyl ester

Table 31: Data of kaempferol-3-O-(2'', 3'', 4''-tri-O-acetyl)-β-D-glucuronic acid methyl ester

State of aggregation	pale yellow solid
Amount [mg]	14.9
Yield [%]	9
m/z $[M+H]^+$	603.1343
Calc *m/z* $[M+H]^+$	603.1344

3.3.3.2 Synthesis of Kaempferol-3-O-β-D-glucuronide

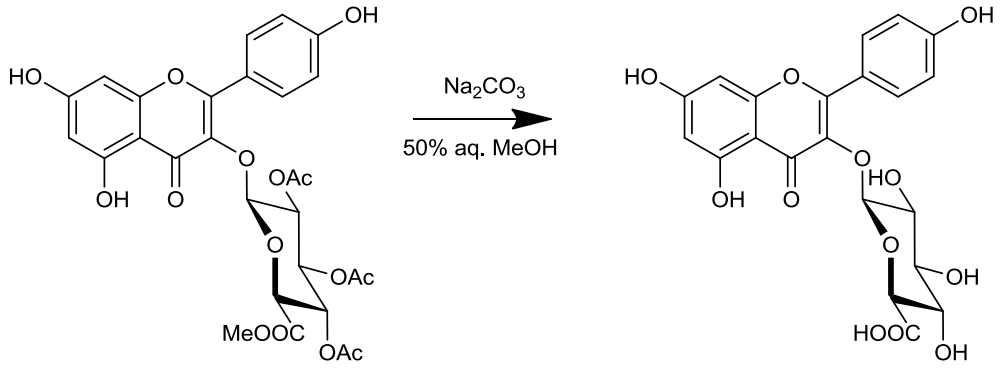

Kaempferol-3-O-(2‘‘, 3‘‘, 4‘‘-tri-O-acetyl)-β-D-glucuronic acid methyl ester (7.5 mg, 32.9 µmol) was dissolved in 15 mL 50% aq. MeOH. After the addition of 0.45 mL aq. sodium carbonate (0.5 M), the reaction mixture was stirred at room temperature for 150 min. After cooling the pH was ajusted ≤ 3 with Dowex 50 W X 4 resin. The mixture was filtrated and the residue was washed with 20 mL 50 % aq. MeOH and 20 mL MeOH. The crude product was purified by semipreparative HPLC.

Chromatographic parameter:

Instrument:	Semipreparative HPLC
Column:	Knauer, Vertex, 16 x 250 mm
Stationary phase:	Eurospher-100 C18-7 µm
Mobile phase:	A: H_2O+0.1% TFA, B: acetonitrile+0.1% TFA
Application:	Liquid injection in 5% aqueous acetonitrile
Fractionation:	19 min
Gradient:	0 min: 10% acetonitrile+0.1% TFA
	15 min: 45% acetonitrile+0.1% TFA
	16 min: 90% acetonitrile+0.1% TFA
	16-18 min: 90% acetonitrile+0.1% TFA
	19 min: 10% acetonitrile+0.1% TFA
Flow:	10 mL/min
Retention Time(t_R):	13.5 min
λ_{max} [nm] at t_R:	222, 263, 348
File:	2013-08/7

Table 32: ^{1}H and ^{13}C NMR spectral data of kaempferol-3-O-β-D-glucuronide (600/150 MHz, 298 K, *J* in Hz, in DMSO-d_6)

Position	^{1}H	^{13}C
2		156.3
3		133.0
4		177.2
5		161.1
6	6.20 (1H, d, 2.1)	98.8
7		164.2
8	6.42 (1H, d, 2.0)	93.7
9		156.3
10		103.9
1´		120.6
2´,6´	8.14 (2H, d, 8.9)	130.9
3´,5´	6.86 (2H, d, 8.9)	115.1
4´		177.2
1´´	5.47 (1H, d, 7.5)	101.1
2´´	3.23-3.18 (1H, m)	73.9
3´´	3.26-3.22 (1H, m)	75.8
4´´	3.35-3.30 (1H, m)	71.5
5´´	3.53 (1H, d, 9.6)	75.8
6´´		169.9

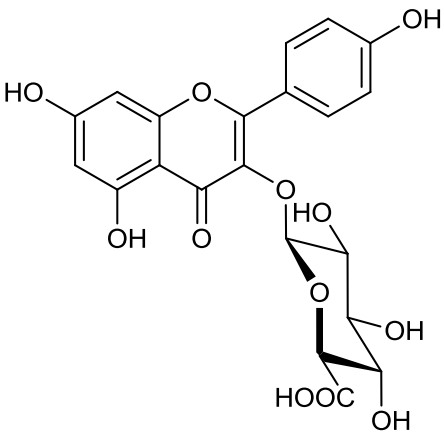

Chemical Formula: $C_{21}H_{18}O_{12}$
Exact Mass: 462.0798
Molecular Weight: 462.3604

Figure 37: Structure of kaempferol-3-O-β-D-glucuronide

Table 33: Data of kaempferol-3-O-β-D-glucuronide

State of aggregation	yellow solid
Amount [mg]	1.7
Yield [%]	30
m/z $[M-H]^-$	461.0721
Calc *m/z* $[M-H]^-$	461.0725
λ_{max} in acetonitrile	267.0, 347.3
Molar absorptivity (n=3) $[L \cdot mol^{-1} \cdot cm^{-1}]$	11640 (267.0 nm)

3.3.4 Synthesis of Kaempferol-7-sulfate

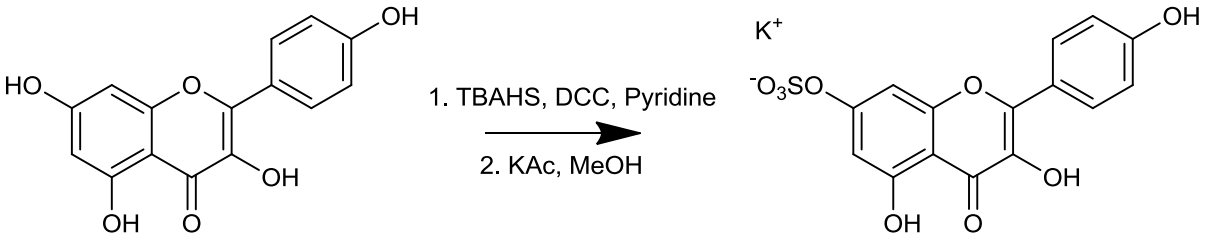

Kaempferol (75.0 mg, 262 µmol) was transferred in a Schlenk flask. *N,N'*-Dicyclohexylcarbodiimide (541.0 mg, 2.62 µmol, 10 eq) and tetrabutylammonium hydrogensulfate (TBAHS, 136.0 mg, 524 µmol, 2 eq) were dissolved in 2 mL and 250 µL pyridine, respectively and added *via* a septum. The reaction mixture was stirred under nitrogen atmosphere and room temperature. After 3 days 4.6 mL of MeOH were added.[53] The dicyclohexylurea precipitates were filtered off and the solvent was removed under nitrogen stream. The crude product was purified by flash column chromatography

Chromatographic parameter:

Instrument:	Flash chromatography
Column:	Merck, SuperVarioPrep® D40, 46 x 186 mm
Stationary phase:	Merck, LiChroprep RP-18 25-40 µm, 30 g, 30 x 100 mm + 5 g precolumn
Mobile phase:	A: H_2O, B: MeOH
Application:	Suspension in 30% MeOH
Fractionation:	35 min
Gradient:	0 min: 30% MeOH 25 min: 75% MeOH 30 min: 100% MeOH 30-35 min: 100% MeOH
Flow:	20 mL/min
Region of retention:	20-25 min, 570–720 mL
File:	120814-1258-1

The combined fractions were dissolved in 2 mL MeOH and the potassium salt of the flavonol sulfate was generated by adding 2 mL saturated, methanolic potassium acetate solution. The suspension was centrigugated at 3000 rcf for 5 min. The precipitate was purified by semipreparative HPLC.

Chromatographic parameter:

Instrument:	Semipreparative HPLC
Column:	Knauer, Vertex, 16 x 250 mm
Stationary phase:	Eurospher-100 C18-7 µm
Mobile phase:	A: H_2O, B: acetonitrile
Application:	Liquid injection in 10% aqueous acetonitrile
Fractionation:	15 min
Gradient:	0 min: 10% acetonitrile
	10 min: 20% acetonitrile
	10-12 min: 20% acetonitrile
	13 min: 10% acetonitrile
	13-15 min: 10% acetonitrile
Flow:	10 mL/min
Retention Time(t_R):	9.4 min
λ_{max} [nm] at t_R:	246, 369
File:	2012-09/192-193

Table 34: ^{1}H NMR spectral data of kaempferol-7-sulfate (300 MHz, 298 K, *J* in Hz, in DMSO-d_6) compared to literature values[53]

Position	^{1}H	$^{1}H_{LIT}$
6	6.55 (1H, d, 2.0)	6.55 (1H, d, 2.0)
8	6.97 (1H, d, 2.1)	6.98 (1H, d, 2.0)
2´,6´	8.06 (2H, d, 8.9)	8.08 (2H, d, 8.9)
3´,5´	6.94 (2H, d, 8.9)	6.93 (2H, d, 8.9)

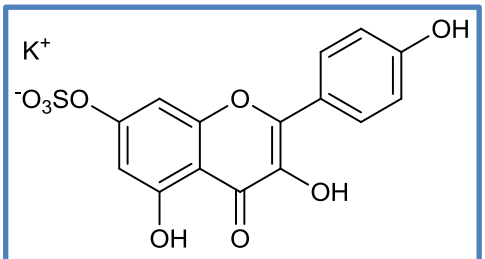

Chemical Formula: $C_{15}H_9KO_9S$
Exact Mass: 403.9604
Molecular Weight: 404.3899

Figure 38: Structure of kaempferol-7-sulfate

Table 35: Data of kaempferol-7-sulfate

State of aggregation	yellow solid
Amount [mg]	2.6
Yield [%]	3
m/z $[M-H]^-$	364.9978
Calc *m/z* $[M-H]^-$	364.9973
λ_{max} in acetonitrile	249.9, 322.1, 366.1
Molar absorptivity (n=3) $[L \cdot mol^{-1} \cdot cm^{-1}]$	9553 (249.9 nm)

3.4 Results and Discussion

Synthesis of Kaempferol-4´-O-β-D-glucuronide

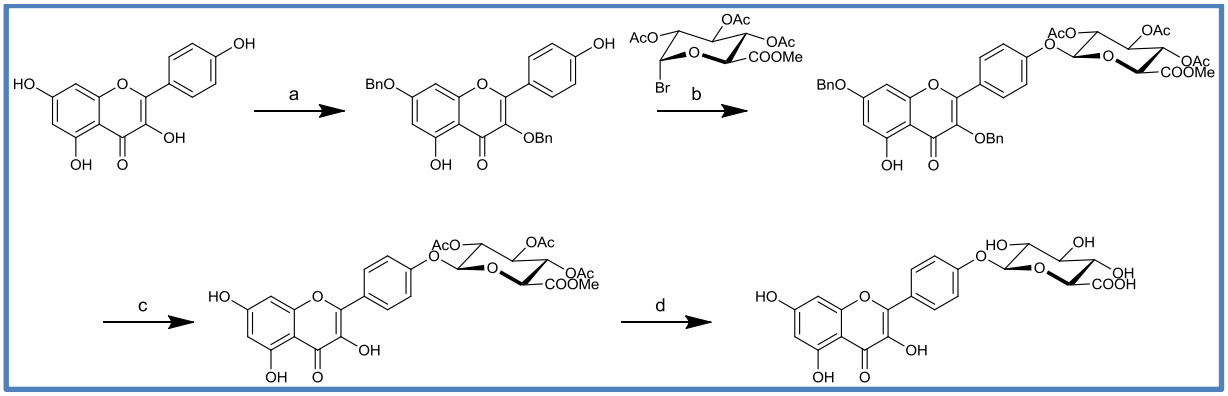

Scheme 1: Synthesis of kaempferol-4´-O-β-D-glucuronide. Reagents and conditions: (a) benzyl bromide, K_2CO_3, DMF, 2h; (b) 1-bromo-2,3,4-tri-O-acetyl-α-D-glucuronic acid methyl ester, Ag_2O, $CaSO_4$, acetonitrile/pyridine, 3.5 h; (c) cyclohexene, $Pd(OH)_2$ on charcoal, reflux, 45 min; (d) Na_2CO_3, MeOH, H_2O, 1.5 h.

The synthesis of kaempferol-4´-O-β-D-glucuronide started with a Williamson ether synthesis. Under alkaline conditions, the organohalide benzyl bromide substitutes to certain hydroxyl functions of kaempferol if an appropriate stoichiometry is used. This S_N2 reaction was accomplished to protect the hydroxyl functions and positions 3 and 7 of the kaempferol as benzyl ethers. Although mono- and tri-benzylated side product were generated, the main compound in the final reaction mixture was 3,7-di-O-benzyl-kaempferol. In the next step, the formation of the glycosidc bond was achieved *via* a modified Koenigs-Knorr reaction. A 1-bromo derivate of the glucuronic acid was activated by silver-I-oxide followed by the substitution to the most reactive free hydroxyl function, which is at position 4´. After purification, the benzyl ether protecting groups were removed by a transfer hydrogenation. Cyclohexene was used as hydrogen donor under palladium catalysis. In the final step, the remaining acetyl protecting groups and the methyl ester were cleaved under

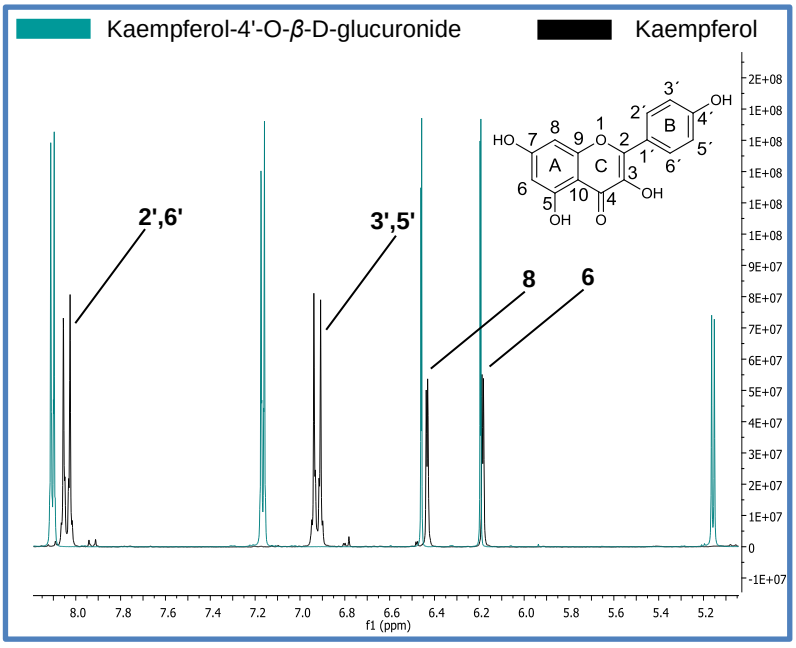

Figure 39: Superimposed ^{1}H NMR spectra of kaempferol and kaempferol-4´-O-β-D-glucuronide

alkaline conditions to yield the desired product. The position of the glucuronic acid at the flavonol was analyzed by 2D NMR, although the comparison of the ^{1}H NMR data of the aglycone and the glucuronide already shows meaningful differences in the chemical shift (**Figure 39**).

For the aromatic protons which are near the substituted hydroxyl group, higher ppm values can be expected. The signals for the protons of the A-ring stay rather unchanged (~6.45 ppm und ~6.18 ppm, respectively), whereas the four protons of the B-ring, especially at position 3´ and 5´ show a downfield shift. These have a chemical shift of 6.92 ppm for the agylcone and 7.18 ppm for the kaempferol-4´-O-β-D-glucuronide. Further on, an additional duplett at 5.18 ppm with coupling constant of ^{3}J = 7.24 Hz proofs the β-configuration of the glucuronic acid.

Further confirmation on the structure was acquired by the analysis of 2D NMR data. Some key sections of this data are presented in **Figure 40** and **Figure 41**.

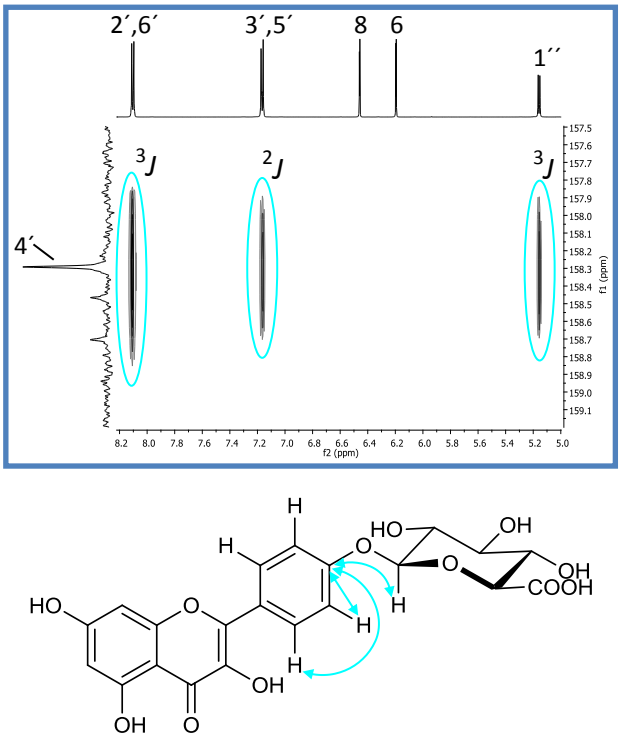

Figure 40: Section of $^{1}H,^{13}C$ HMBC spectral data of kaempferol-4´-O-β-D-glucuronide

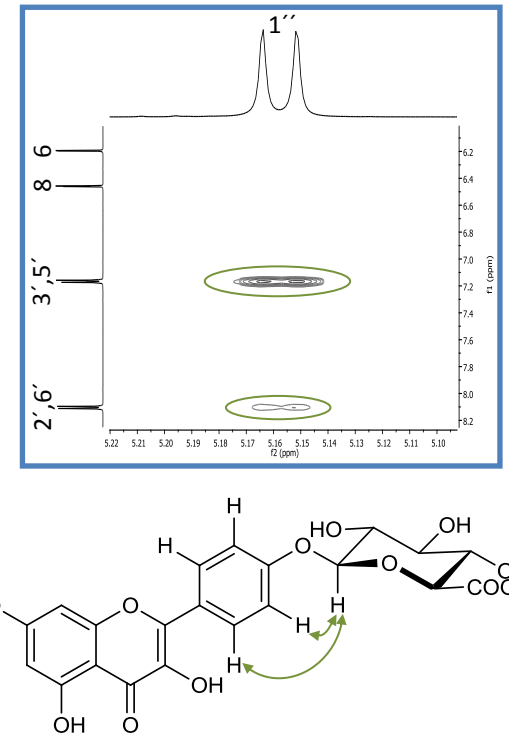

Figure 41: Section of $^{1}H,^{1}H$ NOESY spectral data of kaempferol-4´-O-β-D-glucuronide

Figure 40 shows the cross peaks in the $^{1}H,^{13}C$ HMBC spectra of the carbon at 158.3 ppm with the aromatic protons of the B-ring (H-2´, -6´, -3´, -5´) and the anomeric proton 1´´ (5.18 ppm) of the glucuronic acid as ^{2}J and ^{3}J couplings, respectively. This carbon can be associated to the position 4´, because all other carbon of the B-ring can be excluded based on HSQC (exclusion of 2´,3´,5´,6´) and the chemical shift in combination with HMBC (exclusion of 1´). Further on, another correlation based on the Nuclear Overhausen Effect (NOE) confirms spatial proximity between the anomeric proton and the proton pairs H-2´, -6´ and H-3´, -5´ (**Figure 41**). Consequently, it can be assumed that the distance between the protons is ≤ 5 Å, which makes the detectable energy transfer of the NOE possible. The analytical data clearly verify that the product of the synthesis was kaempferol-4´-O-β-D-glucuronide.

Synthesis of Kaempferol-7-O-β-D-glucuronide and Kaempferol-7,4´-di-O-β-D-glucuronide

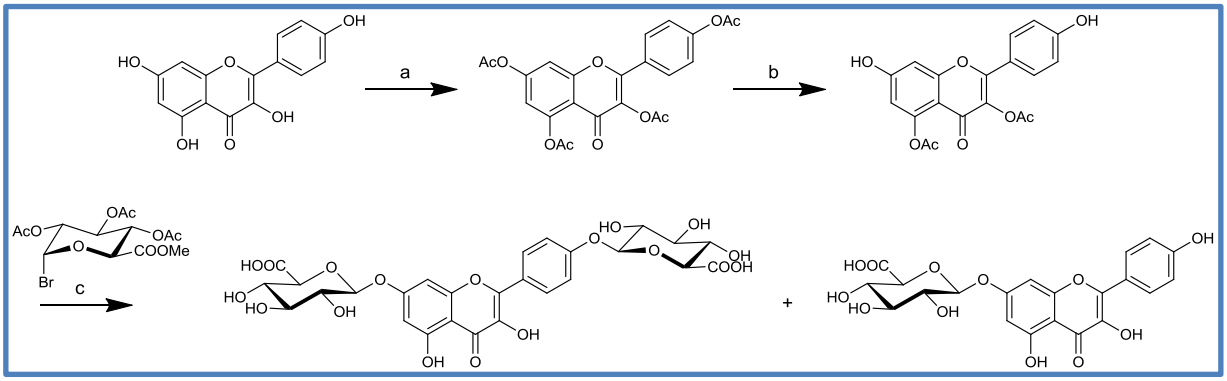

Scheme 2: Synthesis of kaempferol-7-O-β-D-glucuronide and kaempferol-7,4´-di-O-β-D-glucuronide. Reagents and conditions: (a) acetic anhydride, pyridine, reflux, 5 h; (b) *Burkholderia cepacia* lipase, 1-BuOH, THF, 42 °C, 8 days; (c) 1-bromo-2,3,4-tri-O-acetyl-α-D-glucuronic acid methyl ester, Ag_2O, $CaSO_4$, acetonitrile, 4 h; Na_2CO_3, MeOH, H_2O, 1-3 h

The synthesis of kaempferol-7-O-β-D-glucuronide and kaempferol-7,4´-di-O-β-D-glucuronide started with a peracetylation of kaempferol. All four hydroxyl groups of the aglycone were protected as acetic acid esters under alkaline conditions with acetic anhydride. The product was treated with *Burkholderia cepacia* lipase. The addition of 1-butanol enabled a selective transesterification, wherein the protecting groups at position 7 and 4´ were removed, to give the 3,5-diacetylated product. The following modified Koenigs-Knorr glucuronidation was accomplished in a certain stoichiometry to yield in the formation of both desired products, which were again deprotected unter alkaline conditions.

NMR Analysis of Kaempferol-7-O-β-D-glucuronide

The comparison of the ^{1}H NMR spectral data of the glucuronidated product with ^{1}H data of kaempferol shows evidence enough to conclude a substitution at the C-7.

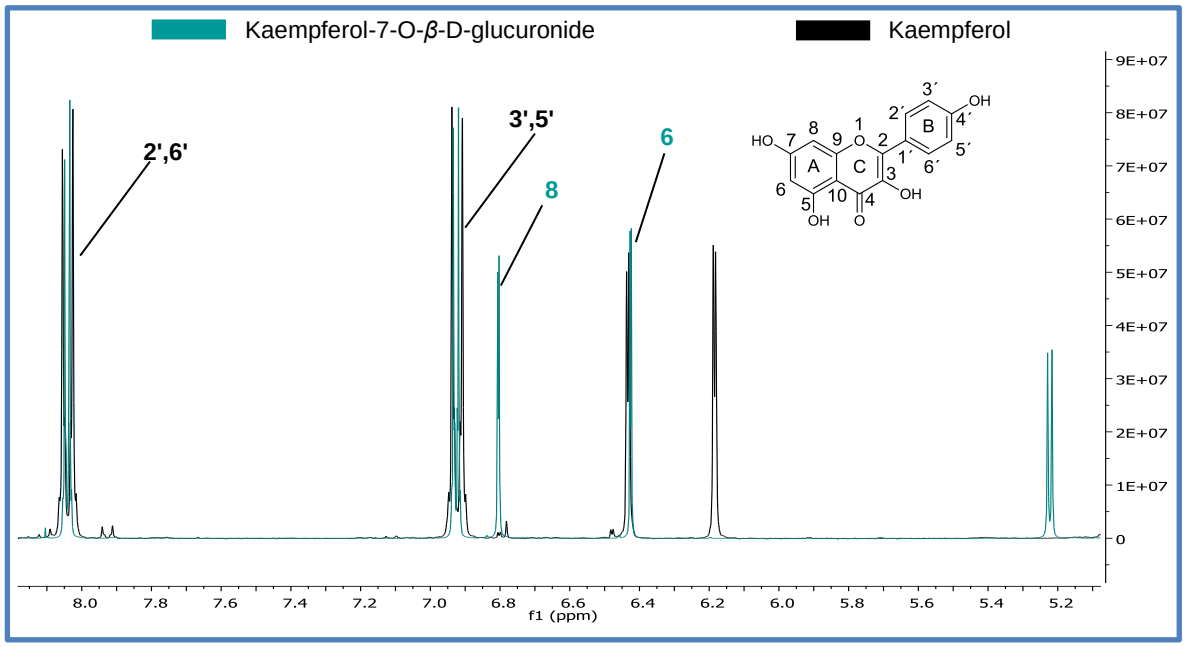

Figure 42: Superimposed ^{1}H NMR spectra of kaempferol and kaempferol-7-O-β-D-glucuronide

Analogously to the signals of kaempferol-4´-O-β-D-glucuronide showing higher ppm values for the aromatic protons of the B-ring due to substitution, **Figure 42** shows the same effect for the aromatic protons of the A-ring. For kampferol-7-O-β-D-glucuronide, the protons of the B-ring remained almost unchanged (~6,92 ppm; ~8,04 ppm). The substitution with a glucuronic acid at position 7 leads for H-8 to a higher chemical shift of 6.80 pm (6.44 ppm for the aglycone). A similar effect can be detected for H-6, where the signal was found at 6.43 ppm for the glucuronide, compared to 6.18 ppm for kaempferol.

Some key correlations of the 2D NMR analysis are presented in **Figure 43** and **Figure 44**. The carbon at position 7 shows cross peaks with the two aromatic protons of the A-ring and the H-1´´ of the glucuronic acid. The latter also gives, due to spatial proximity, a signal in the NOESY with H-6 and H-8.

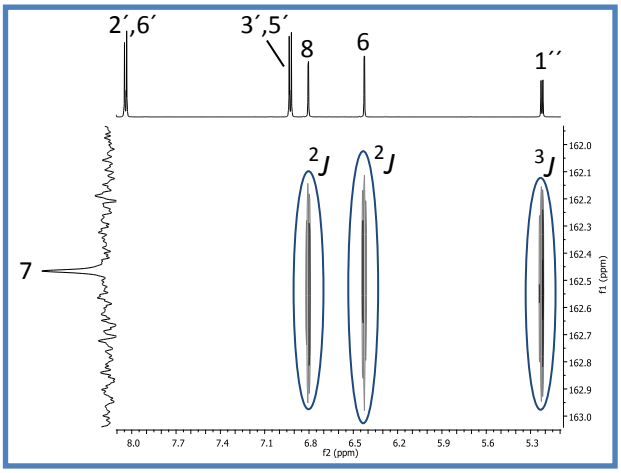

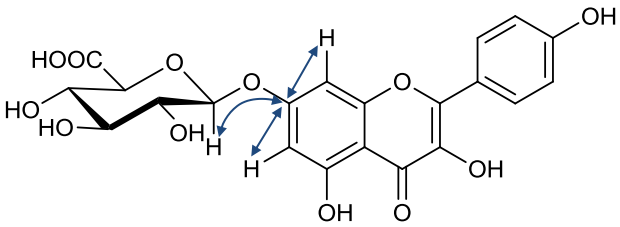

Figure 43: Section of $^{1}H,^{13}C$ HMBC spectral data of kaempferol-7-O-β-D-glucuronide

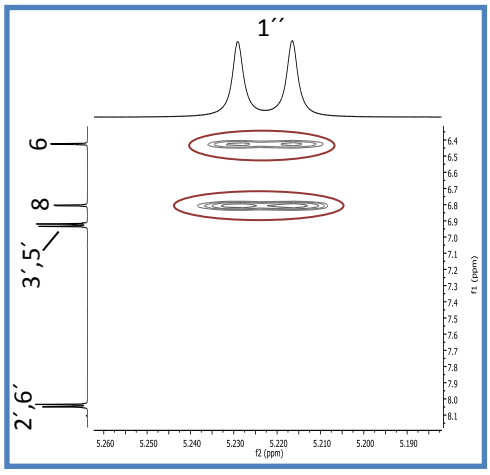

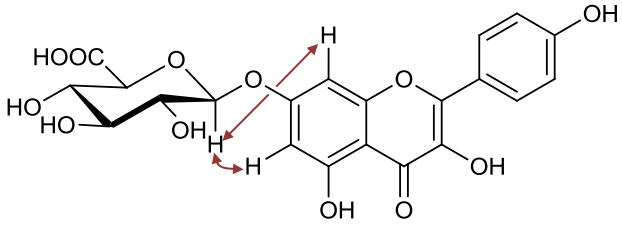

Figure 44: Section of $^{1}H,^{1}H$ NOESY spectral data of kaempferol-7-O-β-D-glucuronide

NMR Analysis of Kaempferol-7,4´-di-O-β-D-glucuronide

The mentioned downfield shift of the aromatic protons in kaempferol-4´-O-β-D-glucuronide and kaempferol-7-O-β-D-glucuronide was consequently also detected and confirmed for kaempferol-7,4´-di-O-β-D-glucuronide. Resonances at higher ppm values were measured for all aromatic protons, the two of the A-ring and the four of the B-ring (**Figure 45**). Further on, two additional dubletts at 5.17 and 5.22 ppm proof the presence of two anomeric protons. The coupling constant is 7.5 Hz for each, which indicated the β-configuration of the glucuronic acids.

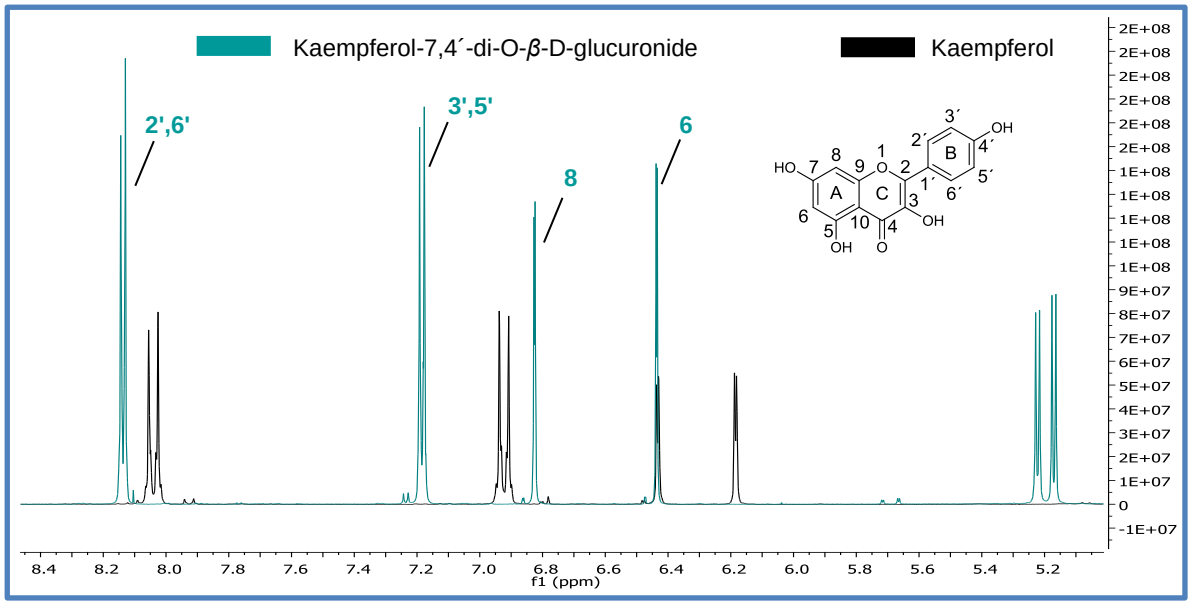

Figure 45: Superimposed ^{1}H NMR spectra of kaempferol and kaempferol-7,4´-di-O-β-D-glucuronide

In the ^{1}H,^{13}C-HMBC (**Figure 46**) the coupling between von C-4´ with H-2´, H-6´ (8.14 ppm) and H-3´, H-5´ (7.18 ppm) as well as to the anomeric proton at 5.17 ppm is clearly visible. Analogously, C-7 shows cross peaks with H-8 (6.83 ppm), H-6 (6.44 ppm) and the other anomeric proton at 5.22 ppm. The cross peak which is not marked based on a correlation between C-5 and H-6.

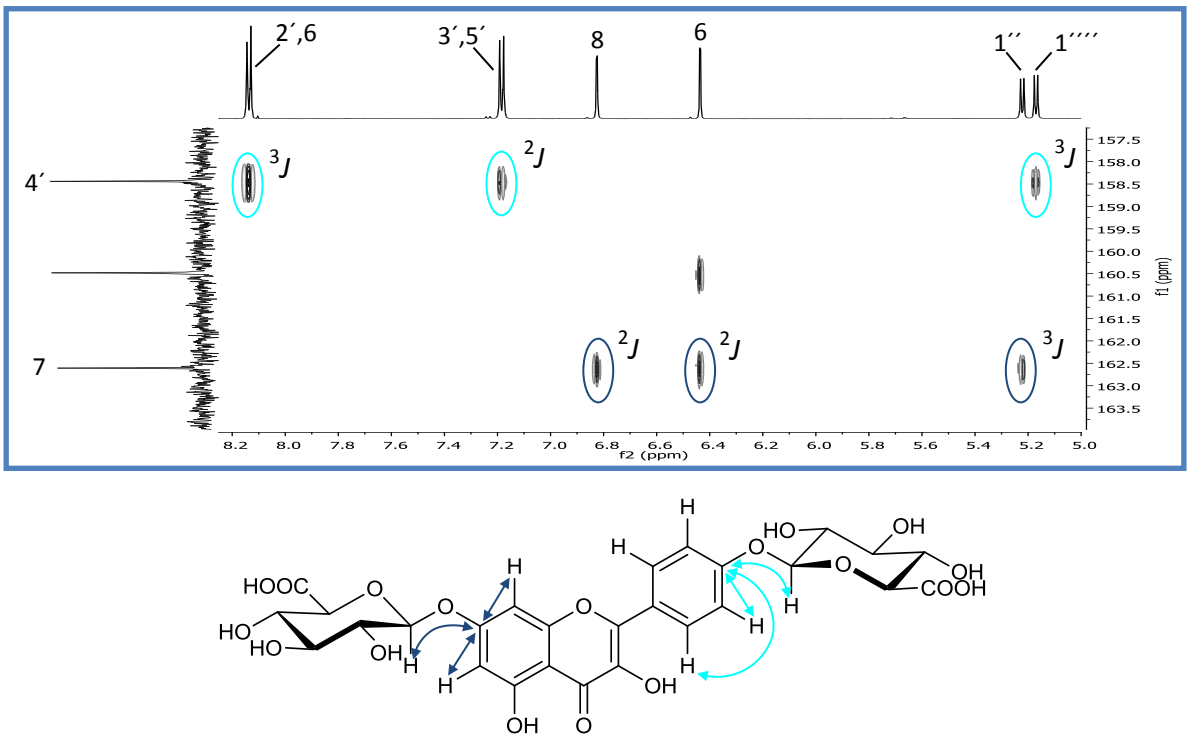

Figure 46: Section of $^{1}H,^{13}C$ HMBC spectral data of kaempferol-7,4´-di-O-β-D-glucuronide

The $^{1}H,^{1}H$-NOESY spectral data again confirms the position of the glucuronic acids (**Figure 47**).

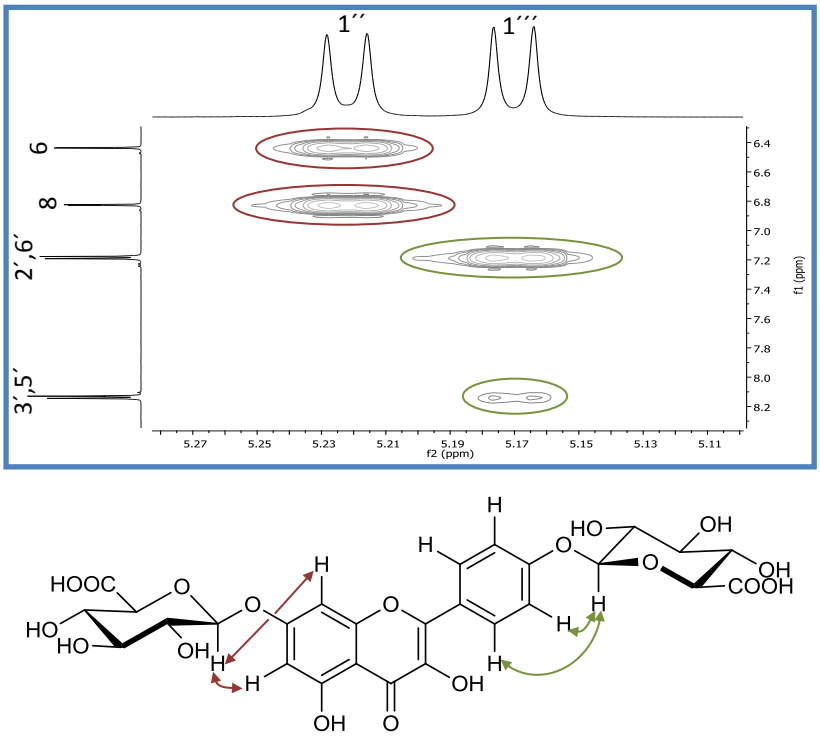

Figure 47: Section of $^{1}H,^{1}H$ NOESY spectral data of kaempferol-7,4´-di-O-β-D-glucuronide

Synthesis of Kaempferol-3-O-β-D-glucuronide

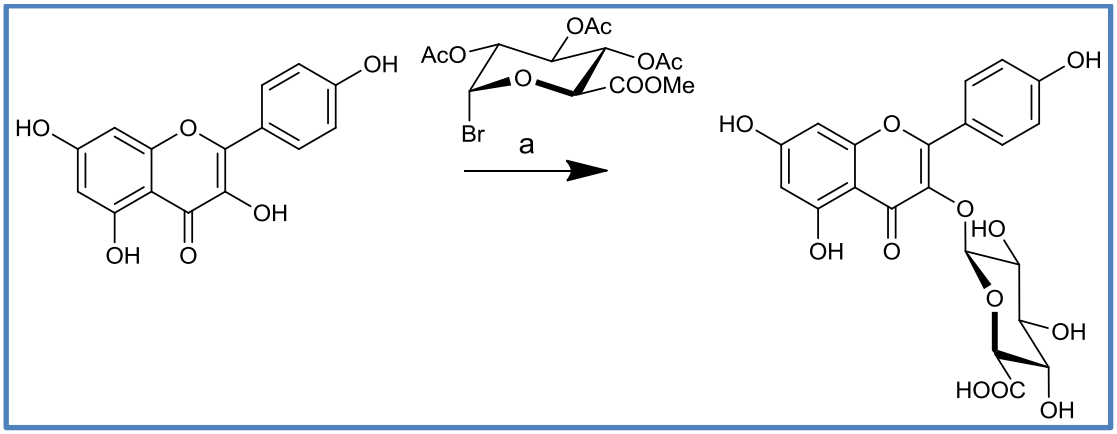

Figure 48: Synthesis of kaempferol-3-O-β-D-glucuronide. Reagents and conditions: (a) 1-bromo-2,3,4-tri-O-acetyl-α-D-glucuronic acid methyl ester, K_2CO_3, DMF, 4 d; following deprotection: Na_2CO_3, MeOH, H_2O, 2 h.

The synthesis of kaempferol-3-O-β-D-glucuronide could be accomplished within two steps, because no primary protection of the aglycone with acetyl- or benzyl groups was necessary. The previous presented glucuronidation by the use of a modified Koenigs-Knorr reaction did not result in the formation of appreciably amounts of any glucuronidated product with this starting materials. In contrast, the desired product was generated under alkaline conditions. Further on, these reaction conditions are most probable also useful for the synthesis of kaempferol-7-O-β-D-glucuronide, which presence can be expected in a fraction after chromatographic purification, due to corresponding shifts in the ^{1}H NMR data.

Concering kaempferol-3-β-D-glucuronide, no remarkable downfield shifts of the aromatic protons of the A-ring and B-ring were observed in comparison to the aglycone, what could be confirmed by the ^{1}H NMR data (**Figure 49**). The presence of the additional dublett at 5.33 (J = 7.4 Hz) again verified the β-configuration of the glucuronic acid.

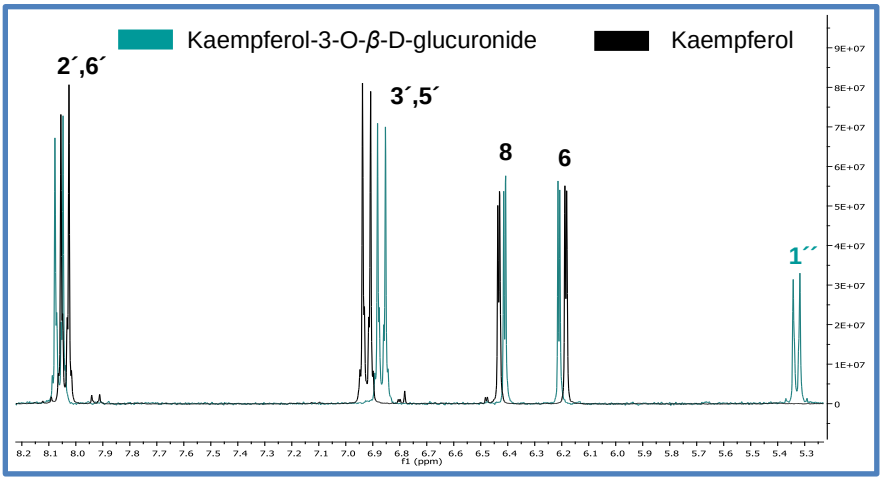

Figure 49: Superimposed ^{1}H NMR spectra of kaempferol and kaempferol-3-O-β-D-glucuronide

Further on, no correlations in the $^{1}H,^{13}C$-HMBC are visible between the anomeric proton 1´´ and any carbon of the A- or B-ring of the flavonol. Just one cross peak with a carbon was detected, which could be assigned to C-3 (**Figure 50**). The $^{1}H,^{1}H$-NOESY spectral data did not show any correlation between the aromatic protons and the proton 1´´.

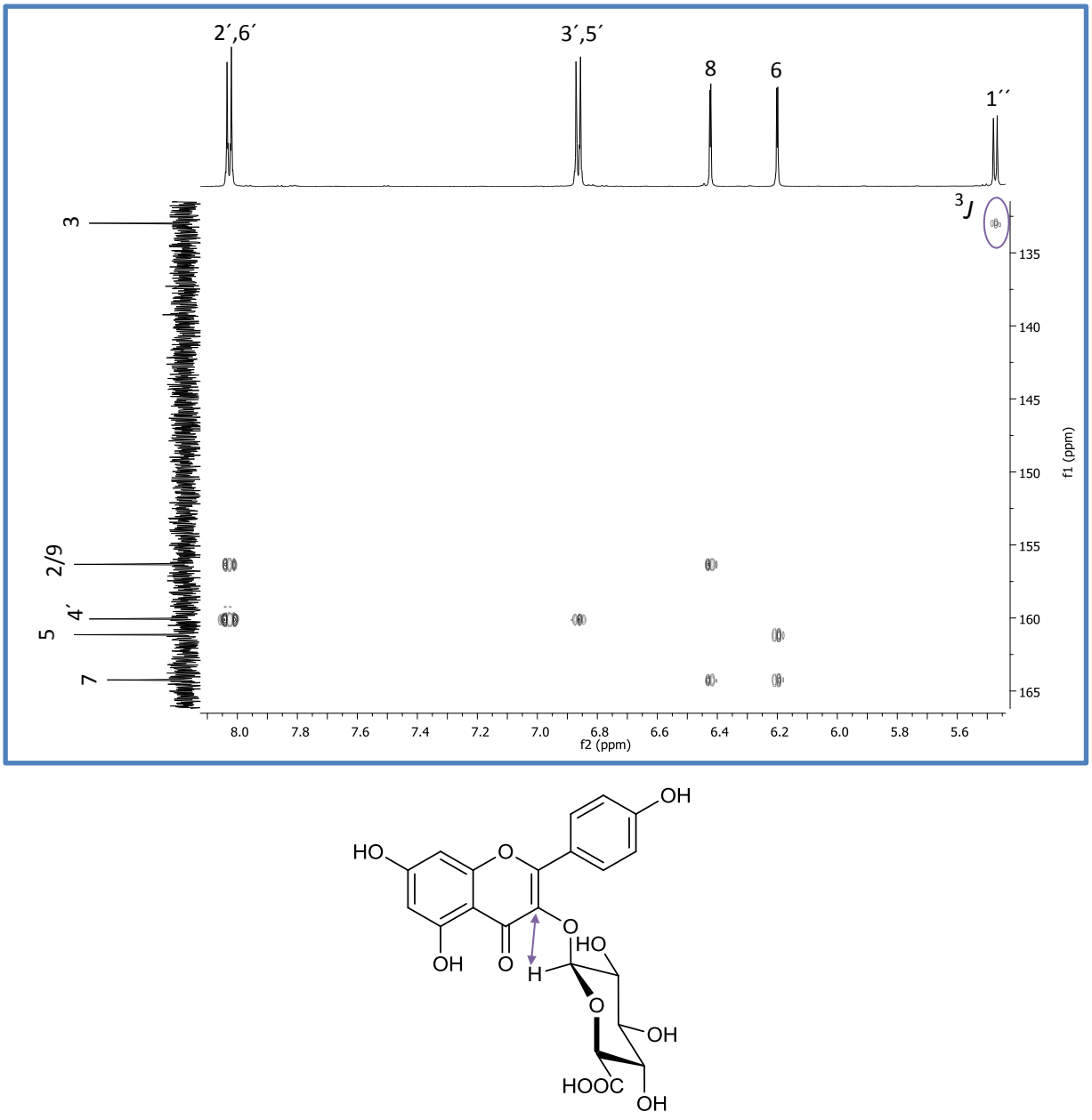

Figure 50: Section of $^{1}H,^{13}C$ HMBC spectral data of kaempferol-3-O-β-D-glucuronide

Synthesis of Kaempferol-7-sulfate

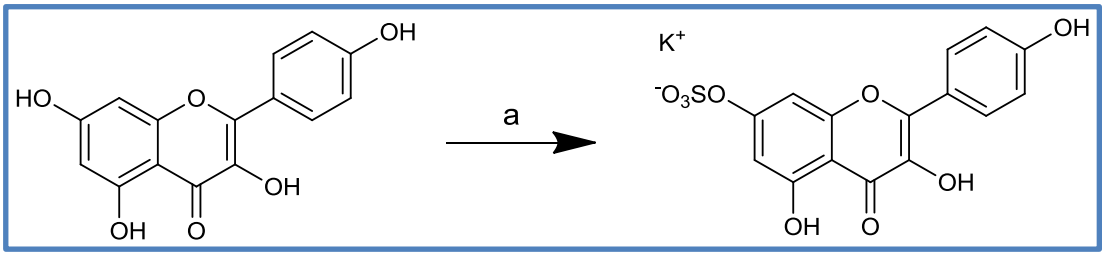

Figure 51: Synthesis of kaempferol-7-sulfate. Reagents and conditions: (a) tetrabutylammonium hydrogensulfate, *N,N´*-dicyclohexylcarbodiimide, pyridine, 2 d; KAc, MeOH.

The synthesis of kaempferol-7-sulfate was accomplished according to literature, but the yield in the present study is much lower (3% ↔ 49%).[59] Barron *et al.* performed the reaction at 4 °C, whereas in the present work the mixture was stirred at room temperature. This increase should, also with regard to the published reaction, enforce the additional sulfation at the hydroxyl functions 3 and 4´, if the stoichiometry concering TBAHS is adequate because the 7-OH group is still the most reactive one. It is more conceivable that the problem of the low yield can be found in the workup of the crude product. Although different chromatographic separation techniques were applied as Barron *et al.* worked with Sephadex LH-20 and in the present study RP-18 silica gel was used, this step should not cause problems. Rather the conversion of the TBA salt to the potassium salt might be the crucial step. The formation of the potassium salt precipitate by the addition of methanolic potassium acetate is probably incomplete. Further experiments have to be made to avoid this significant loss during workup. The presence of a sulfate moiety does not show any additional signal in the ^{1}H NMR, but the electron withdrawing effect of this group results in a downfield shift of H-6 and H-8 (**Figure 52**). The NMR data are in agreement with literature and further confirmation was achieved by HRMS data.

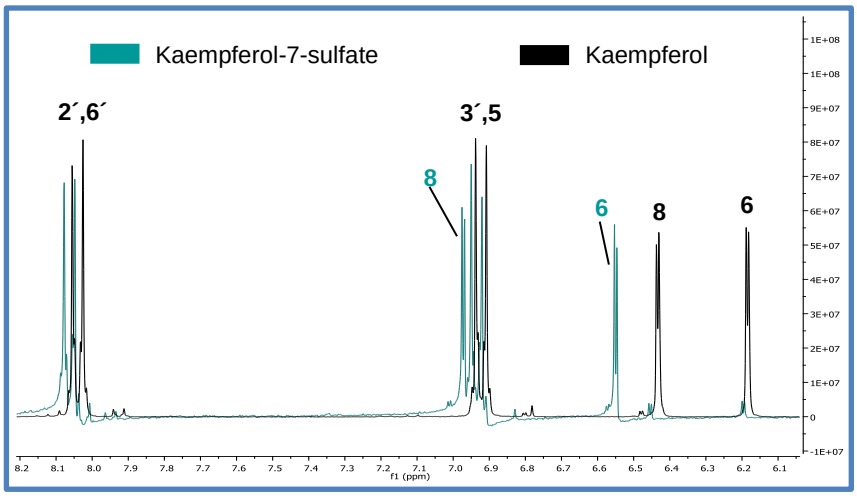

Figure 52: Superimposed ^{1}H NMR spectra of kaempferol and kaempferol-7-sulfate

4 Quantification of Plasma Metabolites

4.1 Introduction

After oral consumption of flavonol glycosides, the compounds will be hydrolyzed to the corresponding sugars and the aglycone. This cleavage can already occur in the oral cavity,[63] but takes place mainly in the jejunum (**Figure 53**).[64,65] The enzymes, which catalyze this reaction are the cytosolic β-glucosidase (CBG) and the lactase phlorozin hydrolase. The latter is a trans-membrane protein, located at the apical side of the enterocytes and enables the hydrolysation in the intestinal lumen.[65] The resulting aglycone has due to its lipophilicity the opportunity to pass the membrane by passive diffusion.[66] Another way for the uptake of the flavonoid glycoside itself into the enterocyte is the active transport *via* a sodium-dependent glucose transporter.[66] A following cleavage of the glycosidic bond by the CBG results also in the formation of the free sugar and the aglycone, which can further be metabolised. Phase-I-metabolism, including among other derivatisations, the attachment of a hydroxyl function by Cytochrom P450, seems to play a negligible part in kaempferol metabolism. At least, kaempferol already has four hydroxyl functions with different reactivity and can thus undergo directly phase-II-metabolism by phenolsulfotransferase (SULT, enterocytes, hepatocytes) and/or uridine-5`-diphospho-glucuronosyltransferase (UGT, enterocytes (UGT1A10), hepatocytes).[67,66] The consequence is the possible conjugation of kaempferol with a sulfate moiety and/or a glucuronic acid. Due to the number of hydroxyl functions,

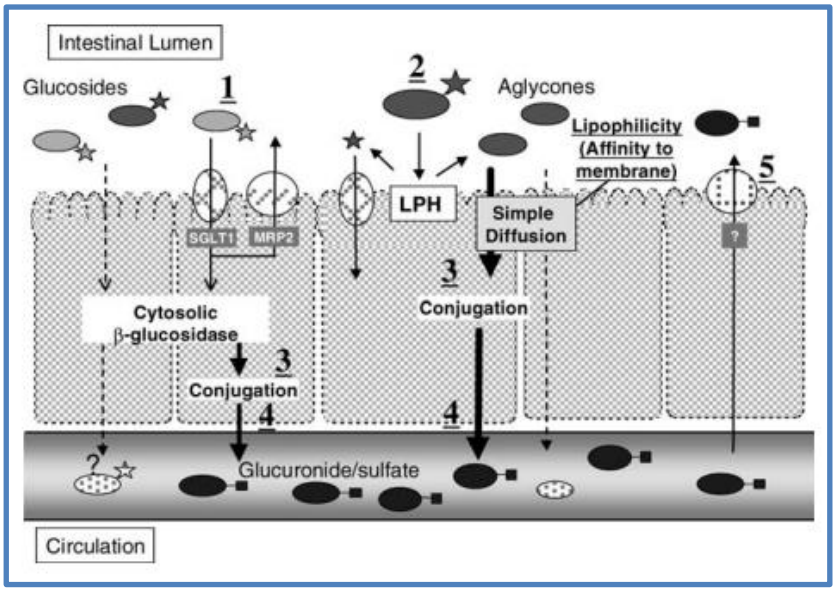

Figure 53: Proposed pathways for small intestinal absorption and metabolism of quercetin glucosides. Annotations: LPH, lactase phloridzin hydrolase; SGLT1, sodium-dependent glucose transporter 1; MRP-2, multidrug resistance-associated protein-2. 1, Quercertin glucosides are directly absorbed *via* SGLT-1 followed by cytosolic β-glucosidase hydrolysis or excretion into the lumen *via* MRP-2; 2, Quercertin glucosides are hydrolyzed by luminal LPH followed by the absorption of resulting aglycones *via* lipophilicity-dependent simple diffusion. 3, Quercertin aglycone in the mucosa is converted into its conjugated metabolites by UDP-glucuronosyltransferase and/or phenol sulfotransferase. 4,5, Conjugated metabolites are transported into the circulatory systems (4) or are excreted into the lumen (5).[109]

different metabolites are conceivable. These compounds can directly be eliminated, but they also undergo enterhepatic circulation (**Figure 54**), which may include again cleavage to form the aglycone, followed by a conjugation with potentially other substituents at different positions.

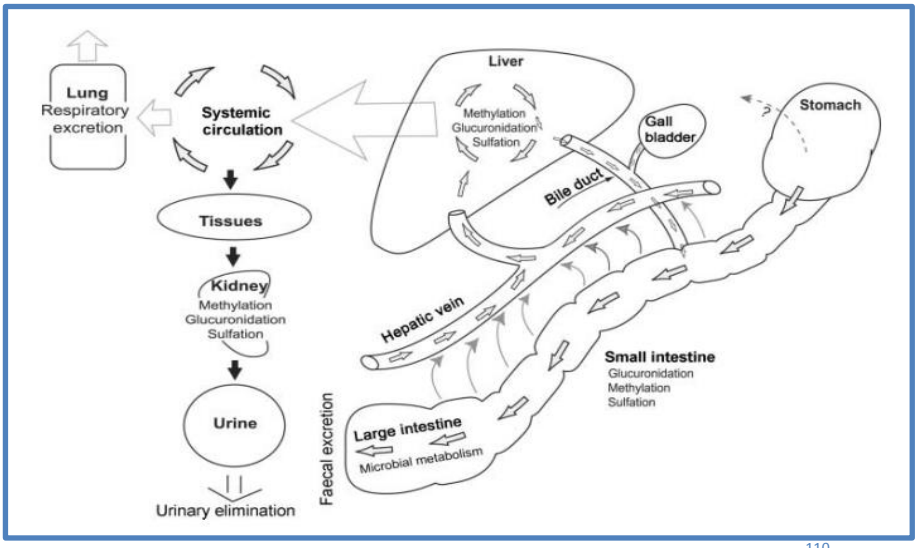

Figure 54: Potential routes of flavonoid absorption, metabolism and elimination[110]

Singh *et al.* (2010) suggested the formation of three kaempferol monoglucuronides after the incubation with UDP-glucuronosyltransferase isoforms. The position of substitution was analyzed according to different λ_{max}.[68] The assumed major metabolites were kaempferol-3-O- and the kaempferol-7-O-β-D-glucuronide. In general this was detected by a hypsochromic shift of band I in the UV spectra (**Table 40**).

Table 36: Hypsochromic shifts of kaempferol glucuronides[68]

Compound	Band II λ_{max} [nm]	Band I λ_{max} [nm]	Δ Shift to aglycone of Band I [nm]
Kaempferol	262.9	366.1	
3-GluA	262.9	348.5	-17.6
7-GluA	262.9	366.1	no change
4´-GluA	262.9	357.8	-8.3

Zhao *et al.* (2010) have discussed the presence of kaempferol-7-O-β-D-glucuronide and kaempferol-3,7-di-O-β-D-glucuronide in bile and blood of rats, respectively.[69] Due to the fact that no characteristic fragmentation peaks of the diglucuronide were reported, the position of the substituents is not clear. Further on, the formation of kaempferol-7-O-β-D-glucuronide is not confirmed by a reference substance, but by the fact, that the 7-OH flavone was predominantly conjugated to form a glucuronide in cultured hepatocytes.[70]

4.2 Material and Methods

4.2.1 Consumable Material

4.2.1.1 Solvents

- H_2O, deionised, further purified by membraPure, Astacus, MembraPure GmbH, Berlin, Germany
- Acetonitrile, LiChrosolv®, ≥ 99.9%, Merck KGaA, Darmstadt, Germany
- Tetrahydrofuran, LiChrosolv®, 99.9%, Merck KGaA, Darmstadt, Germany

4.2.1.2 Chemicals

- Acetic acid, ≥ 99.8%, Merck KGaA, Darmstadt, Germany
- Baicalin, ≥ 99%, Extrasynthese, Lyon, France
- Kaempferol-3-O-β-D-glucuronide, ≥ 98%, Extrasynthese, Lyon, France
- L-Ascorbic acid, 99%, Sigma-Aldrich, Steinheim, Germany
- Sodium acetate, Merck KGaA, Darmstadt, Germany; for sodium acetate buffer, 2 M, pH = 4.7 (adjusted with acetic acid); before use, addition of ascorbic acid (10 mg/mL)
- Sulfatase, from *Helix pomatia*, ≥ 10000 U/g, Sigma-Aldrich, Steinheim, Germany
- Trifluoroacetic acid, 99%, Sigma-Aldrich, Steinheim, Germany
- β-Glucuronidase, type B-10, from bovine liver, ≥ 10100 U/g Sigma-Aldrich, Steinheim, Germany

4.2.1.3 Others

- Eppendorf tubes 3810X, 1.5 mL, Eppendorf AG, Hamburg, Germany
- Syringe filter unit, Perfect-Flow (r), regenerated cellulose, 0.2 µm, 13 mm, WICOM Germany GmbH, Heppenheim, Germany
- Syringe Injekt®-F, 1 mL, B.Braun Melsungen AG, Melsungen, Germany

4.2.2 Instruments

- Pipettes, 0.5-10 µL, 10-100 µL, 100-100 µL, Eppendorf AG, Hamburg, Germany
- Vortex mixer VV3, VWR, Darmstadt, Germany
- Centrifuge, Jouan BR4i multifunction centrifuge, Thermo Electron Corporation, Waltham, MA, USA
- Mass spectrometer:
    - Q-TOF 6540 UHD, Agilent, Santa Clara, USA
    - Electrospray ionization (ESI)
- Analytical HPLC
    - Column: Hibar® 250-4, Purospher® STAR, RP18e (5 µm), Column No.: 027444, Merck KGaA, Darmstadt, Germany
    - Precolumn: LiChroCART® 4-4, Purospher® STAR, RP18e (5 µm), Merck KGaA, Darmstadt, Germany
    - Pump: Hitachi L-2130, VWR, Darmstadt, Germany

- Autosampler: Hitachi L-2200, VWR, Darmstadt, Germany
- Column Oven: Hitachi L-2350, VWR, Darmstadt, Germany
- Diode Array Detector: Hitachi L-2455, VWR, Darmstadt, Germany
- Software, EZChrom Elite, Version 3.3.2 SP2, VWR, Darmstadt, Germany

4.2.2.1 Chromatographic Separation

The following method was used for plasma quantification. For HPLC-MS analysis of plasma samples the same gradient was used, but other solvents, namely A: 10 mM NH_4HCO_3 in H_2O, B: acetonitrile.

Instrument:	Analytical HPLC
Oven:	23 °C
Thermo Unit:	4 °C
Column:	Precolumn: LiChroCART® 4-4, Purospher® STAR RP-18e (5 µm)
	Main Column: Hibar® 250-4, Purospher® STAR RP-18e (5 µm)
Mobile Phase:	A: H_2O/THF 98.3/1.7 + 0.1% TFA, B: acetonitrile
Injection Volume:	20 µL
Flow	1.1 mL/min
Gradient:	0 min: 10% acetonitrile
	0-2 min: 10% acetonitrile
	9 min: 25% acetonitrile
	17 min: 35% acetonitrile
	22 min: 50% acetonitrile
	25 min: 100% acetonitrile
	25-30 min: 100% acetonitrile
	32 min: 10% acetonitrile
	32-39 min: 10% acetonitrile

4.2.3 Sample Preparation

All plasma samples were frozen at -80 °C and were just defrosted to form aliquots for sample preparation. Unless otherwise indicated, the samples were treated at 0 °C.

- 50 µL plasma aliquot
- Addition of 0.5 µL aqueous ascorbic acid solution (c = 202 mmol/L, c_f = 1 mmol/L)
- Addition of the internal standard (IS): 3 µL baicalin solution (c = 50 µmol/L in acetonitrile)
- Addition of 47.5 µL acetonitrile for protein precipitation
- Vortex at 4 °C for 5 min (Level 4.5)
- Centrifugation at 4 °C for 10 min at 14000 rpm
- Filtration: 0.2 µm, regenerated cellulose
- HPLC analysis

4.2.4 Calibration Curve Parameter

For each of the expected metabolite, namely kaempferol-3-O-β-D-glucuronide, kaempferol-7-O-β-D-glucuronide, kaempferol-4'-O-β-D-glucuronide, kaempferol-7,4'-di-O-β-D-glucuronide, kaempferol-7-sulfate and the aglycone kaempferol, a calibration curve was determined based on the following parameters.

- Three times weight of each compound
- Stock solution in DMSO with c = 50 mmol/L
- 2nd stock solution: dilution with acetonitrile to c = 50 µmol/L
- Mixture of equal volumes of each 2nd stock solution → 3rd stock solution
- 1, 2, 2.5, 3, 4, 5, 6, 7 and 9 µL of 3rd stock solution were added to the appropriate amount of blank plasma matrix (supernatant after protein precipitation, centrifugation and filtration) to a final volume of 101 µL
- Addition of 0.5 µL aqueous ascorbic acid solution (c = 202 mmol/L, c_f = 1 mmol/L)
- Addition of the internal standard (IS): 3 µL baicalin solution (c = 50 µmol/L in acetonitrile)
- Basically, 27 values were measured for each compound (9 concentrations), which were corrected according to the Limit of Quantification

4.2.5 Tentative Investigation with Glucuronidase and Sulfatase

- 50 µL of plasma
- Addition of 5 µL glucuronidase (10 mg/mL in sodium acetate buffer) or 5 µL glucuronidase (10 mg/mL in sodium acetate buffer) + sulfatase (1.6 mg)
- Incubation for 2 h at 37 °C and 5% CO_2 in the dark
- Addition of 55 µL acetonitrile for protein precipitation
- Workup according to **4.2.3 Sample Preparation**

4.3 Results and Discussion

For the workup of the plasma samples, a method was developed fullfilling the following prerequisites:

- Recovery ≥ 90 %
- Fast method → avoiding rotation evaporater, centrifugal evaporator or nitrogen stream
- Least possible dilution of the plasma samples with organic solvent for protein precipitation and thus avoiding an unnecessary decrease in the concentration of metabolites with regard to the limit of quantification (LOQ)

For the method development baicalin was added to blank plasma. Acetonitrile was applied as one volume equivalent for protein precipitation. The workup procedure was followed by a modified HPLC method[71] to evaluate the LOQs and the recovery of all reference substances. The chromatographic analyses showed a good separation of the reference substances and the internal standard **(Figure 55**). The formation of a double peak for kaempferol-7,4-di-O-*β*-D-glucuronide required an analysis by HPLC-MS. Thereby, it could be confirmed that the double peak is assignable to one *m/z* value and thus be regarded and integrated as one peak. The resulting limits of quantification for all the expected metabolites are presented in **Table 37**.

Table 37: Chromatographic and analytical data of the references

Compound	t_R [min]	Recovery [%]	LOQ [ng/mL]	f(x)	R^2	Interday precision (n = 6) [%]	Intraday precision (n = 6) [%]
7,4´-DigluA	11.2	84 ± 14	~ 130	3.8364x – 0.0474	0.996	12.0	11.8
3-GluA	14.5	92 ± 16	~ 100	2.5360x + 0.1723	0.959	9.1	7.6
7-GluA	15.3	83 ± 10	~ 60	5.2085x + 0.1163	0.989	10.4	4.6
4`-GluA	16.2	70 ± 7	~ 100	4.0474x + 0.2827	0.981	13.4	8.8
Baicalin, IS	16.6	106 ± 10				5.5	1.3
7-Sul	17.0	139 ± 26	~ 120	1.5873x + 0.1473	0.933	9.1	11.3
Kaempferol	23.5	83 ± 10	~ 50	5.7094x + 0.1018	0.990	6.4	10.3

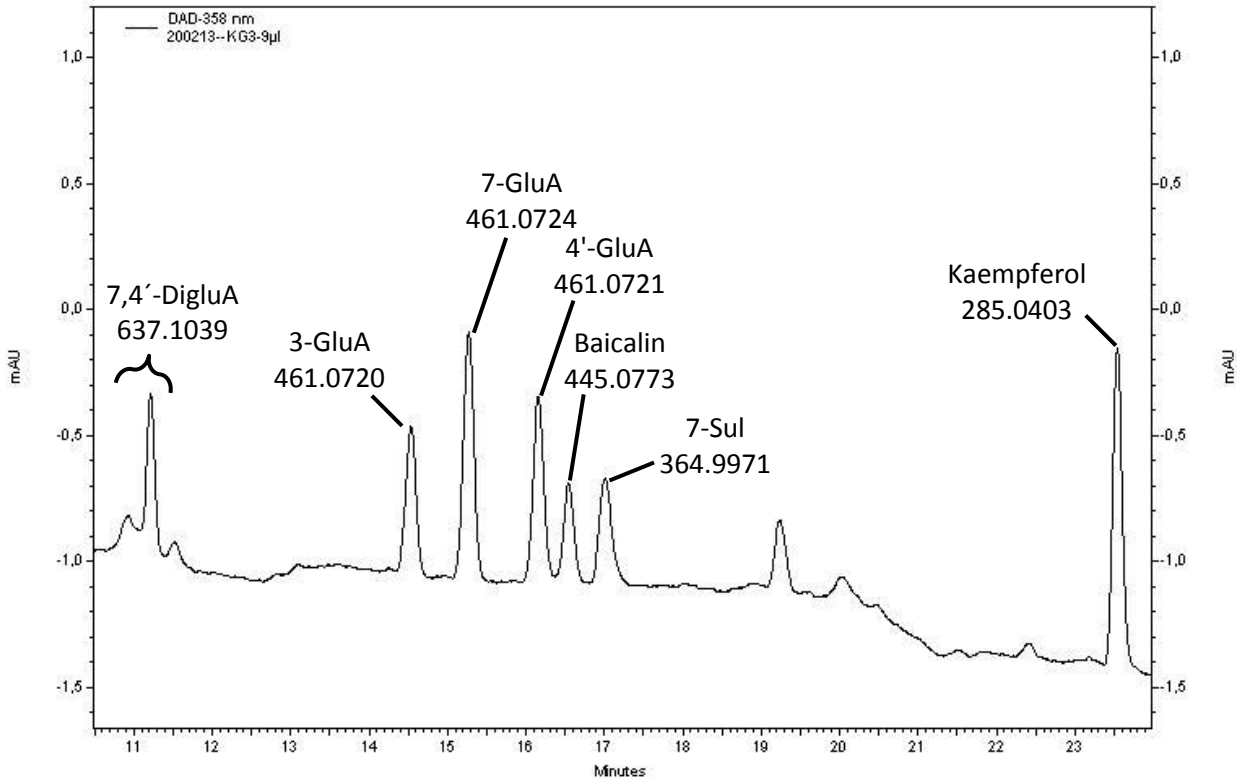

Figure 55: HPLC analysis of all references and the internal standard after addition to blank plasma and usual workup. MS data were obtained from a separate run. CC according to 4.2.2.1

For the following *in vivo* study, the four predominant kaempferol glycosides in the *Ginkgo* folium extract EGb 761® were administered to Spraque Dawley rats equal to the dosage of 600 mg/kg of the extract. As already described in the extract quantification, (page 42) kaempferol rutinoside has the highest content and was consequently used in the highest dose. For each of the five time points (1, 2, 4, 8 and 24 h) the plasma samples of five rats were taken. Unfortunately, only the plasma samples after administration of kaempferol rutinoside could be used for identification and quantification of the major metabolites by HPLC-UV. The other ones, which were obtained after a single dose of kaempferol biloside, acylated kaempferol biloside and kaempferol triglycoside, respectively, were below the limit of detection. This is based in the different contents of the kaempferol glycosides in the extract and consequently different dosage.

To make this more obvious, **Table 38** illustrates dosage and percentage of each kaempferol glycoside and the corresponding kaempferol content compared to the total kaempferol (glycosides) content. Beside, it should be noted, that this calculation based on an approximation which does not regard the other four kaempferol glycosides in EGb 761®,

which could be detected by HPLC-MS analysis. But as already shown, these compounds are present in much lower contents in the extract. Nevertheless, the knowledge on the content of the four low concentrated kaempferol glycosides is not necessary if just the distribution of the kaempferol dosage for the rutinoside, biloside, triglycoside and acylated biloside is regarded.

Table 38: Content of four kaempferol glycosides in EGb 761®, resulting dosage for *in vivo* study and approximation of the kaempferol (glycoside) percentages in EGb 761®

	Rutinoside	Biloside	Triglycoside	Acyl. Biloside
Content in EGb 761® [% w/w]	**2.17**	**0.89**	**1.58**	**1.59**
M [g/mol]	594.16	594.16	740.22	740.20
Dosage for *in vivo* study [mg/kg]	**13.0**	**5.3**	**9.5**	**9.5**
Content based on the four kaempferol glycosides [% w/w]	34.83	14.29	25.36	25.52
≙ Calculated content of kaempferol [% w/w]	**38.72**	**15.88**	**22.63**	**22.77**

This listing shows, that the other three kaempferol glycosides were administered in more or less half of the dosage compared to kaempferol rutinoside, if the percentage of the aglycone is regarded (last line of **Table 38**). Due to this difference, the presence of the corresponding metabolites had to be confirmed by HPLC-MS. A comparison of the corresponding retention times and the *m/z* values with the reference substances is presented below.

4.3.1 Identification of Kaempferol Metabolites

Kaempferol rutinoside was administered at a concentration of 13 mg/kg. After sample workup and HPLC-UV analysis, two signals in the chromatogram could be assigned to the appropriate peaks of the reference substances (**Figure 56**).

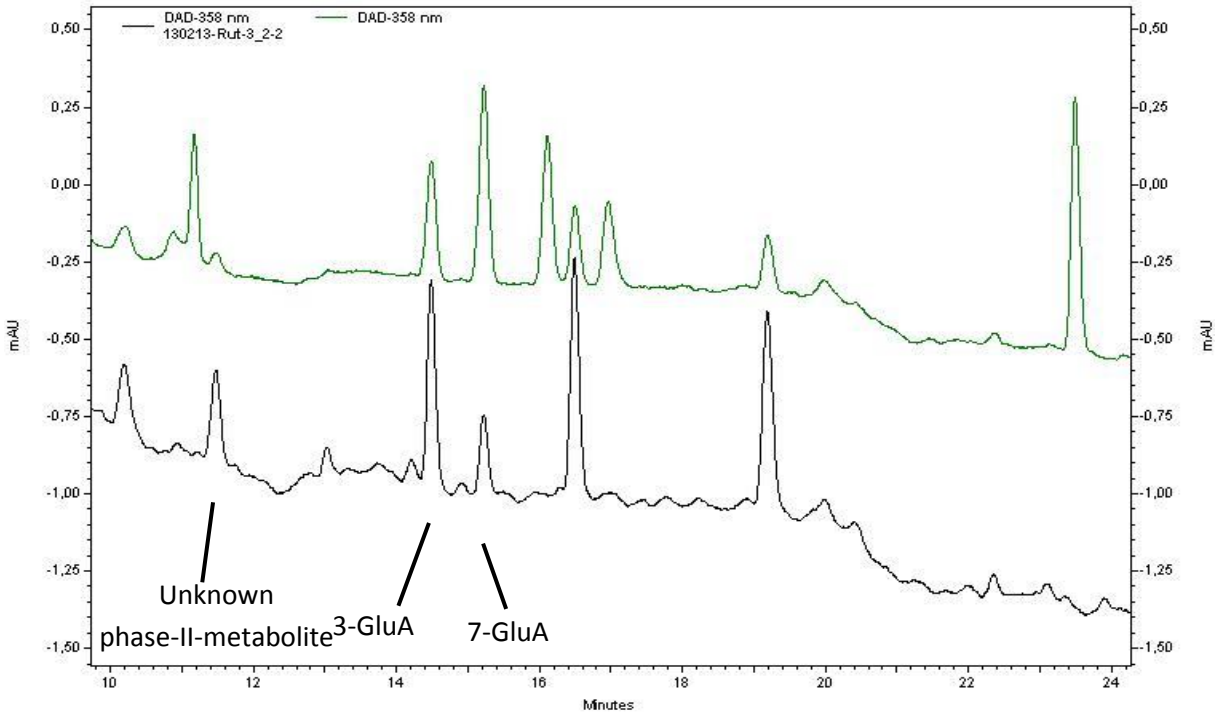

Figure 56: Comparison references (green) and plasma sample (black, 4 h) by HPLC-UV at 358 nm. CC according to 4.2.2.1

The coelution of two compounds in the plasma with the reference substances kaempferol-3-O-β-D-glucuronide (14.6 min) and kaempferol-7-O-β-D-glucuronide (15.3 min) confirmed the presence of these metabolites *in vivo*. Further on, another phase-II-metabolite of kaempferol was detected at 11.6 min, which cannot be assigned to the expected kaempferol-7,4´-di-O-β-D-glucuronide (11.2 min) due to the difference in the retention time.

In order to get an evidence for the identification of this metabolite, one exemplarily chosen plasma sample was treated once with glucuronidase/sulfatase and once solely with glucuronidase. In both cases, the signals for the two monoglucuronides and the unknown metabolite disappeared and almost the same integral for the resulting kaempferol aglycone was measureable (**Figure 57**).

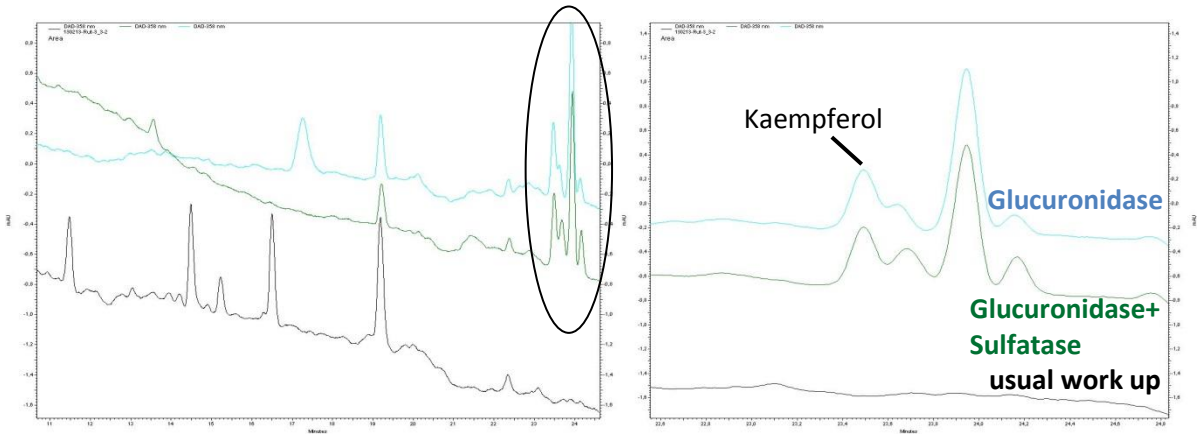

Figure 57: HPLC-UV at 358 nm, test workup of plasma samples (4 h) with glucuronidase and/or sulfatase compared to unhydrolyzed sample. CC according to 4.2.2.1

But interestingly, after the incubation with solely glucuronidase, a further peak occured at a retention time of 17.3 min (**Figure 58**). Due to the difference in the retention time, this signal cannot be assigned to kaempferol-7-sulfate (17.0 min).

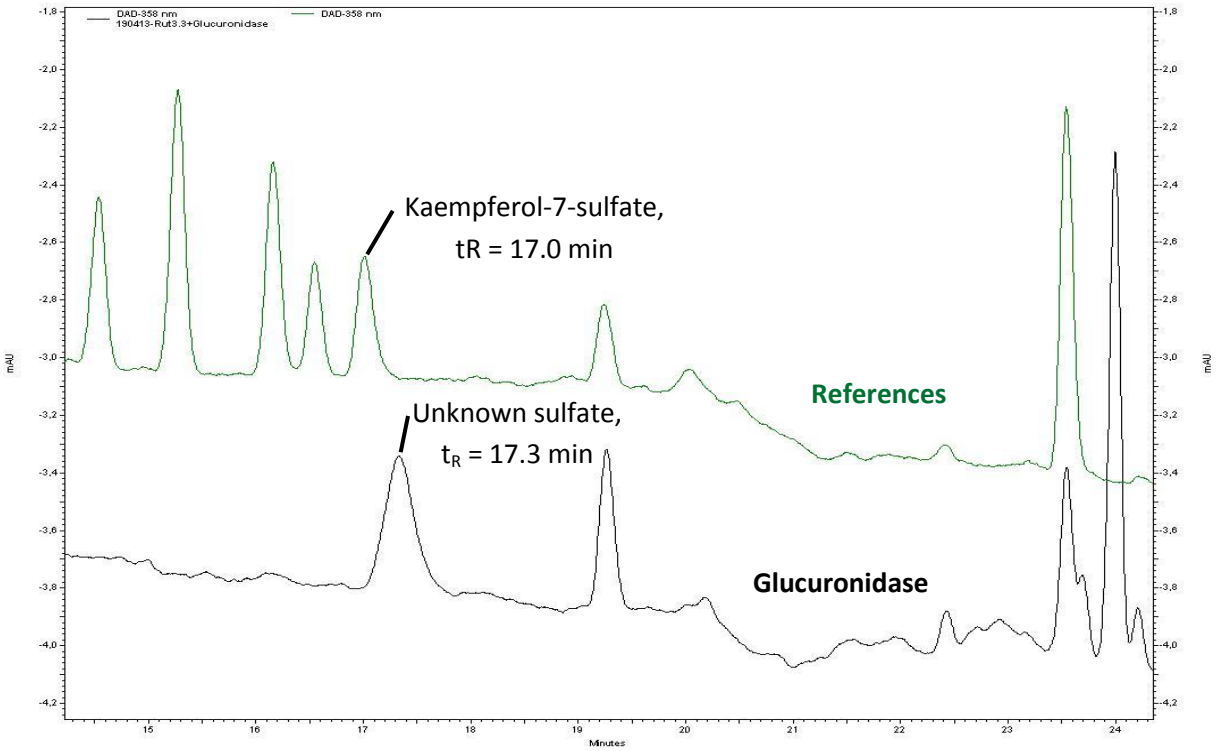

Figure 58: HPLC-UV at 358 nm, test workup of plasma samples (4 h) with glucuronidase compared to references. CC according to 4.2.2.1

Assuming that this peak disappeared after glucuronidase/sulfatase hydrolysis (**Figure 57**), the corresponding compound is most probably conjugated with a sulfate moiety. Further on, a missing increase concerning the kaempferol integral leads to the conclusion, that unfortunately, the hydrolysis products of the corresponding compound after treatment with glucuronidase/sulfatase are unkown. Nevertheless, it can be said that the unkown phase-II-metabolite of kaempferol must be substituted with at least one glucuronic acid and at least one sulfate group. In order to get more structural information and with regard to the plasma samples which were under the LOD by HPLC-UV, an investigation by HPLC-MS was accomplished.

4.3.2 Plasma Analysis by HPLC-MS

The plasma samples which were obtained after the oral administration of the following kaempferol glycosides were not quantifiable by HPLC-UV, nor any metabolites could be detected with this method.

- 3-O-(2-O, 6-O-Bis(α-L-rhamnosyl)-β-D-glucosyl)kaempferol **(Triglycoside)**
- 3-O-(2-O-(β-D-glucosyl-α-L-rhamnosyl)kaempferol **(Biloside)**
- 3-O-(2-O-(6-O-(*p*-Hydroxy-trans-cinnamoyl)-β-D-glucosyl)-α-L-rhamnosyl)kaempferol **(Acylated Biloside)**

In consequence, one plasma sample for each compound was chosen exemplarily at the time point of 4 h and analyzed by a more sensitive HPLC-MS method to identify possible metabolites below the LOD in HPLC-UV. The assignment to a certain metabolite was based on comparison of retention time and *m/z* value (**Table 39**).

Table 39: Results of HPLC-HRMS of plasma samples compared to references

	DigluA t_R [min] *m/z*	**GluA-sulfate** t_R [min] *m/z*	**3-GluA** t_R [min] *m/z*	**4´-GluA** t_R [min] *m/z*	**7-GluA** t_R [min] *m/z*	**7-Sulfate** t_R [min] *m/z*
Reference	3.674 637.1050	not available calc *m/z* $[M-H]^-$ 541.0294	8.335 461.0727	8.926 461.0727	10.142 461.0728	15.477 364.9976
Rutinoside		7.458 541.0295	8.241 461.0726	8.944 461.0732	10.126 461.0730	15.524 364.9969
Biloside		7.428 541.0295	8.261 461.0732	8.893 461.0731	10.121 461.0747	15.531 364.9976
Acylated Biloside		7.417 541.0296	8.254 461.0725	8.870 461.0728	10.127 461.0756	15.488 364.9974
Triglycoside		7.423 541.0294	8.325 461.0728	8.889 461.0727	10.104 461.0736	15.435 364.9973

Overall, the presence of five kaempferol metabolites could be shown, which include the three expected monoglucuronides and the sulfate. Further on, a clear assignment of the previous mentioned unknown metabolite to a mixed kaempferol glucuronide-sulfate can be made. It has to be noted that no signal of a kaempferol diglucuronide was detectable. This does not necessarily exclude the presence of a diglucuronide, because the reference

substance, kaempferol-7,4´-di-O-β-D-glucuronide is eluting very early (3.7 min) and thus the signal is possibly overlapped by some other peak.

Finally, it could be shown that the three major metabolites of kaempferol rutinoside, which are quantifiable, are:

- Kaempferol-3-O-β-D-glucuronide
- Kaempferol-7-O-β-D-glucuronide
- Kaempferol glucuronide-sulfate

4.3.3 Quantification of Kaempferol Metabolites

In the next step, the plasma levels at three different time points (4 h, 8 h, 24 h) were quantified (**Table 40**). After 1 and 2 h, no kaempferol metabolites could be detected. It has to be admit that due to unavailability of a mixed kaempferol glucuronide-sulfate as reference substance, this metabolite was, with regard to the synthesized compounds, quantifed as the only accessible disubstituted kaempferol, namely kaempferol-7,4´-di-O-β-D-glucuronide.

The plasma samples of five rats for each time point were measured three times.

Table 40: Plasma levels after the administration of kaempferol rutinoside, measurements were performed in triplicates, $n_{maximal}$: 5 plasma samples, n.d.: not detectable

Identified metabolite	c [ng/mL] 4 hours	c [ng/mL] 8 hours	c [ng/mL] 24 hours	AUC [ng*h/mL]
GluA-sulfate	273 ± 83, n=5	294 ± 79, n=5	187 ± 30, n=5	4982
3-GluA	383 ± 137, n=4	detectable, n=2	n.d., n=5	
7-GluA	30 ± 6, n=3	n.d., n=5	n.d., n=5	
≙ Calculated concentration of aglycone	400 ± 94	155 ± 42	99 ± 16	

Comparison to published data

In order to discuss the results with published data, just the plasma concentration of the aglycone can be regarded, which had to be calculated.

Within a comparable study from Rangel-Ordóñez *et al*. in 2010, the extract was administered to the same species of rats in a concentration of 600 mg/kg. The resulting maximum plasma concentration of kaempferol (acidic hydrolysis of the phase-II-metabolites was accomplished) was achieved 8 h after administration. They reported a value of 341 ng/mL, but the standard degression is not exactly mentioned and can thus just be estimated to ± 47 ng/mL based on a figure in the publication (**Figure 59**). In our study, the three different kaempferol metabolites were quantified, but these values can be calculated down to the aglycone concentration with the adequate quotient of the molecular masses. The condensed calculated kaempferol concentration are shown in the last line of **Table 40.** Consequently, the maximum plasma concentrations of the aglycone presented in literature with a value of 341 ± 47 ng/mL is very similar to the one in the present study with 400 ± 94 ng/mL. Of course, it has to be mentioned that Rangel-Ordóñez *et al*. administered the extract EGb 761® and thus considerably more kaempferol compared to the solely administration of kaempferol rutinoside. To be more exact and with regard to **Table 38** (page 92), the dosage of kaempferol in our study was about 39% compared to the extract administration. In this context, it can be estimated that a general maximum plasma concentration ~350 ng/mL is conceivable. This value can on one hand be achieved by the administration of the extract and on the other hand just by the content-depended administration of the predominat kaempferol glycoside, namely kaempferol rutinoside.

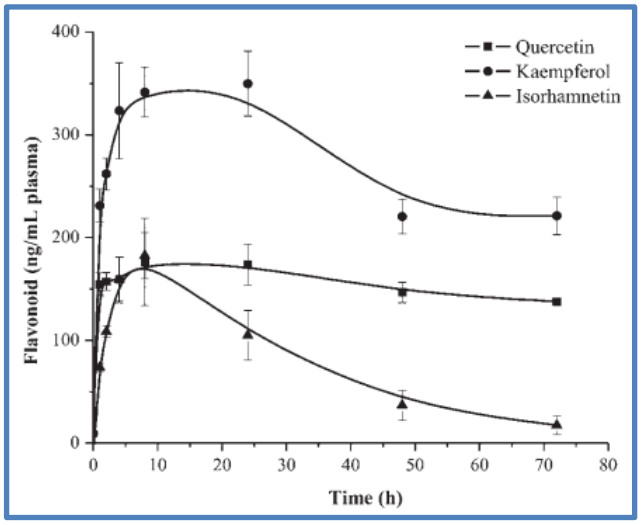

Figure 59: Time course of plasma concentrations of quercetin (squares), kaempferol (circles), and isorhamnetin (triangles) following a single oral dose of 600 mg/kg of EGb 761®. Each point represents the mean ± SEM of six samples[50]

Nevertheless, the differences in both studies should not be left unattended. Beginning with the dosage form, it can be assumed that the following resorption of the compounds is not the same for the extract and the pure kaempferol glycoside, respectively. Further on, the sample workup is not comparable. Rangel-Ordóñez *et al*. performed acidic hydrolysis with 2 M HCl at 90 °C, wherein in the present study no hydrolysis was achieved and the workup procedure was accomplished at maximum 4 °C. Finally, it has to be admit that in the present study, the mixed kaempferol glucuronide-sulfate was quantified based on a calibration curve of kaempferol-7,4´-di-O-β-D-glucuronide. Consequently, the evaluated plasma concentration can have a different value if the exact reference substance is used.

Application of other Detectors

Basically, it can be expected that the oral administration of different kaempferol glycosides does not result in the formation of different metabolites. Nevertheless, a difference in the relative plasma concentration and the time point of maximal plasma concentration are conceivable. The most obvious option for this investigation in the present study would be to adjust the dosage of the biloside, acylated biloside and triglycoside to the same of rutinoside with regard to the kaempferol percentage and thus independent to the content in EGb 761®. But further on, the usage of more sensitve detectors can be discussed.

The use of an electrochemical detector (ED) is basically possible, but it has always be regarded that a hydrolysation of the kaempferol metabolites is not desirable in the present study design. Nevertheless, it is known that at least a glycosilation at 3-OH has no strong effect on the electrochemical behaviour.[72] Consequently, one main metabolite in the present study, kaempferol-3-O-β-D-glucuronide, should be combinable with this method. Further on, Guo *et al.* (1997) reported a linear relationship between oxygen radical absorbance capacity (ORAC) of aqueous extracts from fruits and vegetable including kaempferol glycosides containing plants (e.g. strawberry) and the accessibility for electrochemical detection.[73] The result of the ORAC assay for some of the synthesized kaempferol derivatives are presented further down (page 111). One problem of the ED can be the adsorption of electrochemical products to the surface of the electrode and thus a decrease of the initial capacity, but a method with HPLC-ED might be worth to try.[72]

The use of a fluorescence detector is conceivable, due to the metal chelating activity of kaempferol. For this, a post-column derivatization has to be accomplished, wherein a aluminium chelate complexes is formed.[50] The disadvantage of this method is, that a free 3-OH group is essential for the formation of the complex.[74] Thereby, one of the major metabolites, namely kaempferol-3-O-β-D-glucuronide is not measurable.

5 Pharmacological Characterisation of Kaempferol and Conjugates

5.1 Introduction

Neurotoxicity and Neuroprotection Assay

Neuronal damage can be based on several reasons like i.e. failure in metabolic processes, protein impaired mitochondrial function, increased oxidative damage, defect in the proteasome system, protein aggregation, changes in iron metabolism or events of excitotoxicity and inflammation.[75] Oxidative stress might be a reason for at least some of these failures and is a consequence of a disturbed homeostasis between generation and elimination of reactive oxygen and nitrogen species (ROS, NOS).[75] This oxidative stress can cause damage of proteins, lipids and nucleic acids as well as a disruption of redox signaling.[75] In the nervous system, the tripeptid glutathione prevents this oxidative stress, because it acts as radical scavenger, but also as redox modulator of ionotropic receptor activity and possibly as neurotransmitter.[76] A decrease in the glutathione concentration can enhance oxidative stress and thus cause ailments like Lou Gehrig´s disease, Parkinson´s disease or Alzheimer disease.[76] In the neuroprotection assay, the decrease in cellular glutathione concentration is induced by a high extracellular glutamate concentration (5 mM). To be more specifically, the glutamate/cystine anti-porter is influenced and thus, an imbalance in cystine homeostasis is generated.[77] The following cell death *via* the oxidative pathway showed characteristics of necrosis and apoptosis.[78] The morphological mutations during cell death can be visualized with an electron microscop (**Figure 61**). After 8 h the cells begin to shrink,

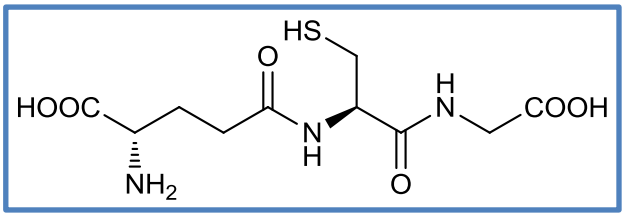

Figure 60: Structure of glutathione

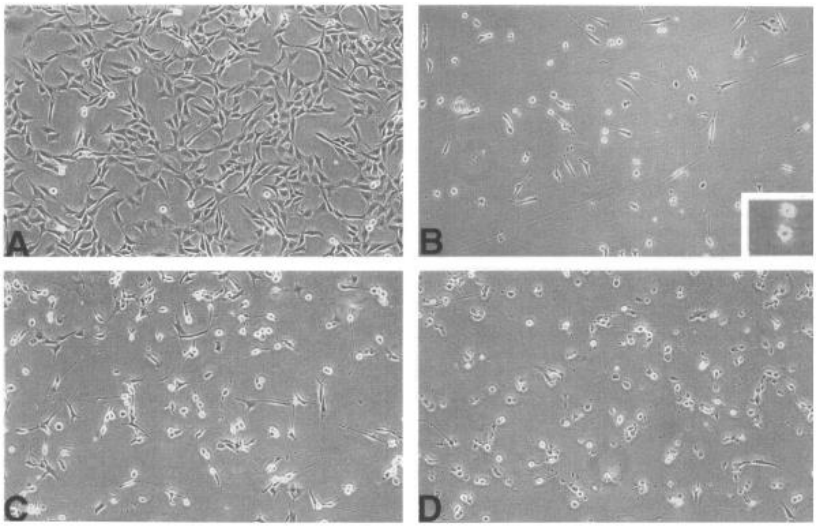

Figure 61: Light microscopic morphology of glutamate-treated HT-22 cells. Cells were untreated (A) or treated with 5 mM glutamate for 8 h (B), 10 h (C), or 14 h (D) before examination under a phase-contrast microscope. Inset in B shows blebs on surface of cells[78]

appear more globulary and show little blebs on the surface. Further 2 h later, several cell organells seem to be swollen or damaged (endoplasmic reticulum, Golgi-apparatus, mitochondria). In contrast, the nuclear morphology is almost stable. After 16-24 h the cells disintegrate and just cellular debris can be seen.[78] The cell viability can finally be measured with the colorimetric MTT assay.

Investigation of anti-oxidative Activity in a cell-free Assay, ORAC Assay

In order to have better comparable values for the antioxidative activity of the synthesized compounds, the Oxygen Radical Antioxidant Capacity (ORAC) assay was chosen as cell-free assay. In general, cell-free systems are easier to handle and also the higher availability and reproducibility cannot be denied.[79] In the ORAC assay, the compound 2,2'-azobis(2-amidinopropane) dihydrochloride (AAPH) is used to generated free radicals. These radicals degrade the also present fluorescein, which results in a weaker light emission at 535 nm (excitation at 485 nm). If the investigated compound shows antioxidant activity, the decrease of the emitted light is decelerated.

Anti-proliferative activity, Proliferation Assay

Cell proliferation comprises an increase in the number of cells as a consequence of cell growth and division. One necessary step for angiogenesis is cell proliferation. Angiogenesis includes the growth of new blood vessels during embryogenesis and wound healing, but is also supportive in certain diseases like i.e. diabetic retinopathy, psoriasis and rheumatoid arthritis and for tumors concerning growing and spreading.[80] The ability of some flavonoids as anti-cancerogenic compounds is based, among others, in anti-oxidative, pro-apoptotic, DNA damaging, anti-angiogenic, and immunostimulatory effects.[81] Suppression of the abnormal angiogenesis might thus be useful for the therapy of these affections.[80]

In the present work, the influence of the synthesized kaempferol derivatives on the cell proliferation of human microvascular endothelial cells (HMEC) was examined. It should be noted that an anti-proliferative effect on the chosen HMEC-1 cells does not necessarily include an anti-angiogenetic activity of the test compound. Among others, also the intervention of cell cycle,[82] induction of apoptotic cell death[83] or a distortion that decreases intracellular acidity and/or increases basicity[84] are possible essentials for an anti-proliferative activity.

Anti-inflammatory Activity, ICAM-1 Assay

Inflammation is basically a response of the immune system as a protective event[85] and is the consequence of several different pathways and signal cascades. One of these pathways includes the increase of the ICAM-1 (Intercellular Adhesion Molecule 1) expression. This is not uncommon for any kind of inflammation and also chronical inflammatory diseases like rheumatoid arthritis, psoriasis and atherosclerosis show an abnormal increase in ICAM-1 expression.

Briefly, the cascade starts with the interaction of a macrophage with a pathogen. This results, among other reactions, in the release of the tumor necrosis factor *α* (TNF-*α*) from the macrophage.[86] The cytokine TNF-*α* for his part activates the nuclear transcription factor NF-κB *via* a cascade, starting at a specific receptor at the membrane of the endothelial cells. In a next step NF-κB induces the expression of ICAM-1, which enables leukocytes to attach and finally pass the endothelial cell layer and thus to reach the location of an infection in the tissue.

Consequently an increase of ICAM-1 can be seen as indication for a proceeding inflammation. The informative concentration of ICAM-1 can be visualized by the use of a specific antibody, which is labeled with fluorescein isothiocyanate (FITC) and detected *via* fluorescence-activated cell sorting (FACS).

5.2 Material and Methods

5.2.1 Consumable Material

- Dulbecco´s Modified Eagle Medium, DMEM, gibco®, Life technologies coorporation, New York, USA
- Dulbecco´s Phosphate Buffered Saline (PBS), Sigma-Aldrich, Steinheim, Germany
- Endothelial cell growth medium + 10% FCS, supplement mix and antibiotics, Provitro GmbH, 10117 Berlin, Germany
- FCS Superior, Biochrom, Berlin, Germany
- Fluorescein, Merck, Darmstadt, Germany
- Kaempferol ≥ 99%, Extrasynthese, Lyon, France
- Mouse anti human CD54: FITC, FITC-labelled mouse antibody against ICAM-1, 0.1 mg/mL, Biozol, Eching, Germany
- Parthenolide, ≥ 97%, Calbiochem, Bad Soden, Germany
- Quercetin, ≥ 98%, Sigma-Aldrich, Steinheim, Germany
- Sodium dihydrogen phosphate monohydrate, 99.0-102.0%, for 75 mM stock solution, Merck, Darmstadt, Germany
- Thiazolyl blue tetrazolium bromide, ~98%, for 4 mg/mL in PBS, Sigma-Aldrich, Steinheim, Germany
- Tryphan blue, dye content ~ 37%, Sigma-Aldrich, Steinheim, Germany
- TTP® Tissue culture testplate 96F, Techno Plastic Products AG, 8219 Trasadingen, Switzerland
- Tumor Necrosis Factor-α, ≥ 97%, Sigma-Aldrich, Steinheim, Germany
- H_2O, deionised, further purified by membraPure, Astacus, MembraPure GmbH, Berlin, Germany
- Xanthohumol, 98%, Nookandeh Institute, Hamburg, Germany
- Sodium dodecyl sulfate, 92.5-100.5%, for 10% solution (m/v), Sigma-Aldrich, Steinheim, Germany
- di-Sodium hydrogen phosphate dihydrate, ≥ 99.5%, for 75 mM stock solution, Merck, Darmstadt, Germany
- DMSO, SeccoSolv®, ≥ 99.9%, Merck KGaA, 64271 Darmstadt, Germany
- Ethanol, ≥ 99.9%, J.T.Baker®, Avantor Performance Materials, Center Valley, PA, USA
- Methanol, EMSURE®, for analysis, 99.9%, Merck KGaA, 64271 Darmstadt, Germany
- Trypsin (1:250)/EDTA (0.5%/0.2%), for 10% solution (v/v) in PBS, Biochrom, Berlin, Germany
- Crystal violett, ACS, Reag. Ph. Eur., for 0.5% solution (m/v) in MeOH, Merck, Darmstadt, Germany

- tri-Sodium citrate dihydrate, for dissolving buffer, 0.05 M in H_2O/EtOH 1:1, Merck, Darmstadt, Germany
- 6-Hydroxy-2,5,7,8-tetramethylchroman-2-carboxylic acid (Trolox), 98%, Fluka, Neu-Ulm, Germany
- 2,2'-Azobis(2-amidinopropane) dihydrochloride (AAPH), 97%, Sigma-Aldrich, Steinheim, Germany

5.2.2 Instruments

- Autoflow IR Direct Heat CO_2 Incubator, Nuaire™, Integra Biosciences GmbH, Fernwald, Germany
- FACScalibur™, Becton Dickinson, Heidelberg, Germany
- Megafuge 1.0R, Thermo Scientific, Waltham, USA
- Tecan SpectraFluor Plus, Tecan Group Ltd. Crailsheim, Germany
- IBM® SPSS® Statictics 20

5.2.3 Neurotoxicity and Neuroprotection Assay

The assay was accomplished according to Kling *et al.* (2013) in 3 experiments (in 4 parallels):

Neuroprotectivity/Neurotoxicity Assay

HT-22 cells were seeded in 96-well plates at a density of $5x10^3$ per well and cultured for 24 h. Subsequently, cells were incubated for another 24 h either with medium or the test compounds with putative cytoprotective activity either in absence (to test for the compounds' self-toxic effects) or presence (to test for the compounds' protective potential against glutamate induced oxidative stress) of 5 mM glutamate. MTT solution (4 mg/mL in PBS) was diluted 1:10 with medium and added to the wells after removal of culture medium. The plates were then incubated for another 3 h. Afterwards, supernatants were removed and 100 µL of lysis buffer (10% SDS, pH 4.1) was added to the wells. Absorbance at 560 nm was determined on the next day using a multiwell plate photometer (Spectra Fluor Plus, Crailsheim, Germany). Results of these cell viability assays are expressed as percentage to untreated control cells. All compounds were dissolved in DMSO and diluted with fresh medium. DMSO concentration was always below 0.1% (v/v).

5.2.4 ORAC Assay

The ORAC assay was accomplished by Gabriele Brunner according to Decker *et al.* (2012) in minimum 4 experiments (in 4 parallels):

The reaction was carried out in 75 mM phosphate buffer (pH 7.4) and the final reaction mixture was 200 µL. Antioxidant (20 µL) and fluorescein (120 µL, 300 nM final concentration) were placed in the wells of a black 96-well plate and the mixture was incubated for 15 min at 37 °C. Then AAPH (Sigma, Steinheim Germany) solution (60 µL; 12 mM final concentration) was added rapidly. The plate was immediately placed into a Spectrafluor Plus plate reader (Tecan, Crailsheim, Germany) and the fluorescence was measured every 60 s for … [260] min with excitation at 485 nm and emission at 535 nm. 6-Hydroxy-2,5,7,8-tetramethylchroman-2-carboxylic acid (Trolox, Sigma, Steinheim Germany) was used as standard (1–8 µM, final concentration). A blank (FL + AAPH) using phosphate buffer instead of antioxidant and Trolox calibration were carried out in each assay. The samples were measured at different concentrations … [1-5 µM]. All reaction mixtures were prepared fourfold and at least four independent runs were performed for each sample. Fluorescence measurements were normalized to the curve of the blank (without antioxidant).[87]

5.2.5 ICAM-1 Assay

The ICAM assay was accomplished by Monika Untergehrer according to Knuth *et al.* (2011) in 3 experiments (in 2 parallels):

Confluent grown human microvascular endothelial cells (HMEC-1)[88] were pretreated either with … [kaempferol, kaempferol-4´-O-β-D-glucuronide, kaempferol-7,4´-di-O-β-D-glucuronide and kaempferol-7-sulfate], parthenolide (Calbiochem, purity ≥ 97%, 5 µM, positive control), or medium (ECGM, endothelial cell growth medium (Provitro) + 10% FKS, + antibiotics, + supplements) as a negative control in 24-well plates. Thirty minutes later, 10 ng/mL TNF-α (Sigma-Aldrich) were added to stimulate the ICAM-1-expression. After 24 hours of incubation (New Brunswick Scientific, 37 °C, 5 %CO_2), cells were washed with PBS, removed from the plate with trypsin/EDTA and fixed with formalin. After incubating with a FITC-labelled mouse antibody against ICAM-1 (Biozol) for 20 min, the fluorescence intensity was measured by FACS analysis (Becton Dickinson Facscalibur™). ICAM-1-expression of cells treated with TNF-α only was set as 100%.[89]

5.2.6 Proliferation Assay

The proliferation assay was accomplished from Sebastian Schmidt according to Schmidt *et al.* (2012) in one experiments (in 6 parallels):

The proliferation assay was performed using an SV-40T transfected human microvascular endothelial cell line (HMEC-1).[88] Cells were incubated at 37 °C under a 5% CO_2/95% air atmosphere at constant humidity. HMEC-1 cells were seeded in 96-well microplates (100 µL, 1.5 × 10^3cells/well) in endothelial cell growth medium with 10% FCS, supplement mix, and antibiotics (all from Provitro). After 24 h (time of cell adhesion for seeded cells), the medium in a reference plate was removed and the cells were stained with crystal violet solution for 10 min, providing a baseline value before the start of proliferation. Cells in other plates were treated with increasing concentrations of each test compound … [kaempferol, kaempferol-4´-O-β-D-glucuronide, kaempferol-7,4´-di-O-β-D-glucuronide and kaempferol-7-sulfate]. After 72 h incubation, cells were stained as previously described. The cells were washed with … [deionized] H_2O, 100 µL of dissolving buffer was added, and the absorbance was measured with a Tecan SpectraFluor Plus at 540 nm. A negative control in the absence of drug (pure solvent, 0.1% DMSO, in hexaplicates) was included in every 96-well plate and normalized to 100% proliferation after 72 h. The inhibitory effects of … [kaempferol, kaempferol-4´-O-β-D-glucuronide, kaempferol-7,4´-di-O-β-D-glucuronide and kaempferol-7-sulfate] were calculated as % proliferation compared to the no-drug control. … . Xanthohumol was used as a positive control.[90]

5.3 Results and Discussion

For the pharmacological characterisation by the cell based assays, kaempferol, kaempferol-4´-O-β-D-glucuronide, kaempferol-7,4´-di-O-β-D-glucuronide and kaempferol-7-sulfate were chosen. The ORAC assay was additionally accomplished with kaempferol-3-O-β-D-glucuronide and kaempferol-7-O-β-D-glucuronide.

5.3.1 Neurotoxicity and Neuroprotection Assay

The tested glucuronides and the potassium salt of kaempferol-7-sulfate did not show any neurotoxicity or neuroprotectivity within the concentration range of 1-25 µM, which is exemplarily shown for kaempferol-7-O-glucuronide in **Scheme 3**.

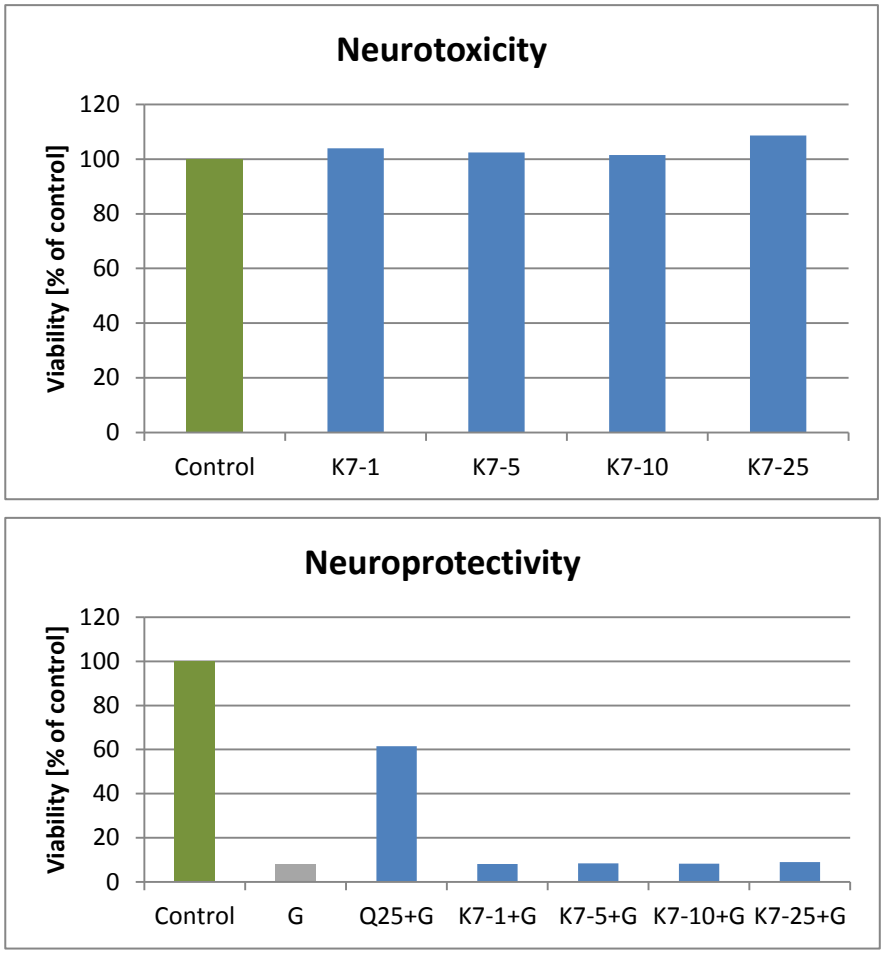

Glutamate 5 mM	-	+	+	+	+	+	+
Quercetin 25 µM	-	-	+	-	-	-	-
K-7-O-GluA [in µM]	-	-	-	+	+	+	+

Scheme 3: Neurotoxicity and neuroprotectivity of kaempferol-7-O-β-D-glucuronide. Experiments were performed in 3 independent experiments (in 4 parallels each). Data were subjected to one-way ANOVA followed by Dunnet's multiple comparison post test using IBM SPSS Statistics Software

Further on, kaempferol showed a very low neurotoxic *in vitro* effect at 25 µM and a neuroprotectivity already at 5 µM. (**Scheme 4**)

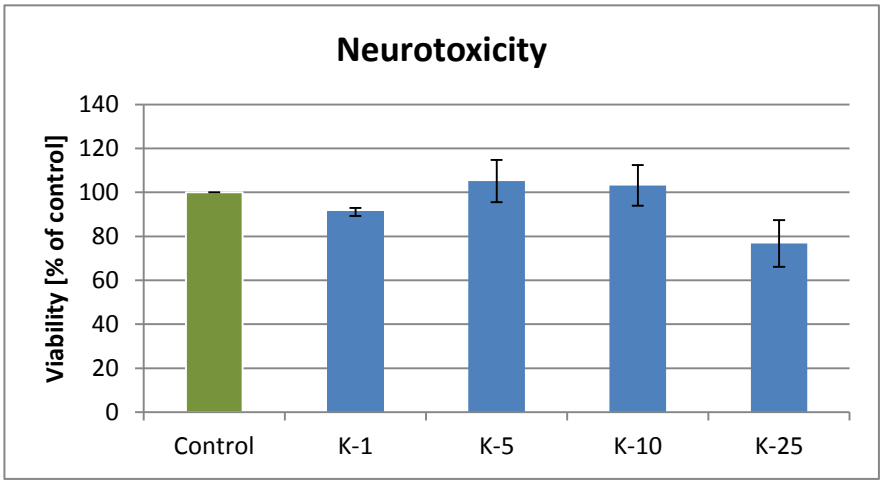

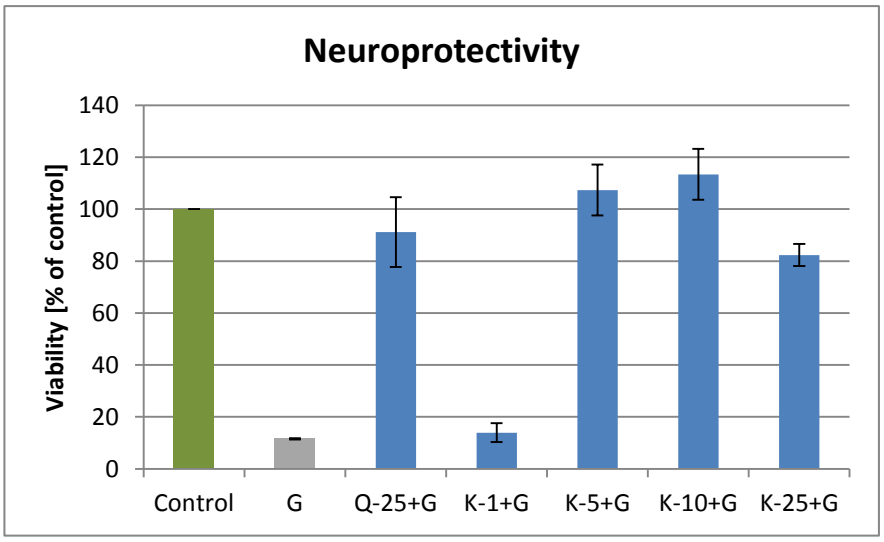

Glutamate 5 mM	-	+	+	+	+	+	+
Quercetin 25 µM	-	-	+	-	-	-	-
Kaempferol [µM]	-	-	-	+	+	+	+

Scheme 4: Neurotoxicity and neuroprotectivity of kaempferol. Experiments were performed in 3 independent experiments (in 4 parallels each). Data were subjected to one-way ANOVA followed by Dunnet's multiple comparison post test using IBM SPSS Statistics Software

The reason for this effect might be seen in the higher hydrophilicity of the glucuronides and the sulfate. The compounds are not able to pass the lipophilic cell membrane and thus, the glutamate induced intracellular oxidative stress cannot be reduced by these compounds. Nevertheless, the structural essentials for a neuroprotectivity are basically present also in the conjugates. Ishige *et al*. have investigated, among others, some flavanols like e.g. catechin.[91] These compounds do not show a neuroprotection in the same assay, whereas kaempferol and eriodictyol do (Kling *et al*. 2013). With regard to the corresponding structures, the additional carbonyl moiety at C-4 seems to play the crucial role (**Figure 62)**. A free hydroxyl function at position 3, as well as a catechol moiety at the B-ring or a C2-C3 double bond are not sufficient for the activity.

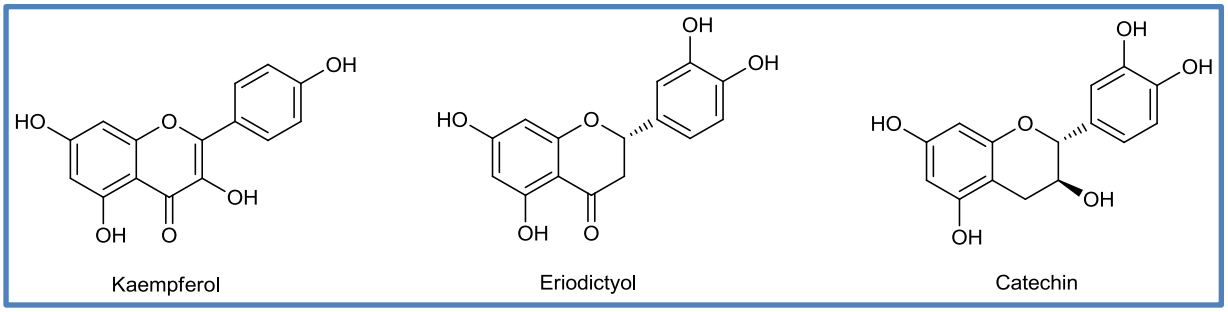

Figure 62: Structures of flavonoids tested in the neuroprotection assay (Kling et al., 2013).

5.3.2 ORAC-Fluorescein Assay

The antioxidant capacities of kaempferol, kaempferol-7-sulfate, kaempferol-3-O-β-D-glucuronide, kaempferol-7-O-β-D-glucuronide, kaempferol-4´-O-β-D-glucuronide and kaempferol-7,4´-di-O-β-D-glucuronide were investigated in relation to Trolox for the free radical generating compound 2,2'-azobis(2-amidinopropane) dihydrochloride (AAPH). Kaempferol showed with a value of 4.8 the highest radical scavenging effect (**Table 41**), which is based in the presence of theoretically four oxidizable hydroxyl functions. Principally, a substitution with a sulfate- or glucuronic acid moiety does reduce the electron density in the aromatic system and results in a lower oxidizability. It can be expected that just the hydroxyl functions at position 3 and 4´ are oxidized (**Figure 63**),[27] which explains the lower antioxidant capacity, if a glucuronic acid is substituted to 3-OH or 4´-OH. Consequently, among the synthesized monoglucuronides, kaempferol-7-O-β-D-glucuronide had with a value of 3.2 the highest anti-oxidant activity. Also concerning kaempferol-7-sulfate, an oxidation at the B- and C- ring is possible and thus, the Trolox equivalent is at a medium value regarding the investigated compounds.

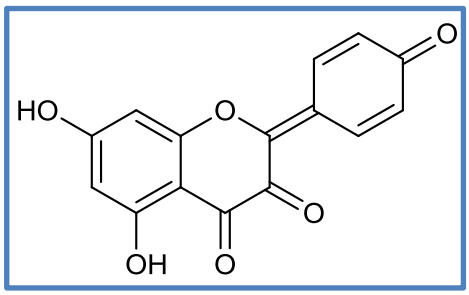

Figure 63: Oxidized form of kaempferol

Table 41: Oxygen radical absorbance capacity (ORAC, Trolox equiv, 1-5 µM) by kaempferol and the synthesized conjugates

Compound	Trolox equivalents	SD
Kaempferol	4.8	± 0.5
Kaempferol-3-O-β-D-glucuronide	2.3	± 0.2
Kaempferol-7-O-β-D-glucuronide	3.2	± 0.3
Kaempferol-4´-O-β-D-glucuronide	1.3	± 0.2
Kaempferol-7,4´-di-O-β-D-glucuronide	1.0	± 0.1
Kaempferol-7-sulfate	2.0	± 0.2

The anti-oxidant activity of kaempferol in relation to Trolox was also analyzed by Guo *et al.* to a value of 2.67 ± 0.13.[92] In this study, also AAPH was used for the free radical generating, but *R*-Phycoerythrin as indicator. The fact that we have applied fluorescein to monitor the radical attack and that the instrument setup is partly different can explain the variation in the obtained values. Nevertheless, a significant anti-oxidant activity of kaempferol cannot be denied.

5.3.3 ICAM-1 Expression

The glucuronide and the sulfate conjugates of kaempferol did not show any decrease in ICAM-1 expression in the tested concentration range (up to 50 µM, **Scheme 5**). For the aglycone a certain effect was detected, but not in a significant manner. Regarding that the anti-inflammatory activity can be based on several pathways, some other assays with regard to further inflammation pathways have do be considered.

The biological relevance of the glucuronides might be more imported *in vivo* due to deglucuronidation during inflammation, which was already shown for luteolin.[20] The *β*-glucuronidase activity increases in rat plasma after the injection of pro-inflammatory lipopolysaccharide (LPS).[93] During the inflammation process, *β*-glucuronidase is known be released by neutrophil granulocytes.[94] Along with the release of *β*-glucuronidase a lower pH value of 4-5 at an inflammation side intensifies the enzyme activity.[93] Kaempferol is known to inhibit moderate the LPS induced NF-κB activiation (~60%, 100 µM),[95] which is an intersection point with the TNF-*α* induced expression of ICAM-1 in the present study, wherein also NF-κB is a necessary transcription factor.

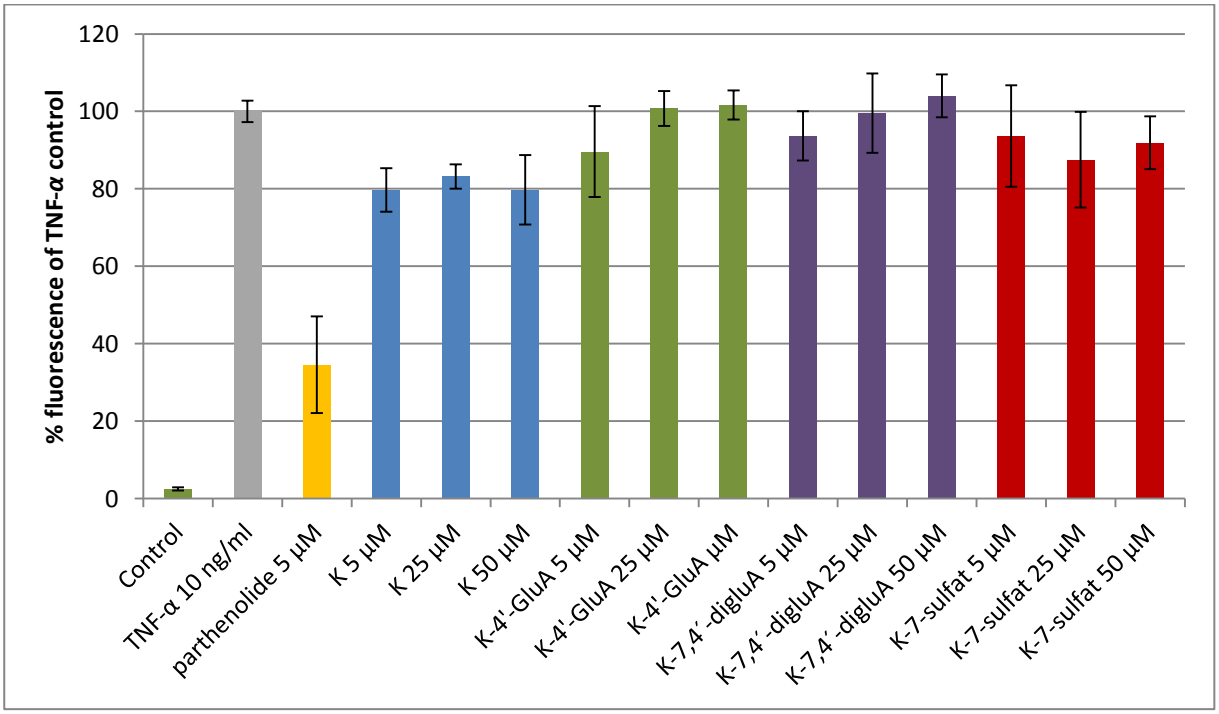

Scheme 5: Inhibition of ICAM-1 expression of kaempferol and some conjugates

5.3.4 Proliferation Assay

Kaempferol showed a concentration dependent anti-proliferativ activity on HMEC-1 cells. This effect possibly based on the already described reduction of Vascular Endothelial Growth Factor (VEGF) gene expression.[96] A VEGF isoform is known to induce angiogenic processes in HMEC cells in biomimetic hydrogels, which includes increased cell proliferation, migration, and survival of apoptosis. A comparable study from the literature showed also inhibition of cell proliferation in HMEC cells of some flavonoids wherein the activity at 50 µM was as follows: quercetin (~40% of control) > naringenin (~70% of control) > catechin (comparable to control).[97] Of course is has to be considered, that the assay setup is not exactly the same, but in combination with the published data some structural key elements can be estimated. The C2-C3 double bond and the C4 keto function seem to play a crucial role, whereas a catechol moiety or a hydroxyl function at C3 have no strong effect. But of course, further data of this assay concering a wide range of different flavonoids are necessary to verify this theory.

Table 42: Anti-proliferative activity of Kaempferol

c (Kaempferol) [µM]	% Cell Control
5	76.4
25	36.7
50	9.7

Although kaempferol has anti-angiogenetic and thus anti-proliferative activity against several tumor cell lines regarding, i.e. ovarian- ,[96] breast-[98] and pancreatic-[99] cell lines, it is widely discussed in literature, whether flavonoids would be suitable for the chemoprevention of certain cancerogenic deseases.

In contrast, the tested kaempferol-4´-O-β-D-glucuronide, kaempferol-7,4-di-O-β-D-glucuronide and the kaempferol-7-sulfate did not show anti-proliferative activity in this assay (80-104% of control). In this context also the deglucuronidation may play a certain role *in vivo*. Tumours have a high metabolic rate and thus a acidosis is a possible consequence.[100] As mentioned above, a pH value of 4-5 intensifies the activity of β-glucuronidase and therefore a liberation of free kaempferol.

6 Summary

Flavonoids are secondary metabolites and almost ubiquitous in many edible plants and thus part of a healthy nutrition. They can be found mainly as glycosides in fruits and other vegetables, but also in some herbal medicines like Tebonin®, which active ingredient is an extract from the leaves of *Ginkgo biloba*. Following to the oral ingestion, these flavonoid glycosides are hydrolyzed in the small intestine. After absorption to the epithelium, the generated aglycone can be conjugated for instance with methyl-, sulfate- or glucuronic acid groups (phase-II-metabolism). This derivatisation initialize the excretion *via* kidney or bile but also results in a distribution of these metabolites in the body *via* the blood circulation. Consequently these flavonoid derivatives have the ability to reach several organs and tissues.

Flavonoids are known to have many benefical effects on health, but whether just the aglycones or also the in vivo conjugates are responsible is not always obvious. These is partly based in the lack of knowledge concerning the in vivo status of the metabolites in the tissues. The questions arises whether conjugates or maybe deconjugated metabolites are substrates for certain enzymes in tissues or organs.

In this work, the main phase-II-metabolites of kaempferol glycosides were identified and quantified in rat plasma. To achive this, the expected metabolites were chemically synthesized and used as reference substance in HPLC analysis. The different kaempferol glycosides for oral application were isolated from flavonol-enriched fractions of the *Ginkgo* folium extract EGb 761® obtained from Dr. Willmar Schwabe GmbH & Co. KG. Single kaempferol glycosides were orally administred to male Spraque Dawley rats, respectively. Finally, kaempferol-3-O-β-D-glucuronide, kaempferol-7-O-β-D-glucuronide and a kaempferol glucuronide-sulfate could be identified as the main metabolites after oral application of kaempferol rutinoside to rats.

The pharmacological investigation of kaempferol and some synthezised derivatives by the neuroprotectivity/neurotoxicity assay, but especially by the ORAC assay, confirmed the frequently mentioned anti-oxidative activity, wherein the aglycone showed the highest capacity. Also an anti-proliferative activity was detected for kaempferol, whereas the conjugates did not show any significant activity in this cell based assay. Similar results were

obtained for the inhibition of ICAM-1 expression were just the aglycone showed a weak activity.

7 Zusammenfassung

Flavonoide sind sekundäre Metabolite in Pflanzen und somit unter anderem Bestandteil einer gesunden Ernährung. In Gemüse und Früchten kommen vor allem die Glycoside dieser Verbindungen vor. Weiterhin findet man Flavonoide in vielen Phytopharmaka wie beispielsweise Tebonin®, dessen aktiver Inhaltsstoff ein Extrakt aus *Ginkgo biloba* Blättern darstellt. Nach oraler Aufnahme werden diese Flavonoidglycoside im Dünndarm hydrolisiert und können über das Dünndarmepithel aufgenommen werden. Der Aufnahme schließt sich eine Derivatisierung an, d.h. die entstandenen Aglykone werden z.B. mit einer Methyl-, Sulfat- oder Glucuronsäure-Gruppe konjugiert (Phase-II-Metabolismus). Der Grund für diese Substitution liegt grundsätzlich darin, die Substanz für die Exkretion über Niere oder Galle zugänglich zu machen, führt aber auch zu einer Aufnahme und Verteilung der Metabolite über den Blutkreislauf. Somit sind diese Verbindungen in der Lage zahlreiche Organe und Gewebe des Körpers erreichen.

Einige gesundsheitsfördernde Eigenschaften von Flavonoiden wurden bereits gezeigt, aber ob diese Effekte auf das Aglykon oder auch auf die Phase-II-Metabolite zurückzuführen sind ist bisher nicht eindeutig geklärt. Dies liegt unter anderem auch daran, dass in-vivo nicht genau bekannt ist, ob und vor allem in welchem Ausmaß die Konjugate in den Geweben wieder zu den Aglykonen umgesetzt werden.

In dieser Arbeit wurden die wichtigsten Phase-II-Metabolite von verschiedenen Kämpferolglykosiden im Plasma von Ratten identifiziert und quantifiziert. Um dies zu ermöglichen, wurden die erwarteten Metabolite chemisch synthesiert und als Referenzsubstanzen für die HPLC-Analyse genutzt. Für die orale Applikation wurden vier Kämpferolglycoside aus mit Flavonolen angereicherten Fraktionen des *Ginkgo* folium Extraktes EGb 761® isoliert, welche von der Dr. Willmar Schwabe GmbH & Co. KG bereitgestellt wurden. Nach oraler Applikation der Glykoside an männliche Spraque Dawley Ratten konnten Kämpferol-3-O-β-D-glucuronid, Kämpferol-7-O-β-D-glucuronid and ein Kämpferol Glucuronid/Sulfat als Hauptmetabolite identifiziert bzw. nach der Gabe von Kämpferolrutinosid auch teilweise quantifiziert werden.

Die Untersuchung von Kämpferol und einiger der synthetisierten Phase-II-Metabolite mittels des Neuroprotektivität/Neurotoxizität Assays, aber vor allem des ORAC Assays, bestätigte die oftmals erwähnte antioxidative Aktivität, insbesondere bzgl. des Aglykons. Dieses zeigt sowohl antiproliferative Eigenschaften als auch eine schwache Hemmung der ICAM-1 Expression. Die synthetisierten Konjugate des Kämpferols zeigten dagegen keine signifikante Aktivität in einem der durchgeführten zellbasierten Assays.

8 Literature

1. Hertog, M.G.L. *et al.* Content of potentially anticarcinogenic flavonoids of tea infusions, wines, and fruit juices. *Journal of Agricultural and Food Chemistry* **41**, 1242-1246 (1993).

2. Crozier, A. *et al. Plant Secondary Metabolites*. (Blackwell Publishing Ltd: Oxford, UK, 2006).

3. Hertog, M.G.L. *et al.* Content of potentially anticarcinogenic flavonoids of 28 vegetables and 9 fruits commonly consumed in the Netherlands. *Journal of Agricultural and Food Chemistry* **40**, 2379-2383 (1992).

4. Koes, R.E. *et al.* The flavonoid biosynthetic pathway in plants: Function and evolution. *BioEssays* **16**, 123-132 (1994).

5. Harborne, J.B. & Williams, C.A. Anthocyanins and other flavonoids. *Natural Product Reports* **18**, 310-333 (2001).

6. Bechtold, T. & Mussak, R. *Handbook of Natural Colorants*. (John Wiley & Sons Ltd: Chichester, UK, 2009).

7. Bowsher, C. *et al. Plant Biochemistry*. (Garland Science, Taylor & Francis Group: New York, USA, 2008).

8. Nelson, D. & Cox, M. *Lehninger Biochemie*. (Springer Verlag Berlin Heidelberg: Berlin, Germany, 2009).

9. Berg, J.M. *et al. Stryer Biochemie*. (Elsevier GmbH, Spektrum Akademischer Verlag: München, Germany, 2007).

10. Fatland, B. *et al.* Molecular characterization of a heteromeric ATP-citrate lyase that generates cytosolic acetyl-coenzyme A in *Arabidopsis*. *Plant Physiologists* **130**, 740-756 (2002).

11. Sasaki, Y. & Nagano, Y. Plant acetyl-CoA carboxylase: structure, biosynthesis, regulation, and gene manipulation for plant breeding. *Bioscience, Biotechnology, and Biochemistry* **68**, 1175-84 (2004).

12. Shorrosh, B.S. *et al.* Molecular cloning, characterization, and elicitation of acetyl-CoA carboxylase from *alfalfa*. *Proceedings of the National Academy of Sciences* **91**, 4323-4327 (1994).

13. Fatland, B. *et al.* Molecular biology of cytosolic acetyl-CoA generation. *Biochemical Society Transactions* **28**, 593-5 (2000).

14. Herrmann, K.M. & Weaver, L.M. The shikimate pathway. *Annual Review of Plant Physiology and Plant Molecular Biology* **50**, 473-503 (1999).

15. Rippert, P. *et al.* Tyrosine and phenylalanine are synthesized within the plastids in *Arabidopsis*. *Plant Physiology* **149**, 1251-60 (2009).

16. Maeda, H. & Dudareva, N. The Shikimate pathway and aromatic amino acid biosynthesis in plants. *Annual Review of Plant Biology* **63**, 73-105 (2012).

17. Winkel-Shirley, B. Flavonoid biosynthesis. A colorful model for genetics, biochemistry, cell biology, and biotechnology. *Plant Physiology* **126**, 485-493 (2001).

18. Arts, I.C. *et al.* Catechin intake and associated dietary and lifestyle factors in a representative sample of Dutch men and women. *European Journal of Clinical Nutrition* **55**, 76-81 (2001).

19. de Kleijn, M.J. *et al.* Intake of dietary phytoestrogens is low in postmenopausal women in the United States: the Framingham study. *The Journal of Nutrition* **131**, 1826-32 (2001).

20. Arai, Y. *et al.* Human nutrition and metabolism dietary intakes of flavonols , flavones and isoflavones by japanese women and the inverse correlation between quercetin intake and plasma LDL cholesterol concentration. *The Journal of Nutrition* **130**, 2243-2250 (2000).

21. Chun, O.K. *et al.* Estimated dietary flavonoid intake and major food sources of U.S. adults. *The Journal of Nutrition* **137**, 1244-52 (2007).

22. Medina, J.H. *et al.* Overview-flavonoids: a new family of benzodiazepine receptor ligands. *Neurochemical Research* **22**, 419-25 (1997).

23. Halliwell, B. Oxygen radicals, nitric oxide and human inflammatory joint disease. *Annals of the Rheumatic Diseases* **54**, 505-10 (1995).

24. Fang, Y.-Z. *et al.* Free radicals, antioxidants, and nutrition. *Nutrition* **18**, 872-9 (2002).

25. Kaur, H. & Halliwell, B. Evidence for nitric oxide-mediated oxidative damage in chronic inflammation. Nitrotyrosine in serum and synovial fluid from rheumatoid patients. *FEBS letters* **350**, 9-12 (1994).

26. Thomsen, L.L. & Miles, D.W. Role of nitric oxide in tumour progression: lessons from human tumours. *Cancer Metastasis Reviews* **17**, 107-18 (1998).

27. Tsimogiannis, D.I. & Oreopoulou, V. The contribution of flavonoid C-ring on the DPPH free radical scavenging efficiency. A kinetic approach for the 3',4'-hydroxy substituted members. *Innovative Food Science & Emerging Technologies* **7**, 140-146 (2006).

28. Birjees Bukhari, S. *et al.* Synthesis, characterization and investigation of antioxidant activity of cobalt–quercetin complex. *Journal of Molecular Structure* **892**, 39-46 (2008).

29. Brown, J.E. *et al.* Structural dependence of flavonoid interactions with Cu^{2+} ions: implications for their antioxidant properties. *Biochemical Journal* **1178**, 1173-1178 (1998).

30. Sugihara, N. *et al.* Anti- and pro-oxidative effects of flavonoids on metal-induced lipid hydroperoxide-dependent lipid peroxidation in cultured hepatocytes loaded with alpha-linolenic acid. *Free Radical Biology and Medicine* **27**, 1313-1323 (1999).

31. Saragusti, A.C. *et al.* Inhibitory effect of quercetin on matrix metalloproteinase 9 activity molecular mechanism and structure-activity relationship of the flavonoid-enzyme interaction. *European Journal of Pharmacology* **644**, 138-45 (2010).

32. Ende, C. & Gebhardt, R. Inhibition of matrix metalloproteinase-2 and -9 activities by selected flavonoids. *Planta Medica* **70**, 1006-8 (2004).

33. Coates, D. The angiotensin converting enzyme (ACE). *The International Journal of Biochemistry & Cell Biology* **35**, 769-73 (2003).

34. Guerrero, L. *et al.* Inhibition of angiotensin-converting enzyme activity by flavonoids: structure-activity relationship studies. *PLOS one* **7**, e49493 (2012).

35. de Vries, J.H. *et al.* Plasma concentrations and urinary excretion of the antioxidant flavonols quercetin and kaempferol as biomarkers for dietary intake. *The American Journal of Clinical Nutrition* **68**, 60-5 (1998).

36. Rice-Evans, C.A. *et al.* Structure-antioxidant activity relationships of flavonoids and phenolic acids. *Free Radical Biology and Medicine* **20**, 933-956 (1996).

37. Li, N. *et al.* Free radical scavengers, antioxidants and aldose reductase inhibitors from Camptosorus sibiricus Rupr. *Zeitschrift für Naturforschung C* **63c**, 66-68 (2008).

38. Liu, H. *et al.* Glycosides from *Stenochlaena palustris*. *Phytochemistry* **49**, 0-5 (1998).

39. Lee, M.-J. *et al.* Effect of flavonol glycosides from *Cinnamomum osmophloeum* leaves on adiponectin secretion and phosphorylation of insulin receptor-beta in 3T3-L1 adipocytes. *Journal of Ethnopharmacology* **126**, 79-85 (2009).

40. Zeng, S. *et al.* Development of a EST dataset and characterization of EST-SSRs in a traditional Chinese medicinal plant, *Epimedium sagittatum* (Sieb. Et Zucc.) Maxim. *BMC Genomics* **11**, 94 (2010).

41. Filip, R. *et al.* Phenolic compounds in seven South American *Ilex* species. *Fitoterapia* **72**, 774-778 (2001).

42. Froelich, S. *et al.* Plants traditionally used against malaria : phytochemical and pharmacological investigation of *Momordica foetida*. *Brazilian Journal of Pharmacognosy* **17**, 1-7 (2007).

43. Mahadevan, S. & Park, Y. Multifaceted therapeutic benefits of *Ginkgo biloba* L.: chemistry, efficacy, safety, and uses. *Journal of Food Science* **73**, R14-9 (2008).

44. Calderón-Montaño, J.M. *et al.* A review on the dietary flavonoid kaempferol. *Mini Reviews in Medicinal Chemistry* **11**, 298-344 (2011).

45. Royer, D.L. *et al.* Ecological conservatism in the "living fossil" *Ginkgo*. *Paleobiology* **29**, 84-104 (2003).

46. *Europäisches Arzneibuch*. (Deutscher Apotheker Verlag Stuttgart, Govi-Verlag-Pharmazeutischer Verlag GmbH Eschborn: Stuttgart, Eschborn, 2011).

47. Hänsel, R. & Sticher, O. *Pharmakognosie und Phytopharmazie*. (Springer Medizin Verlag Heidelberg: Heidelberg, Germany, 2010).

48. *WHO monographs on selected medicinal plants*. (World Health Organization: Geneva, 1999).

49. Fachinformation Tebonin ® konzent ® 240 mg. *Dr. Willmar Schwabe GmbH & Co. KG*

50. Rangel-Ordóñez, L. *et al.* Plasma levels and distribution of flavonoids in rat brain after single and repeated doses of standardized *Ginkgo biloba* extract EGb 761®. *Planta Medica* **76**, 1683-90 (2010).

51. Neu, R. Aromatische Borsäuren als bathohrome Reagentien für Flavone. *Fresenius' Zeitschrift für Analytische Chemie* **82**, 328-332 (1956).

52. Hasler, A. Flavonoide aus *Ginkgo biloba* L. und HPLC-Analytik von Flavonoiden in verschiedenen Arzneipflanzen. (Dissertation, ETH Zürich, 1990).

53. Barron, D. & Ibrahim, R.K. Synthesis of flavonoid sulfates: 1. stepwise sulfation of positions 3, 7, and 4 using *N,N'*-dicyclohexylcarbodiimide and tetrabutylammonium hydrogen sulfate. *Tetrahedron* **43**, 5197-5202 (1987).

54. Bouktaib, M. *et al.* Regio- and stereoselective synthesis of the major metabolite of quercetin, quercetin-3-O-β-D-glucuronide. *Tetrahedron Letters* **43**, 6263-6266 (2002).

55. Vermes, B. *et al.* The synthesis of afzelin, paeonoside and kaempferol 3-O-β-rutinoside. *Phytochemistry* **15**, 1320-1321 (1976).

56. Wagner, H. *et al.* Synthese von Glucuroniden der Flavonoid-Reihe, II. Isolierung von Kämpferol-3-β-D-glucuronid aus *Euphorbia esula* L. und seine Synthese. *Chemische Berichte* **103**, 3678-3683 (1970).

57. Needs, P.W. & Kroon, P. a. Convenient syntheses of metabolically important quercetin glucuronides and sulfates. *Tetrahedron* **62**, 6862-6868 (2006).

58. Bouktaib, M. *et al.* Hemisynthesis of all the O-monomethylated analogues of quercetin including the major metabolites, through selective protection of phenolic functions. *Tetrahedron* **58**, 10001-10009 (2002).

59. Alluis, B. & Dangles, O. Quercetin (=2-(3,4-dihydroxyphenyl)-3,5,7-trihydroxy-4H-1-benzopyran-4-one) glycosides and sulfates: chemical synthesis, complexation, and antioxidant properties. *Helvetica Chimica Acta* **84**, 1133-1156 (2001).

60. Yang, W. *et al.* Synthesis of kaempferol 3-O-(3'',6''-Di-O-E-*p*-coumaroyl)-β-D-glucopyranoside, efficient glycosylation of flavonol 3-OH with glycosyl o-alkynylbenzoates as donors. *The Journal of Organic Chemistry* **75**, 6879-6888 (2010).

61. 10.07.2013 http://www.reseachem.ch/index.php?new_section=kat&new_subitem=0.

62. Li, Y. *et al.* Synthesis of Kaempferol 3-O-[2'',3''- and 2'',4''-Di-O-(E)-*p*-coumaroyl]-α-L-rhamnopyranosides. *Synlett* **7**, 915-918 (2011).

63. Walle, T. *et al.* Flavonoid glucosides are hydrolyzed and thus activated in the oral cavity. *The Journal of Nutrition* 48-52 (2005).

64. Day, A.J. *et al.* Deglycosylation of flavonoid and isoflavonoid glycosides by human small intestine and liver β-glucosidase activity. *FEBS Letters* **436**, 71-75 (1998).

65. Németh, K. *et al.* Deglycosylation by small intestinal epithelial cell beta-glucosidases is a critical step in the absorption and metabolism of dietary flavonoid glycosides in humans. *European Journal of Nutrition* **42**, 29-42 (2003).

66. Walle, T. Absorption and metabolism of flavonoids. *Free Radical Biology and Medicine* **36**, 829-837 (2004).

67. Spencer, J.P.E. Metabolism of tea flavonoids in the gastrointestinal tract. *Proceedings of the Third International Scientific Symposium on Tea and Human Health: Role of Flavonoids in the Diet* 3255-3261 (2003).

68. Singh, R. *et al.* Identification of the position of mono-O-glucuronide of flavones and flavonols by analyzing shift in online UV Spectrum (λ_{max}) generated from an online diode array detector. *Journal of Agricultural and Food Chemistry* **58**, 9384-9395 (2010).

69. Zhao, H. *et al.* Liquid chromatography–tandem mass spectrometry analysis of metabolites in rats after administration of prenylflavonoids from *Epimediums*. *Journal of Chromatography B* **878**, 1113-1124 (2010).

70. Yodogawa, S. *et al.* Glucurono- and sulfo-conjugation of kaempferol in rat liver subcellular preparations and cultured hepatocytes. *Biological and Pharmaceutical Bulletin* **26**, 1120-1124 (2003).

71. Day, A.J. *et al.* Absorption of quercetin-3-glucoside and quercetin-4'-glucoside in the rat small intestine: the role of lactase phlorizin hydrolase and the sodium-dependent glucose transporter. *Biochemical Pharmacology* **65**, 1199-1206 (2003).

72. Hua, L. *et al.* Separation of kaempferols in *Impatiens balsamina* flowers by capillary electrophoresis with electrochemical detection. *Journal of Chromatography A* **909**, 297-303 (2001).

73. Guo, C. *et al.* High-Performance Liquid Chromatography coupled with coulometric array detection of electroactive components in fruits and vegetables: relationship to oxygen radical absorbance capacity. *Journal of Agricultural and Food Chemistry* **45**, 1787-1796 (1997).

74. Hollman, P.C.H. *et al.* Fluorescence detection of flavonols in HPLC by postcolumn chelation with aluminum. *Analytical Chemistry* **68**, 3511-3515 (1996).

75. Dajas, F. *et al.* Neuroprotective actions of flavones and flavonols: mechanisms and relationship to flavonoid structural features. *Central Nervous System Agents in Medicinal Chemistry* **13**, 30-5 (2013).

76. Bains, J.S. & Shaw, C.A. Neurodegenerative disorders in humans: the role of glutathione in oxidative stress-mediated neuronal death. *Brain Research Reviews* **25**, 335-358 (1997).

77. Davis, J.B. & Maher, P. Protein kinase C activation inhibits glutamate-induced cytotoxicity in a neuronal cell line. *Brain Research* **652**, 169-173 (1994).

78. Tan, S. *et al.* Oxidative stress induces a form of programmed cell death with characteristics of both apoptosis and necrosis in neuronal cells. *Journal of Neurochemistry* **71**, 95-105 (1998).

79. Simmonds, N.J. *et al.* Antioxidant effects of aminosalicylates and potential new drugs for inflammatory bowel disease: assessment in cell-free systems and inflamed human colorectal biopsies. *Alimentary Pharmacology & Therapeutics* **13**, 363-372 (1999).

80. Varinska, L. *et al.* Anti-angiogenic activity of the flavonoid precursor 4-hydroxychalcone. *European Journal of Pharmacology* **691**, 125-133 (2012).

81. Lamoral-Theys, D. & Pottier, F. Dufrasne, J. Neve, J. Dubois, A. Kornienko, R.K. and L.I. Natural polyphenols that display anticancer properties through inhibition of kinase activity. *Current Medicinal Chemistry* **17**, 812-825 (2010).

82. Liang, M. *et al.* Anti-hepatocarcinoma effects of *Aconitum coreanum* polysaccharides. *Carbohydrate Polymers* **88**, 973-976 (2012).

83. Wang, S. *et al.* Recent advances in the study of elemene on cancer. *Journal of Medicinal Plants Research* **6**, 5720-5729 (2012).

84. Luzina, E.L. & Popov, A.V. Synthesis and anticancer activity of N-bis(trifluoromethyl)alkyl-N'-thiazolyl and N-bis(trifluoromethyl)alkyl-N'-benzothiazolyl ureas. *European Journal of Medicinal Chemistry* **44**, 4944-4953 (2009).

85. Frank, M.M. & Fries, L.F. The role of complement in inflammation and phagocytosis. *Immunology Today* **12**, 322-326 (1991).

86. Vollmar, A. & Dingermann, T. *Immunologie. Grundlagen und Wirkstoffe*. (Wissenschaftliche Verlagsgesellschaft mbH: Stuttgart, Germany, 2005).

87. Decker, M. *et al.* Design, synthesis and pharmacological evaluation of hybrid molecules out of quinazolinimines and lipoic acid lead to highly potent and selective butyrylcholinesterase inhibitors with antioxidant properties. *Bioorganic & Medicinal Chemistry* **16**, 4252-4261 (2008).

88. Ades, E.W. *et al.* HMEC-1: Establishment of an immortalized human microvascular endothelial cell line. *Journal of Investigative Dermatology* **99**, 683-690 (1992).

89. Knuth, S. *et al.* Catechol, a bioactive degradation product of salicortin, reduces TNF-α induced ICAM-1 expression in human endothelial cells. *Planta Medica* **77**, 1024-6 (2011).

90. Schmidt, S. *et al.* Bi-, tri-, and polycyclic acylphloroglucinols from Hypericum empetrifolium. *Journal of Natural Products* **75**, 1697-1705 (2012).

91. Ishige, K. *et al.* Flavonoids protect neuronal cells from oxidative stress by three distinct mechanisms. *Free Radical Biology and Medicine* **30**, 433-446 (2001).

92. Betancor-Fernández, A. *et al.* Screening pharmaceutical preparations containing extracts of turmeric rhizome, artichoke leaf, devil's claw root and garlic or salmon oil for antioxidant capacity. *The Journal of Pharmacy and Pharmacology* **55**, 981-6 (2003).

93. Shimoi, K. *et al.* Deglucuronidation of a flavonoid, luteolin monoglucuronide, during inflammation. *Drug Metabolism and Disposition* **29**, 1521-1524 (2001).

94. Marshall, T. *et al.* Release of lysosomal enzyme beta-glucuronidase from isolated human eosinophils. *Journal of Allergy and Clinical Immunology* **82**, 550-555 (1988).

95. Hämäläinen, M. *et al.* Anti-inflammatory effects of flavonoids: genistein, kaempferol, quercetin, and daidzein inhibit STAT-1 and NF-kappaB activations, whereas flavone, isorhamnetin, naringenin, and pelargonidin inhibit only NF-kappaB activation along with their inhibitory effect on iNOS expression and NO production in activated macrophages. *Mediators of Inflammation* **2007**, 45673 (2007).

96. Luo, H. *et al.* Kaempferol inhibits angiogenesis and VEGF expression through both HIF dependent and independent pathways in human ovarian cancer cells. *Nutrition and Cancer* **61**, 554-563 (2009).

97. Hakimuddin, F. *et al.* Selective cytotoxicity of a red grape wine flavonoid fraction against MCF-7 cells. *Breast Cancer Research and Treatment* **85**, 65-79 (2004).

98. Choi, E.J. & Ahn, W.S. Kaempferol induced the apoptosis via cell cycle arrest in human breast cancer MDA-MB-453 cells. *Nutrition Research and Practice* **2**, 322-5 (2008).

99. Zhang, Y. *et al. Ginkgo biloba* extract kaempferol inhibits cell proliferation and induces apoptosis in pancreatic cancer cells. *The Journal of Surgical Research* **148**, 17-23 (2008).

100. Neri, D. & Supuran, C.T. Interfering with pH regulation in tumours as a therapeutic strategy. *Nature Reviews Drug Discovery* **10**, 767-777 (2011).

101. Calgarotto, a. K. *et al.* A multivariate study on flavonoid compounds scavenging the peroxynitrite free radical. *Journal of Molecular Structure: THEOCHEM* **808**, 25-33 (2007).

102. 20.08.13. http://img.fotocommunity.com/images/Pflanzen-Pilze-Flechten/Heilpflanzen/Ginkgo-a25418104.jpg.

103. Bedir, E. *et al.* Biologically Active Secondary Metabolites from *Ginkgo biloba*. *Journal of Agricultural and Food Chemistry* **50**, 3150-3155 (2002).

104. Tang, Y. *et al.* Coumaroyl flavonol glycosides from the leaves of *Ginkgo biloba*. *Phytochemistry* **58**, 1251-1256 (2001).

105. Hasler, A. *et al.* Complex flavonol glycosides from the leaves of *Ginkgo biloba*. *Phytochemistry* **31**, 1391-1394 (1992).

106. Pietta, P. *et al.* Identification of flavonoids from *Ginkgo biloba* L., *Anthemis nobilis* L. and *Equisetum arvense* L. by high-performance liquid chromatography with diode-array UV detection. *Journal of Chromatography A* **553**, 223-231 (1991).

107. Vanhaelen, M. & Vanhaelen-fastre, R. Countercurrent chromatography for isolation of flavonol glycosides from *Ginkgo biloba* leaves. *Journal of Liquid Chromatography* **11**, 2969-2975 (1988).

108. Nasr, C. *et al.* Kaempferol coumaroyl glucorhamnoside from *Ginkgo biloba*. *Phytochemistry* **25**, 770-771 (1991).

109. Murota, K. & Terao, J. Antioxidative flavonoid quercetin: implication of its intestinal absorption and metabolism. *Archives of Biochemistry and Biophysics* **417**, 12-17 (2003).

110. Kay, C.D. Aspects of anthocyanin absorption, metabolism and pharmacokinetics in humans. *Nutrition Research Reviews* **19**, 137-46 (2006).

9 Posters

Bücherl D, Heilmann J. **Towards the Synthesis of Phase-II Metabolites of Kaempferol.** 5th International Conference on Polyphenols and Health. Sitges, Barcelona, 17-20 October 2011.

Bücherl D, Erdelmeier C, Nöldner M, Koch E, Heilmann J. **Identification and Quantification of Metabolites in Plasma of Rats treated with major Kaempferol Glycosides occurring in *Ginkgo biloba* Extract EGb 761®.** DPhG annual Conference. Freiburg, 9-11 October 2013.

10 List of Figures